A Macrophage Migration Inhibitory Factor interactome screen identifies a complex of Jab1/CSN5 and Valosin-containing protein as an important mediator in the ubiquitin proteasome system

Inaugural Dissertation
submitted to the Faculty of Medicine
in partial fulfillment of the requirements
for the PhD-Degree
of the Faculty of Medicine
of the Justus Liebig University Giessen

by
Cayli Sevil
of
Ankara, TURKEY

Giessen (2008)

From the Department of Anatomy and Cell Biology
Director / Chairman: Prof. Dr. E. Baumgart-Vogt
of the Faculty of Medicine of the Justus Liebig University Giessen

First Supervisor and Committee Member: Prof.Dr. Andreas Meinhardt
Second Supervisor: Prof. Dr. Jürgen Bernhagen
Committee Members: Prof. Dr. Dr. Hans Michael Piper,
Privatdozent Dr. Sandip Kanse

Date of Doctoral Defense: 24.09.2008

CONTENTS

1. INTRODUCTION

1.1. The history of MIF

Macrophage migration inhibitory factor (MIF) was one of the first cytokines to be identified (Bloom and Bennett, 1966; David, 1966). MIF was first described as a T cell-derived cytokine that inhibits the random migration of macrophages. Between 1970 and 1989, MIF was reported to enhance monocyte and macrophage functions. However, biological activities of MIF remained uncertain until the cloning of the human MIF gene was achieved in 1989 (Weiser et al., 1989). In 1991, research for new regulators of inflammation led to re-discovery of MIF as a molecule released, similar to a hormone, by cells of the anterior pituitary gland after exposure to the endotoxin lipopolysaccharide (LPS) (Bernhagen et al., 1993). This important observation indicated that MIF could be a mediator that links the endocrine and immune systems. Within a few years, bio-active recombinant MIF proteins and neutralizing antibodies were produced and a proinflammatory profile of MIF by acting or promoting cytokine expression has emerged (Bernhagen et al., 1994). Interestingly, it was observed that low levels of glucocorticoids promote MIF release from monocytes and macrophages (Calandra and Bucala, 1995), which was opposed by the concept that MIF is a proinflammatory cytokine and glucocorticoids usually exert powerful anti-inflammatory actions. MIF then was found to be acting in an autocrine or paracrine manner within the host-defence system to block the effects of glucocorticoids on LPS-induced cytokine release (Bacher et al., 1996). Studies concerning the molecular mechanism of MIF revealed that the influence between the pro- and anti-inflammatory actions of MIF and glucocorticoids appear to act as a counterregulatory system that aids the maintenance of homeostasis (Bucala, 1996; Barnes and Karin, 1997).

Using X-ray crystallography the crystal form and unique ribbon structure of rat and human MIF was defined in 1996 (Muhlhahn et al., 1996; Sugimoto et al., 1996; Suzuki et al., 1996). The three dimensional structure and its resemblance to prokaryotic enzymes pointed to a potential enzymatic activity of MIF. Later, MIF has been reported to have two different catalytic activities: tautomerase (Bendrat et al., 1997; Rosengren et al., 1997; Swope et al., 1998) and thiol-protein oxidoreductase (Kleemann et al., 1998a; Kleemann et al., 1998b; Kleemann et al., 1999). MIF-knockout mice were generated in 1999 and reported to be

healthy (Bozza et al., 1999). After 2000, several functions of MIF were described by different studies mentioned below.

1.2. MIF-mediated signaling pathways

1.2.1. MIF-mediated ERK1/ERK2 activation

MIF was found to activate extracellular signal-regulated kinase 1 (ERK1)/ERK2, members of the family of mitogen-activated protein kinases (MAPKs) (Mitchell et al., 1999). MIF-induced activation of ERK1/ERK2 was dependent on protein kinase A and associated with increased cytoplasmic phospholipase A2 (PLA2) enzyme activity. PLA2 is an important intracellular link in the activation of the pro-inflammatory cascade, resulting first in the production of arachidonic acid and then of prostaglandins and leukotrienes. PLA2 also is a key target of the anti-inflammatory effects of glucocorticoids. ERK1/ERK2-mediated induction of PLA2 is one mechanism where MIF could override the immunosuppressive effects of steroids (Mitchell et al., 1999).

The extracellular domain of CD74, the cell-surface form of the MHC class-II-associated invariant chain has been reported to bind MIF (Leng et al., 2003). CD74 was involved in many activities of MIF such as activation of ERK1/ERK2, cell proliferation and the production of prostaglandin E2 (PGE2). However, the intracellular domain of CD74 does not contain motifs that can interact with signal-transducing molecules. Therefore the question arises whether CD74 would be the unidentified receptor for MIF.

1.2.2. MIF inhibits p53 activity

An interesting study indicating that MIF works as a negative regulator of p53-mediated growth arrest and apoptosis has provided a link between MIF, inflammation, cell growth and tumorigenesis (Hudson et al., 1999). Following this finding, it was reported that the proinflammatory function and the viability of MIF-deficient macrophages were diminished compared with wild-type cells after incubation with LPS (Mitchell et al., 2002). NO was thought to be a crucial mediator of increased apoptosis in MIF-deficient macrophages stimulated with LPS, although MIF-deficient and wildtype macrophages produced equal levels of NO. Indeed, MIF was found to inhibit NO-induced intracellular accumulation of p53. Inhibition of p53 by MIF required serial activation of ERK1/ERK2, PLA2, cyclooxygenase 2 (COX2) and PGE2. In parallel to these results, MIF was reported to interact

with the E2F–p53 pathway to sustain normal and malignant cell growth (Petrenko et al., 2003).

1.2.3. MIF regulates Toll-like receptor 4 expression

Toll-like receptor (TLR) plays an essential role in the innate immune response by detecting conserved molecular products of microorganisms (Medzhitov et al., 1997; Medzhitov, 2001). TLR4 is the receptor for LPS, the major component of the cell wall of the gram-negative bacteria (Takeda et al., 2003). MIF-deficient macrophages were found to be hyporesponsive to LPS and Gram-negative bacteria, as shown by reduced cytokine production due to the downregulation of expression of TLR4 (Roger et al., 2001; Roger et al., 2003). MIF upregulates the expression of TLR4 by acting on the ETS family of transcription factors, which are crucial for transcription of the mouse TLR4 gene. Therefore, MIF facilitates the detection of endotoxin-containing bacteria, enabling cells to respond rapidly to invasive bacteria.

1.2.4. MIF stimulates glycolysis

An unexpected role for MIF in the regulation of glycolysis was documented with *in vitro* and *in vivo* studies (Benigni et al., 2000). It was shown that MIF controls peripheral glucose metabolism and mediates the catabolic effects induced by severe inflammatory responses. The addition of recombinant MIF to differentiated rat muscle cells increased synthesis of fructose bisphosphate. In the same study, it is implicated that the catabolic effect of TNF-α on muscle cells was mediated by MIF, which served as an autocrine stimulus for fructose bisphosphate production. TNF-α administered to mice decreased serum glucose levels and increased muscle fructose bisphosphate levels and pre-treatment with a neutralizing anti-MIF antibody completely inhibited these effects. Anti-MIF antibody also prevented hypoglycaemia and increased muscle fructose bisphosphate levels in TNF-α–knockout mice that were administered LPS, supporting the contribution of MIF to these inflammation-induced metabolic changes. Briefly, MIF was found to be a positive, autocrine stimulator of insulin release, suggesting an important role for MIF in the control of host glucose and carbohydrate metabolism.

1.2.5. MIF inhibits Jab1/CSN5 activity

An interaction between MIF and c-Jun-activation domain-binding protein 1 (Jab1) known as the fifth component of the COP9 signalosome (Jab1/CSN5) was shown by using a yeast two-hybrid system (Kleemann et al., 2000). In the same study, it is observed that MIF and Jab1/CSN5 are co-localized in the cytoplasm and that MIF inhibits the positive regulatory effects of Jab1/CSN5 on the activity of JNK and AP1 (Kleemann et al., 2000). Moreover, Jab1/CSN5 was found to activate Jun N-terminal kinase (JNK), phosphorylate c-Jun and function as a co-activator of activator protein 1 (AP1), a transcription factor that is involved in cell growth, transformation and cell death (Shaulian and Karin, 2002).

1.2.6. MIF activates the AKT pathway

Although the inhibition of p53 mediated apoptosis by MIF was indicated (see 1.2.2), MIF-induced AKT pathway was also shown to prevent apoptosis and promote cell survival in fibroblasts, HeLa cervix carcinoma cells and various breast cancer cell lines (Lue et al., 2007). The phosphoinositide-3-kinase (PI3K)/AKT signaling pathway plays an crucial role in the cellular response to growth factors and regulates key cellular functions such as growth, metabolism, migration, apoptosis and survival (Song et al., 2005). PI3K/AKT signalling is initiated by activation of receptor tyrosine kinases or G-protein-coupled receptors (Wetzker and Bohmer, 2003). Activation of PI3K/AKT causes different cellular responses, but most importantly, AKT activation leads cell survival and prevents cell to resist apoptosis. It was shown that the MIF-induced AKT pathway transmits signaling through the MIF binding protein CD74 and the upstream kinases Src and PI3K. Additionally, MIF-induced AKT activation led to inactivation of pro-apoptotic proteins, namely BAD and Foxo3a. In agreement with these result, apoptosis inhibition by MIF was abolished by overexpression of the AKT pathway inhibitor PTEN showing that this inhibition occurred without assistance of p53. Briefly, a cell survival effect of MIF was proven through PI3K/AKT and its downstream pathways in fibroblast and different cancer lines.

1.2.7. MIF regulates leukocyte migration

Although MIF was discovered as an inhibitor of random macrophage migration (David, 1966), the mechanisms underlying MIF-regulated cell migration and the proteins involved have not been studied for many years. Recent study has revealed that MIF is a

functional noncognate ligand for the chemokine receptors CXCR2 and CXCR4, and therefore controls inflammatory and atherogenic leukocyte recruitment (Bernhagen et al., 2007).

In this study, MIF was shown to facilitate chemotaxis of monocytes and T cells, rapid integrin activation and calcium influx through CXCR2 or CXCR4. MIF was indicated to directly bind to CXCR2 and compete with cognate ligands for CXCR4 and CXCR2 binding. The CXCR2 and CD74 interaction found in this study suggested a new signaling pathway via a functional CXCR2-CD74 complex. Additionally, *in vivo* experiments also provided several lines of evidence that MIF deficiency diminished monocyte adhesion to the arterial wall in atherosclerotic mice and MIF-induced leukocyte recruitment. Briefly, MIF was identified as a crucial CXCR2 ligand in advanced atherosclerosis. Blockade of MIF in mice with advanced atherosclerosis causes plaque regression and reduced monocyte and T-cell contents in plaques. In light of these important findings, chemokine-like functions of MIF and a regulatory role in inflammation and atherogenesis were discovered (Bernhagen et al., 2007).

1.2.8. MIF modulates the activation of AMPK pathway

MIF was found to exert one of its metabolic effects on AMP-activated protein kinase (AMPK) pathway (Miller et al., 2008). AMPK, an important regulator of both glycolysis and glucose uptake during cellular stress, protects the heart against ischaemic injury and apoptosis. AMPK affects different pathways. For example; AMPK stimulates 6-phosphofructo-2-kinase activity and glycolysis in the heart (Marsin et al., 2000), induces glucose transporter-4 (GLUT4) translocation (Russell et al., 1999), increases ischaemic glucose uptake (Russell et al., 2004) and limits myocardial injury and apoptosis (Xing et al., 2003). MIF is shown to be released in the ischaemic heart, where it stimulates AMPK activation through CD74. This stimulation promotes glucose uptake and protects the heart during ischaemia-reperfusion injury. MIF germ line deletion impairs ischaemic AMPK signaling in the mouse heart. Additionally, MIF release in human fibroblasts and AMPK activation during hypoxia were diminished. For these reasons, MIF received new attention as a modulator of the activation of the cardio-protective AMPK pathway during ischaemia. These results create a link between inflammation and metabolism in the heart. MIF expression was also thought to have an impact on the response of the human heart to ischaemia by the AMPK pathway.

AMPK is known as a potential target molecule for the treatment of many diseases, because of its metabolic actions that increase skeletal muscle glucose uptake and suppress

hepatic glucose production. AMPK is also a potential molecule in ischemic heart disease, because of its cardio-protective effects and potential role in ischemic conditions (Sukhodub et al., 2007). For these reasons, it is believed that treatment with MIF or MIF agonist's might be a therapy targeted at AMPK activation during acute myocardial ischemia or infarction.

1.3. Role of MIF in pathogenesis

MIF has been shown to participitate in the pathogenesis of several acute and chronic inflammatory diseases as summarized in Table 1 modified from (Lue et al., 2002).

Table1: Human pathologies associated with MIF in systems and organs

Pathogenesis	**References**
Sepsis and toxic-shock syndrome	(Bernhagen et al., 1993; Bozza et al., 1999)
Delayed-type hypersensitivity	(Bernhagen et al., 1996)
Adjuvant and antigen-induced arthritis	(Mikulowska et al., 1997; Leech et al., 1998)
Glomerulonephritis	(Lan et al., 1996; Yang et al., 1998)
Acute lung injury	(Makita et al., 1998)
Allograft rejection	(Brown et al., 1999)
Inflammatory bowel disease (colitis)	(de Jong et al., 2001)
Gastrititis, Pancreatitis	(Huang et al., 2001; Sakai et al., 2003)
Atherogenesis	(Lin et al., 2000)
Encephalomyelitis	(Denkinger et al., 2003)
Uveoretinitis	(Kitaichi et al., 2000)
Systems and organs	**Pathogenesis**
Immune system	sepsis, septic shock and allograft rejection
Lung	adult respiratory distress syndrome, asthma, tuberculosis and Wegener's granulomatosis
Kidney	glomerulonephritis
Bones and joints	rheumatoid arthritis, polychondritis
Gastrointestinal tract	colitis and Crohn's disease
Skin	atopic dermatitis, psoriasis and systemic sclerosis
Endocrine system	type–2 diabetes and pancreatitis
Brain	multiple sclerosis and neuro-Behcet's disease
Eye	uveitis and iridocyclitis
Heart and vasculature	atherosclerosis
Ear	otitis

1.4. Cell and tissue distrubition of MIF

Besides the immune system, MIF has a broad cell and tissue distribution. Previously, T cells were thought to be the main cellular source of MIF in the immune system. However, many cells such as monocytes, macrophages, blood dendritic cells, B cells, neutrophils, eosinophils, mast cells and basophils have been shown to express MIF (Baugh and Bucala, 2002; Lue et al., 2002). Notably, MIF is expressed by cells and tissues that are in direct contact with the host's natural environment, such as the lung, the epithelial lining of the skin, gastrointestinal and genitourinary tracts. Additionally, high levels of MIF expression were noticed in several tissues of the endocrine system, especially in organs such as hypothalamus, pituitary and adrenal glands (Calandra et al., 1994; Meinhardt et al., 1996; Bacher et al., 1997; Fingerle-Rowson et al., 2003).

1.5. MIF interacting proteins

Through its interaction with a variety of proteins, MIF display diverse activities in a cell. MIF was shown to regulate the activity of JNK and AP1 by directly interacting with Jab1/CSN5 (Kleemann et al., 2000). A recent study showed that MIF not only interacts with Jab1/CSN5, the fifth component of the COP9 signalosome (CSN) (see 1.6 and 1.7 for details), but also CSN6 due to their MPN domain (Burger-Kentischer et al., 2005). Jab1/CSN5 plays an important role as a subunit of the CSN complex in animals as well as in plants. The CSN complexes interact with SCF (Skp1/Cullin/F-box protein) E3 ubiquitin ligase complex and deconjugate Nedd8 from Cullin (Cope et al., 2002). In particular, removal of Nedd8 is carried out by the isopeptidase activity that resides in the MPN domain metalloenzyme JAMM motif of Jab1/CSN5. This motif is only functional in the content of the CSN complexes (Cope and Deshaies, 2006). The deneddylation of Cullin results in increased activity in SCF ligases which target p27 and Cyclin E for ubiquitin-dependent proteolysis (Cope and Deshaies, 2003, 2006).

MIF was shown to interact with PAG, a thiol-specific antioxidant. The interaction of MIF and PAG showed a reduction of the dopachrome tautomerase activity of MIF (Jung et al., 2001). In another study, hepatopoietin (HPO) was found to interact with both MIF and Jab1/CSN5, which implicated modulation of the AP-1 pathway (Li et al., 2004).

Recent work has identified CD74 as a cell surface binding receptor for MIF (Leng et al., 2003). However, not all cells targeted by MIF express CD74 on their surface and CD74

does not contain an intarcellular domain for signal transduction, so it is suggested that CD74 could be a docking or an adaptor protein which could present MIF to other proteins.

Although the direct interaction between insulin and MIF was not defined, co-localization of insulin with MIF in secretory granules of pancreatic islet and the regulation of glucose-induced insulin release was studied (Waeber et al., 1997). More recently, a direct interaction of MIF with myosin-light-chain-kinase isoform (MLCK) was identified (Wadgaonkar et al., 2005) suggesting a role of MLCK in the regulation of non-muscle cytoskeletal dynamics and pathobiologic vascular events.

1.6. MIF affects the activity of the Ubiquitin Proteasome System (UPS)

A recent investigation has shown that the optimal composition and activity of SCF ubiquitin ligases, which are known to play an important role in the UPS, is maintained through the Jab1/CSN5-MIF interaction (Nemajerova et al., 2007a). MIF inhibits Jab1/CSN5 function by preventing it from interacting with other cellular proteins targeted by the COP9 signalosome (CSN), especially the Cullins (Nemajerova et al., 2007a). Cullin1 belongs to SCF (E3 Ubiquitin ligase) which is known to control both the specificity and timing of substrate ubiquitinylation. The SCF complex consists of three different components: Rbx1 (Ring box-1), Cullin1 (Cul1, scaffold protein), Skp1 (adaptor protein) and the F-box family proteins, which are responsible for substrate recognition (Cardozo and Pagano, 2004). The main catalytic core of SCF is the Rbx1 and Cul1 subunits (Figure 1). The activity of the SCF is stimulated by attachment of an ubiquitin-like protein called Nedd8 to the Cullins (neddylation) (Bornstein et al., 2006). In a converse manner, deneddylation of cullins was achieved by the CSN/COP9 signalosome with the Jab1/CSN5 subunit directly cleaving of Nedd8 (Cope et al., 2002). Importantly, deneddylated cullins are segregated by inhibitory Cand1 (Figure 1) (Liu et al., 2002). Thus, SCF activity is sustained by dynamic cycles of assembly and disassembly, where both inhibitory protein Cand1 and CSN interacting with MIF play a negative role (Petroski and Deshaies, 2005). In this context, MIF binding to Jab1/CSN5 regulates the cycle and activity of the SCF complex. Briefly, the mechanism how MIF affects the activity of the UPS is shown in figure 1.

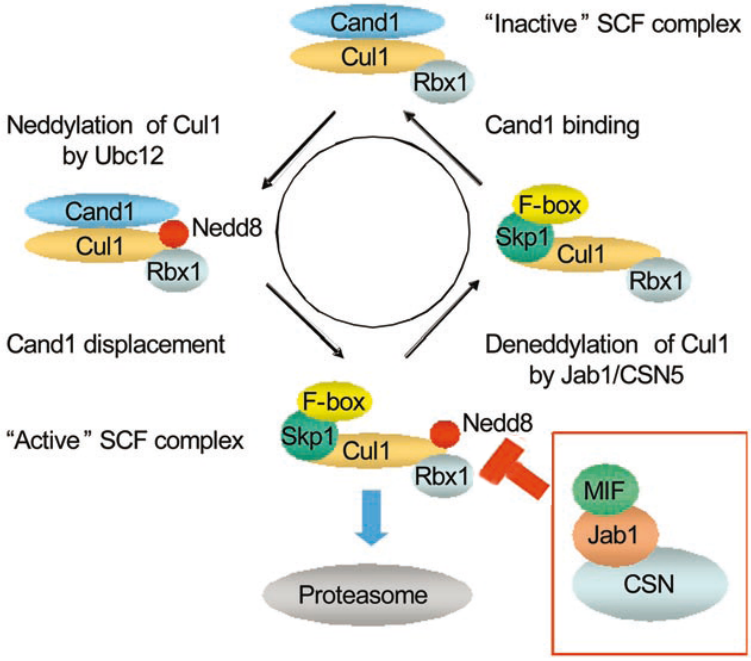

Figure 1: MIF-Jab1/CSN5 interaction regulates SCF activity.
The SCF E3 ubiquitin ligase is composed of Cullins, Skp1 and F-box proteins. Deneddylation (removal of Nedd8 from Cullin1) is achieved by Jab1/CSN5. Following deneddylation of Cullins, Skp1 and F-box proteins are replaced by the inhibitory protein Cand-1. MIF binds to Jab1/CSN5 and prevents it from interacting with Cullins targeted by CSN. Modified from (Nemajerova et al., 2007b).

1.7. The COP9 signalosome (CSN)

One of the most important regulatory components of the UPS is the COP9 signalosome (CSN). Deng and co-workers first identified the CSN in *Arabidopsis* (COP stands for constitutive photomorphogenesis) as a suppressor of light-dependent development (Wei et al., 1994; Wei and Deng, 1999). The mammalian CSN complex, also known as the Jab1/CSN5 containing signalosome, was isolated and co-purified with the 26S proteasome (Seeger et al., 1998).

CSN fractionates as a 450–550-kDa complex in gel filtration columns and consists of eight subunits called CSN1 to CSN8. A characteristic feature of the CSN subunits is the presence of two domains known as the PCI/PINT (Proteasome, COP9 signalosome, Initiation factor 3/Proteasome subunits, Int-6, Nip-1, and TRIP-15) and the MPN/MOV34 family (Mpr1 Pad1-N-terminal) domains (Aravind and Ponting, 1998). These two domains are also found in three large protein complexes: CSN, the 26S proteasome lid subcomplex, and eukaryotic translation initiation factor 3 (eIF3) (Glickman et al., 1998; Wei et al., 1998). The 26S

proteasome (see details in 1.8, figure 3) carried out the non-lysosomal protein degradation in eukaryotic cells, is composed of the 20S catalytic core particle (CP) and the 19S regulatory particle (RP). Remarkably, each of the eight CSN subunits share pair-wise homology with a corresponding lid component, suggesting that CSN and the lid may have a common evolutionary ancestor. The CSN has several biochemical activities explained below:

1.7.1. The Metalloprotease Activity of CSN and Deneddylation of SCF

Jab1/CSN5 contains a metalloprotease motif referred to as JAMM (Jab1/MPN domain-associated metalloisopeptidase) or MPN+ motif. Mutations in this motif of Jab1/CSN5 abolish the activity. Similarly, RPN11, the Jab1/CSN5 paralog in the proteasome lid, contains the same JAMM/MPN+ motif, which consists the major de-ubiquitinating activity of the 26S proteasome (Verma et al., 2002). Although some other proteins posses JAMM/MPN+ (Maytal-Kivity et al., 2002; McCullough et al., 2004; Bellare et al., 2006), both Jab1/CSN5 and RPN11 harbor the metalloisopeptidase activity only when they assemble into the CSN complex or the 26S proteasome, respectively (Cope et al., 2002). The metalloprotease activities of Jab1/CSN5 and RPN11 are likely regulated in accordance with other activities of the complex such as deubiquitinylation and deneddylation.

Another important function of the CSN has received attention in molecular biology. Jab1/CSN5 is involved in deneddylation of the SCF complex due to its functional MPN motif. The SCF ubiquitin ligase complex is the major target of CSN. SCF represents a type of E3 (Ubiquitin ligase) enzyme that catalyzes a key step in ubiquitin conjugation to the target proteins. Similar to the ubiquitin conjugation pathway, the neddylation pathway is catalyzed by an enzymatic cascade involving Nedd8-activating enzymes, whereas deneddylation is catalyzed by a metalloisopeptidase activity centered within the Jab1/CSN5 subunit (Cope et al., 2002). Active cycles of neddylation and deneddylation are required to maintain the SCF activity toward its target substrates.

1.7.2. CSN-Associated Protein Kinase Activity and Deubiquitinylation Activity

The CSN was found to phosphorylate c-Jun (Ser63 and Ser73), IκBα and the NF-κB precursor, p105, as well as the tumor suppressor p53 (Ser149, Thr 150, and Thr 155) *in vitro* (Seeger et al., 1998; Bech-Otschir et al., 2001). The CSN itself is a target of phosphorylation, since phosphorylation sites of some subunits have been noted (Henke et al., 1999).

Recently, reports demonstrated ubiquitin isopeptidase activities associated with the CSN (Groisman et al., 2003; Zhou et al., 2003; Hetfeld et al., 2005; Schweitzer et al., 2007). Deubiquitinylation activities of the CSN are explained in two ways: CSN either deconjugates ubiquitin from mono-ubiquitinated substrates or depolymerize the polyubiquitin chains (Groisman et al., 2003). The former activity requires the metalloprotease domain in Jab1/CSN5 (Groisman et al., 2003), suggesting that cleavage of the ubiquitin- or Nedd8-monoconjugates shows similar mechanisms, whereas the latter activity is associated with the CSN (Zhou et al., 2003; Hetfeld et al., 2005; Schweitzer et al., 2007). Briefly, these findings indicate that the CSN has both deneddylation and de-ubiquitinylation activities either by possessing activities on their own or by selectively associating different deubiquitinylation enzymes.

1.7.3. Protein degradation

Jab1/CSN5 facilitates the 26S proteasome-dependent degradation of several proteins, including p27Kip, Luteinizing hormone receptor (LHR), p53, estrogen receptor, Smad4, Smad7, Id1, Id3, and IκBα (Li et al., 2000; Wan et al., 2002; Berse et al., 2004; Kim et al., 2004; Yun et al., 2004; Callige et al., 2005).

Protein degradation is deployed to modulate the steady-state abundance of proteins and to switch cellular regulatory circuits from one state to another by elimination of proteins. In eukaryotes, the protein degradation that occurs in the cytoplasm and nucleus is carried out by key regulatory proteins via the UPS. Among these regulatory proteins, both CSN (COP9 signalosome) and VCP control the degradation of certain substrates (Ye et al., 2001; Wei and Deng, 2003).

1.8. Ubiquitin Proteasome System (UPS)

The UPS has an essential function in eukaryotes by controlling the levels of crucial intracellular regulatory proteins. The UPS cycles in two phases; ubiquitinylation and degradation. In the initial ubiquitinylation phase, Ub (Ubiquitin) is activated through the ATP-dependent formation of a thiol ester with a cysteine residue of Ub-activating enzyme (E1), then transferred to a cysteine residue of an Ub conjugating enzyme (E2) and finally, transferred to a lysine residue of the substrate in a reaction catalyzed by an Ub-protein ligase (E3). Ub is linked to the substrate through an isopeptide bond. The activation and ligation reactions involve the carboxyl group of the final amino acid of Ub (G76) (Figure 2) (Pickart, 2001b, a).

The attachment of a single ubiquitin molecule (monoubiquitinylation) onto a substrate has been assigned to different functions such as lysosomal sorting, endocytosis and trafficking (Schnell and Hicke, 2003) (Figure 2).

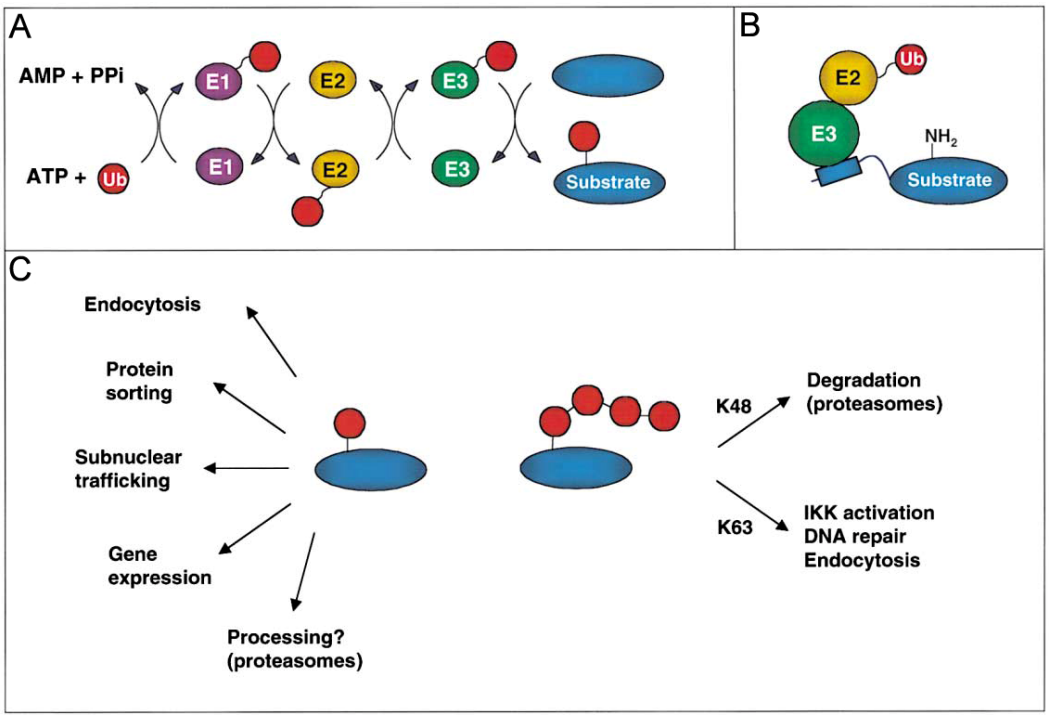

Figure 2: Ubiquitin Conjugation and Signalling
A: Ubiquitin is activated by E1 (Ubiquitin activating enzyme) and subsequently transfered to E2 (Ubiquitin conjugating enzyme). The substrate (blue box) and the E2 enzyme both bind specificially to E3 (Ubiquitin protein ligase) and the activated ubiquitin is then transferred to the substrate. **B:** The E3 binds its substrate and its specific E2 partner at separate sites. The substrate is frequently recognized through an ubiquitinylation signal **C:** some of the known functions of monoubiquitinylation **(left)** and polyubiquitinylation **(right).** Lysine 48 (K48) linkages recognized by the 26S proteasome for degradation and K63 linkages involved in

multiple pathways, including DNA damage, protein trafficking, ribosomal function and inflammation response. From (Pickart, 2001b)

In the second phase of the UPS cycle, the proteasome recognizes the substrate via the poly-Ub chain. The substrate is degraded to small peptides and Ub is recovered by specific deubiquitinating enzymes. Like conjugation, proteasomal degradation is also ATP dependent. The 26S proteasome is a remarkable protein machine that catalyzes the signal-dependent unfolding and proteolysis of its substrates (Schwechheimer and Deng, 2001; Pickart and Cohen, 2004). It is made up of two kinds of complexes (Figure 3). The 20S core complex is a cylindrical stack. It harbors the proteolytic active sites, which face a large interior chamber. Substrate unfolding and recognition of polyUb tag are carried out by the 19S complex that is located at either end of the 20S complex. Each 19S complex contains 15–20 subunits; including six ATPases that are located proximal to the 20S barrel and are likely to promote ATP-dependent substrate unfolding and translocation.

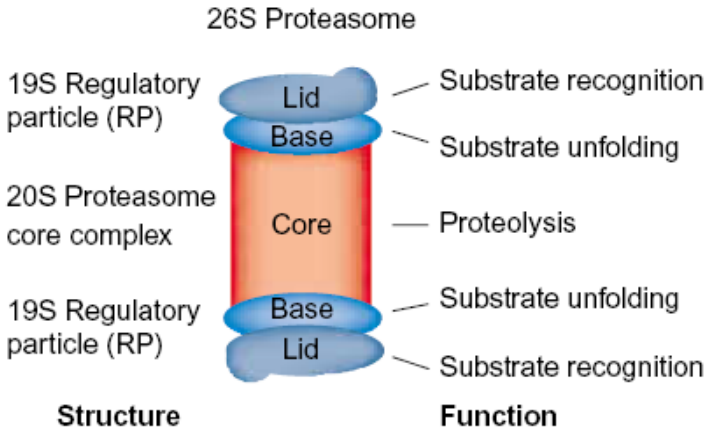

Figure 3: Structural and functional representation of the 26S proteasome.
The 26S proteasome consists of a 19S regulatory particle (divided into lid and base subcomplexes) and a 20S proteolytic core. Functions of each particle are indicated on the right side. From (Schwechheimer and Deng, 2001).

1.9. VCP dependent proteasomal degradation

The 97-kDa valosin-containing protein (p97 or VCP) plays essential roles in ubiquitin-proteaosome proteolysis, which depend on an ability to recognize ubiquitin signals. Ubiquitin interaction with VCP and its cofactors play an important role in VCP-regulated processes. VCP acts as a chaperone in the UPS, thus regulating the various cellular functions through this pathway. VCP is ubiquitous, essential, and highly abundant in cells, accounting for more than 1% of the total cellular protein.

VCP is a member of the type II AAA (**A**TPases **A**ssociated with a variety of **A**ctivities) ATPases, which are characterized by the presence of two conserved ATPase domains, also called AAA domains (Neuwald et al., 1999; Zwickl and Baumeister, 1999; Vale, 2000; Maurizi and Li, 2001; Ogura and Wilkinson, 2001). VCP, also known as VAT in archaebacteria, CDC48 in yeast, TER94 in Drosophila, p97 in Xenopus, and VCP in plants and mammals is one of the most highly evolutionarily conserved proteins (Frohlich et al., 1991; Pamnani et al., 1997).

VCP molecule is composed of N-terminal domain (N), two ATPase domains (D1 and D2), and a C-terminal domain (C). The N domain binds to polyubiquitin chains and thus is responsible for substrate recognition. Both D1 and D2 are required for providing the chaperone activity (Figure 4) (Wang et al., 2003).

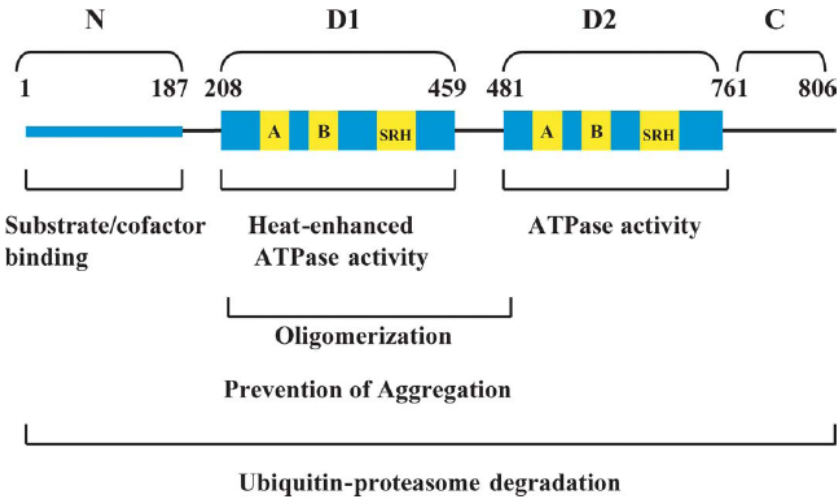

Figure 4: The structural–functional relationship of VCP domains.
A: Walker A, B: Walker B and SRH: the **S**econd **R**egion of **H**omology motifs in D1 and D2 domains of VCP. From (Wang et al., 2004).

Electron microscopy (EM) studies indicated that VCP has a barrel-like homo-hexameric structure that comprises two stacked hexameric rings made of the respective AAA modules (Wang et al., 2003).

VCP is involved in many other cellular activities such as cell cycle progression (Cao K, 2004), homotypic membrane fusion after mitosis, and disassembly of the spindle at the end of mitosis (Kondo et al., 1997; Cao et al., 2003; Wojcik et al., 2004), retrograde translocation of misfolded proteins from the ER (Ye et al., 2001; Braun et al., 2002; Jarosch et al., 2002), degradation of polyubiquitinated proteins by the proteasomes (Ghislain et al., 1996; Dai and Li, 2001), and activation of transcription factors (Hitchcock et al., 2001; Rape et al., 2001) in addition to degradation of proteins.

VCP, with the help of cofactors, specifically binds the ubiquitinylated protein and chaperons the protein before passing it to the 26S proteasome for degradation (Figure 5). After substrate ubiquitinylation, VCP likely uses the energy generated from ATP hydrolysis to segregate the protein complex, singles the ubiquitinylated protein, and presents it to the proteasome for degradation. As an example: in unstimulated cells NF-κB is located in the cytoplasm in an inactive form in physicall association with the inhibitory IκB proteins (Karin and Ben-Neriah, 2000; Santoro et al., 2003). In response to stimulation, NF-κB can be activated and IκBα is rapidly phosphorylated and polyubiquitinylated (Karin and Ben-Neriah, 2000). Following that, VCP binds the polyubiquitinylated IκBα and likely dissociates it from the NF-κB complex (Dai et al., 1998). After dissociation, the NF-κB dimer translocates into the nucleus to regulate its target genes. In the meantime, VCP chaperones the polyubiquitinylated IκBα to the 26S proteasome for irreversible degradation (Dai et al., 1998). In light of this example, figure 5 displays how the ubiquitinylated proteins are guided to the proteasome or to other signaling pathways via VCP.

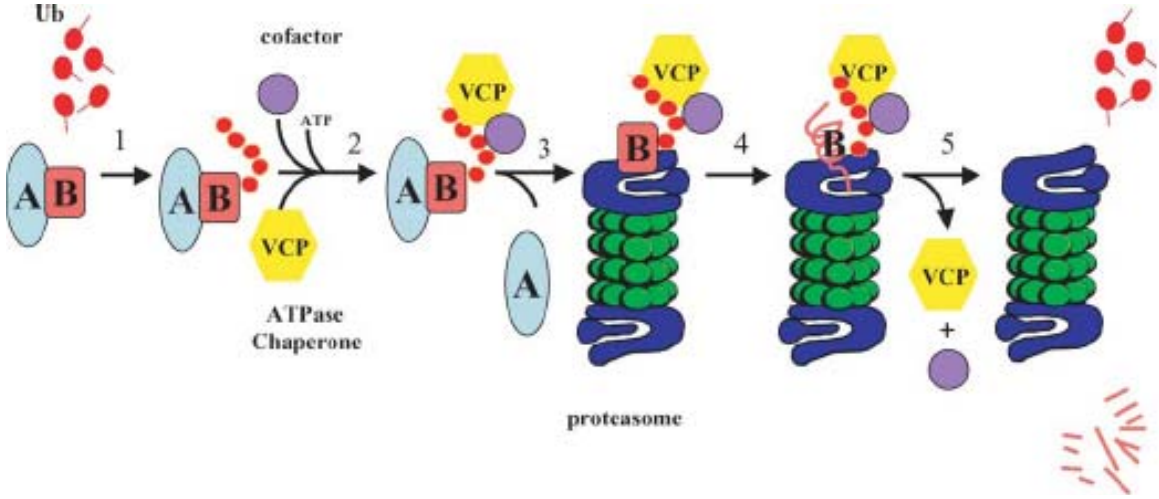

Figure 5: A role of the molecular chaperone VCP in the UPS.
Step 1 shows protein B polyubiquitinylation, which tags the protein for proteasomal degradation. In step 2, VCP together with other cofactor(s), binds to protein B via the N domain of VCP and the poly-Ub chain on protein B. In step 3, the VCP/cofactor complex disassembles the protein A/B complex using the energy generated from VCP-catalyzed ATP hydrolysis. Dissociated protein B is then chaperoned to other intracellular locations or to the proteasome for degradation (steps 4 and 5), from (Wang et al., 2004).

1.10. Aim of the study

Macrophage migration inhibitory factor (MIF) is a ubiquitously expressed, predominantly cytoplasmic protein that has been implicated in the regulation of cell growth, development and many acute as well as chronic inflammatory diseases (Lue et al., 2002; Mitchell, 2004). A search for intracellular MIF-binding partners by the yeast two-hybrid system yielded Jab1/CSN5 as MIF interacting protein (Kleemann et al., 2000). MIF binds to the metalloprotease MPN domain of Jab1/CSN5 and inhibits Jab1/CSN5 function by preventing it from interacting with other cellular proteins. Recent studies point to a regulatory role of MIF on the UPS (Nemajerova et al., 2007b) suggesting that MIF controls proteasomal activity via inhibiting the deneddylating activity of Jab1/CSN5. Nonetheless, despite this recent progress in understanding MIF-mediated signaling pathways, the molecular modes of MIF action and the functional partner(s) underlying its role in protein degradation and intracellular regulatory systems (specially the UPS and ERAD) remain unclear. By using a systematic approach the aim of this study was to identify and characterize of new MIF interacting partners and to reveal the relevance of these interactions for cellular functions.

2. ABBREVIATIONS

aa	Amino acid(s)
Amp	Ampicillin
AMSH	associated molecule with the SH3 domain of STAM
AP-1	Activator protein 1
APS	Ammonium persulphate
ATP	Adenosine 5'-triphosphate
bp	Base pair
BSA	Bovine serum albumin
°C	Degree Celsius
cDNA	Complementary DNA
CHAPS	3-[(3-Cholamidopropyl)-dimethyl-ammonio] – propanesulfonate
COX-2	Cyclooxygenase-2
COP	Constitutive photomorphogenesis
cPLA2	cytosolic phospholipase A2
CXCR2	CXC chemokine receptor 2
CXXS	Cys-Xaa-Xaa-Cys motif
DAPI	4', 6'-diamino-2-phenylindole, dihydrochloride
DCME	L-dopachrome methylester
DMEM	Dulbecco's Minimal Essential Medium
DMSO	Dimethyl sulfoxide
DNA	Deoxyribonucleic acid
DNase	Deoxyribonuclease
dNTPs	2'-deoxynucleoside-5'-triphosphates
ds	Double strand
DTT	Dithiothreitol
DUB	Deubiquitinase
E. coli	*Escherichia coli*
ECL	Enhanced chemiluminescence
et al.	and others
EDTA	Ethylene diamine tetraacetic acid
ERAD	Endoplasmic reticulum associated degradation

ERK1/2	Extracellular signal-regulated kinases
FCS	Fetal calf serum
FLAG	N-DYKDDDDK-C (octapeptide)
FRET	Fluorescence Resonance Energy Transfer
g	gram or gravity, depending on the context
GST	Glutathione S-Transferase
HEPES	4-(2-hydroxyethyl)-1-piperazineethanesulfonic acid
HIF-1	Hypoxia inducible transcription factor 1
His	Histidine
HRP	Horse radish peroxidase
IPTG	Isopropyl β-D-thiogalactopyranoside
IEF	Isoelectric focusing
JAB1	Jun-activation domain-binding protein 1
JNK	c-Jun N-terminal kinase
kb	Kilo base pair.
kD	Kilo Dalton
LB	Luria Bertani medium
LPS	Lipopolysaccharide
M	Molar
MALDI MS	Matrix-assisted laser desorption ionization MS
MAPK	Mitogen-activated protein kinase
mg	Milligram
MES	Morpholinoethane sulfonic acid
MIF	Macrophage migration inhibitory factor
min	Minute
ml	Milliliter
mol	Mol
MOPS	3-(N-Morpholino)-propanesulfonic acid
mRNA	*messenger* RNA
MW	Molecular weight
n	nano (10^{-9})
NaCl	Sodium chloride
NCBI	National Center for Biotechnology Information
NHS	Normal horse serum

NP-40	Nonidet P-40
PAG	Proliferation associated-gene
PAGE	Polyacrylamide gel electrophoresis
PBS	Phosphate buffered saline
PCR	Polymerase chain reaction
PDGF	Platelet derived growth factor
PFA	Paraformaldehyde
PGE2	Prostaglandin E2
Pgk-1	Phosphoglycerate kinase 1
pH	-log c[H^+]
PMSF	Phenylmethylsulfonyl fluoride
PVDF	Polyvinylidenfluorid
RISC	RNA-induced silencing complex
RNA	Ribonucleic acid
RNAi	RNA interference
RNase	Ribonuclease
rpm	Revolutions per minute
RP S19	Ribosomal protein S19
RT	Room temperature
SCF	Skp1-Cullin-F-box protein
SDS	Sodium dodecylsulphate
sec	Second
siRNA	short interfering RNA
shRNA	short hairpin RNA
ss	single strand
STAM	signal transducing adaptor molecule
TAE	Tris-acetate-EDTA
TAP	Tandem affinity purification
TBE	Tris-borate-EDTA
TE	Tris-EDTA
TEMED	N-N'-N'-Tetramethylendiamin
TLR	Toll like receptor
TNF-α	Tumor necrosis factor alpha
Tris	Tris (hydroxymethyl)-amino-methane

U	Unit
UPS	Ubiquitin proteasome system
USP15	Ubiquitin specific proteinase 15
UV	Ultraviolet
V	Volt
VCP	Valosin-containing protein
Vh	Volt hour
v/v	Volume per volume
w/v	Weight per volume
wt	wild type
µ	Micro
µg	Microgram
µl	Microliter
µM	Micromolar

3. MATERIALS

3.1. Chemicals

Acetic acid	Merck, Darmstadt
Acrylamide 30%	Roth, Karlsruhe
Agarose	Invitrogen, Karlsruhe
Bacto-Tryptone	BD Bioscience, Sparks
Bacto-yeast extract	BD Bioscience, Sparks
Biotin	Sigma-Aldrich, Steinheim
Bromophenol blue sodium salt	Sigma-Aldrich, Steinheim
Calcium chloride	Merck, Darmstadt
CHAPS	AppliChem, Darmstadt
Chloroform	Merck, Darmstadt
Brilliant Blue G-Colloidal Concentrate	Sigma-Aldrich, Steinheim
Dexamethasone	Sigma Aldrich, Steinheim
2'-Deoxynucleoside 5'-triphosphate	Gibco, Neu-Isenburg
Dimethyl sulfoxide	Merck, Darmstadt
di-potassium hydrogen phosphate	Merck, Darmstadt
di-sodium hydrogen phosphate	Merck, Darmstadt
1,4-Dithiothreitol	Roche, Mannheim
Ethanol	Sigma-Aldrich, Steinheim
Ethidiumbromide	Roth, Karlsruhe
Ethylene diaminetetraacetic acid disodium salt	Merck, Darmstadt
Formamide	Merck, Darmstadt
Geneticin	Invitrogen, Karlsruhe
Glutathione	Amersham, Freiburg
Glycerol	Merck, Darmstadt
Glycine	Sigma-Aldrich, Steinheim
Guanidine hydrochloride	Sigma-Aldrich, Steinheim
4-(2-hydroxyethyl)-1-piperazineethanesulfonic acid	Roth, Karlsruhe
Igepal CA-630 (NP-40)	Sigma-Aldrich, Steinheim
Isopropylthio-β-D-galactoside	Serva, Heidelberg
Iodoacetamide	Bio-Rad, München

Imidazole	Fluka, Steinheim
Leupeptin	Sigma-Aldrich, Steinheim
Lipopolysaccharide	Sigma-Aldrich, Steinheim
Magnesium chloride	Merck, Darmstadt
Magnesium sulfate	Sigma-Aldrich, Steinheim
Mangan chloride	Merck, Darmstadt
β-Mercaptoethanol	AppliChem, Darmstadt
Methanol	Sigma-Aldrich, Steinheim
MG132 (proteasome inhibitor)	Calbiochem, Germany
Morpholinoethane sulfonic acid	Serva, Heidelberg
3-(N-Morpholino)-propanesulfonic acid	Serva, Heidelberg
Non-fat dry milk	Bio-Rad, München
Paraformaldehyde	Merck, Darmstadt
Phenylmethylsulfonyl fluoride	Sigma-Aldrich, Steinheim
Ponceau S	Roth, Karlsruhe
Potassium chloride	Merck, Darmstadt
Rotiphorese Gel 30	Roth, Karlsruhe
Sodium acetate	Roth, Karlsruhe
Sodium azide	Merck, Darmstadt
Sodium chloride	Sigma-Aldrich, Steinheim
Sodium citrate	Merck, Darmstadt
Sodium carbonate	Roth, Karlsruhe
Sodium dodecyl sulfate	Merck, Darmstadt
Sodium periodate	Sigma-Aldrich, Steinheim
Sodium thiosulfate	Roth, Karlsruhe
N,N,N',N'-Tetramethylethylenediamin	Roth, Karlsruhe
Tris(hydroxymethyl)aminomethane	Roth, Karlsruhe
Triton X-100	Sigma-Aldrich, Steinheim
Trypan blue	Gibco, USA
Tween-20	Roth, Karlsruhe
Urea	Merck, Darmstadt
Zeocin	Invitrogen, Karlsruhe

3.2. Enzymes

Taq Polymerase	Promega, Mannheim
T4 DNA Polymerase	Promega, Mannheim
EcoRI	Promega, Mannheim
XhoI	Promega, Mannheim
NdeI	Promega, Mannheim
BglII	Promega, Mannheim
HindIII	Promega, Mannheim
T4 DNA Ligase	Promega, Mannheim
DNase	Promega, Mannheim
RNase	Promega, Mannheim
TEV protease	Invitrogen, Germany

3.3. Antibodies

Antibody	**Manufacturer**	**Dilution**
Primary antibodies		
Rabbit α-rat MIF	(Kim, 2003)	1:20,000
Mouse α-MIF	Picower Institute, Manhasset, NY	1:200
Mouse α-RP S19	University of Rome, Italy	1:500
α-GST-HRP	Amersham, Freiberg	1:5,000
Rabbit α-Jab-1	Santa Cruz, USA	1:500
α-Biotin-HRP	Amersham, Freiburg	1:1,500
Mouse α-VCP	ABR, USA	1:1,000
Rabbit α-VCP	Santa Cruz, USA	1:200
Goat α-Pgk-1	Santa Cruz, USA	1:200
Goat α-Fetuin	Santa Cruz,USA	1:200
Mouse FLAGM2	Sigma, Stenheim	1:10,000
α –His-HRP	Sigma, Stenheim	1: 8,000
Mouse α-p-Akt	Cell Signalling, USA	1:1,000
Rabbit α-Akt	Santa Cruz, USA	1:500
Rabbit α-Ubiquitin	Santa Cruz, USA	1:500
Rabbit α-RPN11	Biomol, Hamburg	1:1,000
Rabbit α-CSN1	Biomol, Hamburg	1:1,000
Mouse α-Myc (9E10)	Santa Cruz, USA	1:3,000
Rabbit α-Iκβα	Santa Cruz, USA	1:500

Rabbit α-Cullin1	Abcam, UK	1:250
Rabbit α-Nedd8	Axxora, USA	1:500
Rabbit α-peroxiredoxin-1	Abcam, UK	1:500

Secondary antibodies

Goat α-rabbit-HRP	ICN, Ohio, USA	1:10,000
Donkey α-rabbit IgG-Cy3	Chemicon, Hampshire, UK	1:1,000
Donkey α-mouse IgG-FITC	Dianova, Hamburg	1:1,000
Donkey α-goat IgG	Santa Cruz, USA	1:1,000
Rabbit α-mouse IgG	Cell Signaling , USA	1:100

3.4. Cells

NIH 3T3 (mouse fibroblasts)	(Research group of Dr.O. Eickelberg, Giessen, Germany)
HEK 293T (human epithelial kidney cells)	(Research group of Prof. T. Chakraborty, Giessen, Germany)
264.7 RAW macrophages (mouse macrophage cells)	(Cell Lines Service, Eppelheim, Germany)
HeLa (human cervical carcinoma cells)	(Research group of Prof. T. Chakraborty, Giessen, Germany)

3.5. Recombinant proteins

Human MIF	produced in own laboratory
His-VCP	produced in own laboratory
GST-Jab1/CSN5	produced in own laboratory
Mouse PDGF	R&D Bioscience, Germany
Mouse and Human TNFα	eBioscience, Germany
Ubiquitin chains (Ub2-7), K48-linked	Biomol, Hamburg

3.6. Kits

Bradford kit	Roth, GmbH, Karlsruhe
Gel Extraction Kit	Qiagen, Hilden
Maxiprep Plasmid Purification Kit	Genomed GmbH, Löhne
Miniprep Kit	Genomed GmbH, Löhne
PCR Purification Kit	Qiagen, Hilden
Silver staining Kit	Invitrogen, Karlsruhe
QIAX II DNA extraction Kit	Qiagen, Hilden
FLAG purification Kit	Sigma, Steinheim

3.7. Cell Culture Media and Antibiotics

Ampicillin sodium salt	Ratiopharm, Ulm
Kanamycin sodium salt	Ratiopharm, Ulm
Bovine serum albumin	Invitrogen, Karlsruhe
Dulbecco's Minimal Essential Medium	PAA Laboratories, Cölbe
Fetal calf serum	Invitrogen, Karlsruhe
L-Glutamine	PAA Laboratories, Cölbe
MEM Non Essential Amino Acids	PAA Laboratories, Cölbe
Penicillin/Streptomycin	PAA Laboratories, Cölbe
RPMI 1640 medium	PAA Laboratories, Cölbe
Trypsin	PAA Laboratories, Cölbe
Ultrasaline A	PAA Laboratories, Cölbe
Optimem-serum free	Invitrogen, Karlsruhe

3.8. Equipment

Biofuge Fresco	Heraeus, Hanau
Cell culture incubator	Binder, Tullingen
Clean bench	BDK, Sonnenbühl-Genkingen
Confocal laser scanning microscope TCS SP2	Leica, Wetzlar
Easypet 4420 Pipette	Eppendorf, Hamburg
Electronic balance SPB50	Ohaus, Giessen
Gel Jet Imager 2000	Intas, Göttingen

Heater Block DB-2A	Techne, Cambridge, UK
Horizontal Mini Electrophoresis System	PEQLAB, Erlangen
Microwave oven	Samsung, Schwalbach
Mini centrifuge Galaxy	VWR International
Mini-Rocker Shaker MR-1	PEQLAB, Erlangen
Fluorescence microscope	Carl Zeiss, Jena
PCR system	Biozyme, Oldendor
Potter S homogenizer	B. Braun, Melsungen
Power supply units	Keutz, Reiskirchen
Pre-Cast Gel System	Invitrogen, Karlsruhe
SDS gel electrophoresis chambers	Invitrogen, Karlsruhe
Semi-dry-electroblotter	PEQLAB, Erlangen
Vertical electrophoresis system	PEQLAB, Erlangen
Ultrasonic homogenizer	Bandelin, Berlin
Ultrospec 2100 pro	Biochrom, Cambridge,UK
2D-PAGE system	BioRad, München

3.9. Miscellaneous

Bio-Rad Protein Assay	BioRad, München
Complete Freund's adjuvant	Sigma-Aldrich, Steinheim
Carrier ampholytes	BioRad, Hercules, CA
DNA High and Low Mass Ladder	Invitrogen, Karlsruhe
DNA Ladder (100bp and 1kb)	Promega, Mannheim
DAPI	Vector, Burlingame,USA
Enhanced chemiluminescence (ECL) reagents	Amersham, Freiburg,
Fugene Transfection Reagent	Roche, Mannheim
Glutathione Sepharose 4B	Amersham, Freiburg
Hoechst 33342	Sigma-Aldrich, Steinheim
Hybond ECL nitrocellulose membrane	Amersham, Freiburg
IPG Strips (11 cm)	BioRad, München
Lipofectamine 2000	Invitrogen, Carlsbad
NAP^{TM}-5 Sephadex G-25 column	Amersham, Freiburg
Ni-Agarose Beads	Novagen, Germany

NuPAGE 4-12% Novex Bis-Tris gel	Invitrogen, Karlsruhe
Protein size markers	Invitrogen, Karlsruhe
PVDF membrane	Millipor, Germany
Sterile plastic ware for cell culture	Sarstedt, Nümbrecht
Streptavidine beads	Novagen, Darmstadt
SYBR Green I Nucleic Acid Gel Stain	Roche Diagnostics, Mannheim
Sephacryl S-200 column 10/30 HR column	Pharmacia, Germany
Transwell filter system	Corning, Schiphol, NL
X-ray Hyperfilm	Amersham, Freiburg

3.10. Bacterial strains

E.coli DH5α, *E.coli* XL1-Blue, *E.coli* BL21 (DE3)

3.11. Expression constructs

1. pCMV-MIF (produced in own laboratory)
2. pN3-CTB-MIF (produced in own laboratory)
3. pBudCE4.1-birA (produced in own laboratory)
2. pET28$^{a\,(+)}$ His-VCP (Dr. P.Colleman, The Babraham Institute, Cambridge)
3. pFLAG-CMV6-VCP (Prof. M Tagaya, Tokyo University, Japan)
4. pFLAG-CMV-N (aa 1–198), ND1 (aa 1–470), D1 (aa 199–470), and D2 (aa 471–806) domains of VCP (Dr. S. Fang, Maryland University, Biotechnology Institute)
5. pCIneoJab1/CSN5 (Prof. J. Bernhagen, Univerity of Aachen, Germany)
6. pcDNA3-Jab1/CSN5 (Prof. J. Bernhagen, Univerity of Aachen, Germany)
7. pCMV.HA-Ubiquitin (Dr. R. Bohmann, University of Rochester, NY, USA)
8. pGEX-4T$_1$-Jab1/CSN5 (Prof. J Bernhagen, Univerity of Aachen, Germany)
9. pcDNA3-HA/Jab1 deletion mutants, 1-110, 110-191, and 1-191 (Prof. S. Jaewhan, Sungkyunkwan University, Korea).
10. pSUPER vector (Prof. M. Eilers , Marburg University, Germany*)*

3.12. siRNAs

1. Negative control (Cat#:AM4621), Applied Biosystems, Darmstadt
2. VCP (Cat#: AM16708), Applied Biosystems, Darmstadt
3. Jab1/CSN5 (target sequence: GCUCAGAGUAUCGAUGAAAtt), Applied Biosystems, Darmstadt
4. CSN1 (target sequence: GAACCUUUAACGUGGACAUtt), Applied Biosystems, Darmstadt
5. UPS 15 (target sequence: GCACGUGAUUAUUCCUGUUtt), Applied Biosystems, Darmstadt

3.13. Oligonucleotides cloned into pSUPER vector

Oligonucleotides were purchased from Sigma (Steinheim, Germany). The 19mer target sequences are underlined. Scrambled (scr.) oligonucleotides were cloned to pSuper vector as a control.

Table II: 64mer oliginucleotides cloned to pSUPER vector for MIF, VCP and Jab1/CSN5

Name	Sequence
MIF forward	5'-GATCCCC**CCGCAACTACAGTAAGCTG**TTCAAGAGA**CAGCTTACTGTAGTTGCGG**TTTTTGGAAA -3'
MIF reverse	5'AGCTTTTCCAAAAA**CCGCAACTACAGTAAGCTG**TCTCTTGAA**CAGCTTACTGTAGTTGCGG**GGG-3'
MIF scr.forward	5'-GATCCCC**GCCAACATCGACATATCGG**TTCAAGAGA**CCGATATGTCGATGTTGGC**TTTTTGGAAA-3'
MIF scr.reverse	5'AGCTTTTCCAAAAA**GCCAACATCGACATATCGG**TCTCTTGAA**CCGATATGTCGATGTTGGC**GGG-3'
VCP forward	5'-GATCCCC**GGGCACATGTGATTGTTAT**TTCAAGAGA**ATAACAATCACATGTGCCC**TTTTTGGAAA-3'
VCP reverse	5'AGCTTTTCCAAAAA**GGGCACATGTGATTGTTAT**TCTCTTGAA**ATAACAATCACATGTGCCC**GGG-3'
VCP scr.forward	5'-GATCCCC**GATCGGTATTAGCAGCTAG**TTCAAGAGA**CTAGCTGCTAATACCGATC**TTTTTGGAAA-3'
VCP scr.reverse	5'AGCTTTTCCAAAAA**GATCGGTATTAGCAGCTAG**TCTCTTGAA**CTAGCTGCTAATACCGATC**GGG-3'
Jab1/CSN5 forward	5'-GATCCCC**GCTCAGAGTATCGATGAAA**TTCAAGAGA**TTTCATCGATACTCTGAGC**TTTTTGGAAA-3'
Jab1/CSN5 reverse	5'AGCTTTTCCAAAAA**GCTCAGAGTATCGATGAAA**TCTCTTGAA**TTTCATCGATACTCTGAGC**GGG-3'
Jab1/CSN5 scr.forward	5'-GATCCCC**CGTGACTGAAGATAGACGA**TTCAAGAGA**TCGTCTATCTTCAGTCACG**TTTTTGGAAA-3'
Jab1/CSN5 scr.reverse	5'AGCTTTTCCAAAAA**CGTGACTGAAGATAGACGA**TCTCTTGAA**TCGTCTATCTTCAGTCACG**GGG-3'

4. METHODS

4.1. Cell culture techniques

4.1.1. Cell lines and cell culture

NIH 3T3 (mouse fibroblasts), HEK 293T (human epithelial kidney cell), 264.7 RAW (mouse monocyte-macrophage cell) and HeLa (human cervical carcinoma cell) lines were used for the studies. Cells were cultured in Dulbecco's modified Eagle's medium (DMEM), containing 2 mM glutamine supplemented with 10% heat-inactivated fetal calf serum, 100 U/ml penicillin/streptomycin, 2.7% ultrasaline A and grown in an incubator under 5% CO_2 atmosphere at 37°C. Cells were allowed to grow until 80-90% confluency, washed twice with PBS and then splitted at a ratio of up to 1:8 every 2 to 4 days by means of detachment using 1 ml Trypsin/EDTA (0.5 g/L Trypsin, 0.2 g/L EDTA) per 75 cm^2 culture flask. Incubation time was 2-3 minutes at 37°C. Trypsin was then inhibited by adding 7 ml DMEM medium containing 10% FCS, subsequently cells were collected by centrifugation (500 x g for 10 minutes at RT). The resulting cell pellet was resuspended in medium and seeded in new culture flasks.

4.1.2. Cell counting and cell viability assessment

The trypan blue dye was used to determine the number of viable cells present in a cell suspension. Cells were harvested and 20 µl of the cell suspension was mixed with a volume (20 µl) of a 0.08% dye solution. The cell suspension was transferred to the edge of the hematcytometer and allowed to spread evenly. Viable cells possess intact cell membranes that exclude trypan blue and therefore unstained, whereas nonviable cells reveal characteristic blue cytoplasm. The cell concentration was calculated as cell number per ml: cell number / number of squares x 2 x 10^4.

4.1.3. Cell freezing and thawing

The cell suspension was diluted 1:1 with freshly prepared freezing medium (70% DMEM, 10% FCS and 20% DMSO). For freezing, cells were first incubated at -80ºC overnight and then store in liquid nitrogen. To thaw the cells, a vial was transfered to an incubator (37ºC) for 2 minutes and then plated directly with the fresh medium.

4.1.4. Transfection

Transfection means the introduction of foreign material into eukaryotic cells. It typically involves the opening of transient pores or 'holes' in the cell plasma membrane to allow the uptake of molecules, such as supercoiled plasmid DNA or siRNA constructs. In this study, three transfection types were used as described below.

4.1.4.1. Transient transfection

Cells were seeded in 6-well plates one day before transfection at a density of 2 x 10^5 cells and transiently transfected with 1 µg of expression plasmid using FuGene 6 (Roche) according to the product manual. 0.5 µg of DNA per construct in double tranfections and 0.33 µg of DNA per construct in triple transfections were used. Total DNA/well was kept constant at 1 µg. 24h after transfection gene expression was assayed by immunoblotting.

4.1.4.2. Stable transfection

For stable transfection pBudCE4.1-birA and pN3-CTB-MIF were linearized with Xho I and EcoRI, respectively, and transfected, alone or combined (pBudCE4.1-birA) into NIH 3T3 cells using Lipofectamine (Invitrogen) following the manufacturer's instructions. Antibiotic selection started with 800 µg/ml Geneticin (for pN3-CTB-MIF) and 600 µg/ml Zeocin (for pBudCE4.1-birA) and was gradually reduced in three steps after 4 weeks up to 100 µg/ml Geneticin and 150 µg/ml Zeocin. Clones were checked by immunobloting with rabbit anti-rat-MIF antiserum and streptavidin HRP conjugate for expression of a biotinylated 22 kDa MIF fusion protein. After five to eight weeks clones were isolated using small sterile filter discs soaked in trypsin solution. The highest efficiency of biotinylation was achieved with the addition of 0.1 mg/ml of biotin to the medium.One clone with strong expression of the MIF fusion protein and one control clone expressing birA only were cultured in DMEM supplemented with 10% FCS, biotin (0.1 mg/L), Geniticin (100 µg/ml) and Zeocin (150 µg/ml) at 37°C.

4.1.4.3. siRNA transfection

For transient knockdown, cells were seeded in 6-well plates at 30-50 % confluency 24h before siRNA tranfection. Immediately before transfection, cells were washed twice and

then resuspended in OptiMEM serum free medium (Invitrogen). Transfection of siRNA (100 pmol final concentration) was performed in Opti-MEM medium according to the manufacturer's protocol (Lipofectamine 2000, using 4µl transfection reagent/100 pmol siRNA). After 6h transfection, medium was replaced 6h later with serum containing DMEM and cell culture was continued for 72h.

4.1.5. Stimulation of cells with activators and inhibitors

TNF-α (10-100 ng/ml), LPS (10-100 ng/ml), MIF (50-100 ng/ml) and PDGF (10-50 ng/ml) were used for stimulation of cells and incubated for certain time points starting from 5 min to 1h. MG132 (50 µM) was used for 1h to block to proteasome activity.

4.1.6. AKT activation assays

1 x 10^6 NIH 3T3 fibroblasts were seeded in 24-well plates and incubated in DMEM medium containing 10% FCS for 24h. Medium was changed and cells were cultured in DMEM containing 0.5% FCS for 24h. rMIF in 20 mM sodium phosphate buffer, pH 7.2, was added to the cells at a final concentration of 50 ng/ml. As a negative control, cells were incubated with buffer, obtained from a batch of the final dialysis refolding buffer. As a positive control PDGF (20 ng/ml) was used. All additions were performed within the incubator to minimize temperature changes and all reagents added were pre-warmed. Incubations were stopped at the indicated times (0–60 min) by washing the cells twice with cold PBS. Then, cells were lysed with lysis buffer (PBS, pH 7.4, containing 1% NP-40, 0.5% sodium deoxycholate, 1 mM EDTA, 1 x proteinase inhibitor cocktail and 1 mM sodium orthovanadate). Cell lysates were prepared as described in section 4.2.1.

4.2. Protein-biochemical methods

4.2.1. Cell lysate preparation

Cells were grown in a 75 cm^2 culture flaks to 80% confluency, washed twice with ice-cold PBS and incubated on ice with 1 ml of lysis buffer (50 mM Tris-Cl pH 8.0, 150 mM NaCl, 1 mM EDTA, 1% NP-40, 1 µM leupeptin, 1 mM PMSF) for 15 min with occasional rocking. Cells were scraped out, transferred to an Eppendorf tube and disrupted by passage through a 21 Gauge needle, subjected to sonication (two 10 sec bursts at 200-300 W with a 10

sec cooling period in between) followed by centrifugation at 13,000 x g for 10 min at 4°C.

4.2.2. Protein concentration measurement (Bradford, 1976)

The Bradford dye assay was used to determine the concentration of proteins in a solution. The assay reagent was prepared by diluting 1 volume of the dye stock (Protein Assay, BioRad) with 4 volumes of distilled H_2O. The solution appears brown, and has a pH of 1.1. Bovine serum albumin (BSA) at concentrations of 0, 250, 500, 1000, 1500, 2000 µg/ml were used as standards. Both the standards and the samples were prepared in PBS and 1ml assay reagent was mixed with 20 µl sample or standard. After 5 min incubation time they were measured at 595 nm absorbance in a spectrophotometer.

4.2.3. Affinity purification

4.2.3.1. Purification and elution of biotin tagged protein

Biotinylated MIF (biotin.MIF) and associated components were purified from the NIH 3T3 cell lysate by affinity selection on a streptavidin agarose matrix. Cytoplasmic extracts (prepared as described in 4.2.1) from cells expressing biotin.MIF and biotin ligase birA or birA only were incubated with 50 µl streptavidin-agarose beads (Novagen) for 1.5h at room temperature by rotating wheel. Following incubation, beads were washed three times with lysis buffer. Between washing steps, beads were pelleted by centrifugation and bound proteins were eluted by boiling for 10 min in 1 x SDS sample buffer (62.5 mM Tris pH 6.8, 2% SDS, 5% glycerol, 0.3% bromophenol blue, 0.9% (v/v) β-mercaptoethanol), separated on a 4-12 % NuPAGE Bis-Tris gel (Invitrogen).

4.2.3.2. TEV-protease digestion on strepavidin beads

In order to remove the biotin tag from Biotin.MIF, proteins were eluted from the streptavidin beads by incubation with Tobacco Etch Virus (TEV) protease that recognizes the seven specific amino acid sequences Glu-X-X-Tyr-X-Gln-Ser. Following affinity purification with streptavidin beads, 150 µl TEV digestion buffer (Invitrogen, prepared according to the manufacturer protocol) was incubated with beads for 1h at 30°C by rotation. Following TEV digestion, beads were collected by centrifugation and the supernatant containing cleaved MIF and potential MIF partners was transferred to a new Eppendorf tube. To increase the protein

concentration, TEV eluates from 3 experiments were combined and protein from 450 µl eluate was precipitated with cold acetone (four times sample volume) overnight at -20ºC. Precipitated proteins were separated by 1D- and 2D-SDS-PAGE analysis.

4.2.4. 1D-SDS polyacrylamide gel electrophoresis

Discontinuous sodium-dodecyl-sulphate (SDS) polyacrylamide gel electrophoresis (Laemmli 1970) was performed to analyze protein expression in cell lysates. An 18% resolving gel solution (375 mM Tris-HCl pH 8.8, 0.1% SDS, 18% acrylamide, 0.05% APS, 0.05% TEMED) was poured into the assembled gel mold between two glass plates separated by 1 mm thick spacers leaving about 1 cm space for the stacking gel solution (125 mM Tris-HCl pH 6.8, 0.1% SDS, 4% acrylamide, 0.05% APS, 0.1% TEMED). Samples were prepared in 1 x SDS gel sample buffer (62.5 mM Tris pH 6.8, 2% SDS, 5% glycerol, 0.3% bromophenol blue, 0.9% (v/v) β-mercaptoethanol) and boiled for 5 min to denature the proteins. After polymerization of the stacking gel, the comb was removed and the gel mounted in the electrophoresis chamber. Electrode reservoirs were filled with 1x SDS electrophoresis buffer (25 mM Tris, 1.44% glycine, 0.1% SDS), the wells were cleaned and samples loaded. Electrophoresis was performed at 150 V constant. For immunoprecipitation, samples NuPAGE 4-12% precast gradient-gels were used, which were run in 1x MES buffer (50 mM MES, 50 mM Tris, 3.46 mM SDS, 1.025 mM EDTA) or 1x MOPS (50 mM MOPS, 50 mM Tris, 3.46 mM SDS, 1.025 mM EDTA) at constant 200 V for 1h.

4.2.5. 2D-SDS polyacrylamide gel electrophoresis

Proteins were resuspended in 130 µl of isoelectric focusing (IEF) sample rehydration buffer (8 M urea, 50 mM DTT, 4% CHAPS, 0.2% carrier ampholytes, 0.0002% Bromophenol Blue) at room tempature. After placing samples in a rehydration tray, linear strips (IPG Strips, BioRad) were placed face down in a tray containing sample rehydration buffer. IEF strip rehyration was maintained at room temperature overnight. IEF was performed for a total of 10.000 Volt-hours with the voltage conditions: 250 V for 15 min, ramping to 4000 V over 2h and maintenance at 4000 V for about 3h. Prior to running the second dimension, the IEF strips were equilibrated for 15 min in fresh equilibration buffer 1 (6 M urea, 20% glycerol, 2% SDS, 0.375 M Tris-HCl pH 8.8, 130 mM DTT). For another 15 min, equilibration was performed in equilibration buffer 2 (6 M urea, 20% glycerol, 2% SDS, 0.375 M Tris-HCl pH 8.8, 135 mM iodoacetamide). The IEF strips were washed twice with 1x SDS electrophoresis buffer (see

4.2.4), placed on 12.5% SDS gel and sealed with a 3% agarose solution. Vertical second dimension was run at 160 V for 45 min.

4.2.6. Immunoblotting

Proteins were separated on 10-18% SDS-PAGE gel and electro-transferred to a nitrocellulose membrane at 100 mA per gel/membrane for 90 min using a semi-dry blot system. After blotting, the membrane was incubated in blocking buffer (5% (w/v) non-fat dry milk in PBS containing 0.1% Tween-20) for 1h at RT. Subsequently, the membrane was incubated overnight at RT or 4°C with the first antibody diluted in blocking buffer or as stated in the text. After washing (3 x 10 min) with PBS-Tween, the membrane was incubated for 1h at RT with a secondary antibody diluted in blocking buffer. Three washing steps (10 min each) with PBS-Tween were performed before the membrane was incubated with ECL Detection Reagent (1:1 mixture (v/v) of Reagent 1 and Reagent 2) for 60 sec. The membrane was wrapped in plastic foil, exposed to X-ray film for 1-15 min, which was subsequently developed.

4.2.7. SDS Gel Staining and protein analysis by MALDI

4.2.7.1. Silver staining

Proteins separated on 1D- and 2D-SDS polyacrylamide gel electrophoresis were subsequently silver stained as described previously with minor modifications (Blum et al., 1987). Gels were placed in a fixation solution (50% methanol, 10% acetic acid) for 1h and washed with 30% ethanol for 30 min to remove the acetic acid. Gels were then sensitized for 1 min with 0.02% sodium thiosulfate and rinsed three times with deionized water followed by incubation in silver staining solution (0.2% silver nitrate, 0.075% formaldehyde) for 30 min. Gels were then transferred into a new clean tray, rinsed twice with deionized water and placed in developing solution (6% sodium carbonate, 0.03% formaldehyde, 2% sodium thiosulfate from sensitizing solution) until protein spots were clearly visible. The development reaction was terminated by replacement of the developing solution with a stop solution (fixing solution) for 15 min. Stained gels were rinsed twice with deionized water for 15 min to remove remaining fixing solution and placed in a preserving solution (30% ethanol, 5% glycerol) for 2 h. For longer storage, gels were air-dried for 3 days using Gel Air Dryer (Sigma) with a cellophane support.

4.2.7.2. Coomassie blue staining

After electrophoresis gels were incubated in fixing solution (7% glacial acetic acid in 40% (v/v) methanol) for 1h. Staining solution was prepared by mixing 4 parts of 1x Brilliant Blue G-Colloidal with 1 part methanol and the gel was incubated overnight with gentle shaking. The gel was then rinsed for 60 sec with destaining solution I (10% acetic acid in 25% (v/v) methanol) to reduce the background staining, followed by destaining solution II (25% methanol) until a sufficient destaining level was reached. For documentation purposes the gel was scanned and dried between cellophane on air.

4.2.7.3. Image and protein analysis (MALDI)

After performing Coomassie and Silver staining, lanes from 1D-SDS-PAGE and spots from 2D-SDS-PAGE were cut into slices and proteins in all slices were digested with trypsin separately (Shevchenko et al., 1996). Extracted peptides were separated and sequenced by LC-coupled ESI-tandem MS on a Q-TOF instrument (Q-TOF ultima, Waters) under standard conditions. Proteins are identified by searching peptide fragment spectra against all entries in the NCBI database using MASCOT as search engine.

4.2.8. Co-immunoprecipitation

Cells were washed once in ice cold PBS and then lysed in 500 µl RIPA buffer containing proteinase inhibitors (50 mM Tris-HCl pH 7.5, 150 mM NaCl, 5 mM EDTA, 10 mM K_2HPO_4, 10% v/v glycerol, 1% NP–40, 0.15% SDS, 1 mM Na_3VO_4, 1 mM sodium molybdate, 20 mM NaF, 0.1 mM PMSF). Cells were disrupted by passing the cell suspension through 21-gauge needles and then centrifuged at 13,000 x g for 10 min at 4°C. After clearance of lysate, supernatants (500µl) were diluted (1:2) with IP (immunoprecipitation) buffer [20 mM Tris-HCl pH 8.0, 150 mM NaCl, 2 mM EDTA, 1% NP-40, 20 mM NaF, protease inhibitor cocktail (Sigma)] and incubated on a permanent rotator (10 r.p.m.) at 4°C for 3h to overnight with 30 µl Protein G-Sepharose 4B Fast Flow beads (Amersham) preloaded with respective antibodies (1-2 µg). Afterwards, the beads were washed three times with 1 ml ice-cold IP buffer. After complete removal of the buffer, immune complexes were collected by centrifugation, resuspended in 25 µl of 3x SDS–PAGE sample buffer and boiled for 10 min at 95°C. The IP samples were separated on a NuPAGE 4-12% Novex Bis-Tris gel (Invitrogen) and either blotted to Nitrocellulose membranes (Amersham) or stained with

colloidal Coomassie staining solution.

4.2.9. Expression and purification of recombinant GST-Jab1/CSN5 and His-VCP

Jab1/CSN5 was expressed as a fusion protein with GST tag and VCP was expressed as a fusion protein with His tag. For expression of GST-Jab1/CSN5 or His-VCP, *E. coli* BL21 DE3 competent cells were transformed with the pET28$^{a\ (+)}$ His-VCP or pGEX-4T$_1$-Jab1/CSN5 constructs (bacterial transformation described in section 4.3.1). Positive transformants were inoculated in to 5 ml 2YT medium (1.6% tryptone, 1% yeast extract and 1% NaCl, pH 7.0) containing antibiotics (kanamycin for His-VCP, ampicillin for GST-Jab1/CSN5) and cultured overnight in a shaker at 37°C.

To optimize expression conditions, 50 ml of 2YT medium (2% (w/v) bactotryptone, 1 % (w/v) yeast extract, 100 mM NaCl, pH 7.0) containing 50 µg/ml antibiotics (kanamycin or ampicillin) was inoculated with 500 µl of overnight culture. Cultures were kept at 37°C in a shaking incubator until OD_{600} = 0.5. The culture was split in two equal parts and 1 ml aliquot from each culture was saved and prepared for SDS-PAGE. One culture was induced by adding IPTG to a final concentration of 0.5 mM and incubation was continued at 37° with shaking. At different time points of induction (1, 2 and 3h), 1 ml from each culture were transferred to a microfuge tube, the OD_{600} was measured and each pellet was prepared for SDS-PAGE. The samples were mixed with 1x SDS sample buffer, boiled at 95°C for 3 min, stored on ice and then loaded onto 12.5 % SDS-PAGE. The gel was stained with Coomassie.

For large scale expression 5 ml of an overnight culture was inoculated into 400 ml 2YT medium (supplemented with 100 µg/ml ampicillin or kanamycin) and incubated at 37°C until an OD_{600} of 0.5 was reached. Expression was induced by adding IPTG to a final concentration of 0.5 mM and incubation was continued at 37°C for 3h. Cells were harvested by centrifugation at 3,000 x g at 4°C for 30 min. The supernatant was discarded and the cell pellet was resuspended in ice-cold PBS (50 µl PBS for each ml of culture). The cells were lysed by sonication (10 short burst of 10 sec followed by intervals of 30 sec for cooling) and a small aliquot was saved after this step. Cell lysates were treated with Triton X-100 to a final concentration of 1% and gently mixed for 30 min to solubilize the fusion protein. Centrifugation at 1200 x g for 10 min at 4°C removed the cell debris and the supernatant was transferred to a new tube. An aliquot of supernatant and pellet was saved for analysis by SDS-PAGE to identify the fraction that contains the fusion protein.

Supernatant contained His-VCP or GST-Jab1/CSN5 were further resuspended in lysis buffer (50 mM Tris-HCl, 1mM EDTA, 100 mM NaCl, pH 8.0), treated with 1mg/ml lysozyme and DNAase I for 30 min on ice. Lysed cells were centrifuged at 14,000 x g for 15 min at 4°C and the pellet containing mainly inclusion bodies was washed four times with lysis buffer. The resuspended inclusion body pellet was incubated with denaturation buffer (6 M guanidium hydrochloride, 10 mM DTT in PBS) at room temperature on a rotating plate for 30 min and centrifuged at 4°C at 12.000 rpm for 15 min. After incubation with denaturation buffer, the cleared lysate was dialyzed against PBS pH 7.8 containing 0.5 mM PMSF and 1 mM DTT for 4h. After dialysis, the cleared cell lysate incubated with 50% Ni-NTA slurry (1 ml bed volume for 10 ml lysate) at 4°C for 60 min. The matrix was then washed twice with 50 mM NaH_2PO_4 pH 8.0, 300 mM NaCl, and 20 mM imidazole. Bound protein was eluted with 50 mM Na_2HPO4, 300 mM NaCl, 250 mM imidazole, pH 8.0 and dialyzed against PBS pH 7.8 containing 0.5 mM PMSF and 1 mM DTT. The purity of the eluted protein was estimated by SDS-PAGE.

For the purification of GST-Jab1/CSN5, supernatant containing GST-Jab1/CSN5 was subjected to Glutathion Sepharose 4B chromatography at 4°C 2h. The matrix was washed twice with 5 bed volumes of PBS (140 mM NaCl, 2.7 mM KCl, 10 mM Na_2HPO_4, 1.8 mM KH_2PO4) and bound proteins were eluted with 10 mM Glutathione in 50 mM Tris-HCl pH 8.0 (GST-Jab1/CSN5 was purified by Suada Fröhlich and Dr. Jörg Klug).

4.2.10. *In vitro* pull-down assays

4.2.10.1. His-VCP pull-down

His-VCP (1 µg) was immobilized with 30 µl (50% slurry) of Ni-NTA beads by incubation at RT on a rotating wheel for 1h. In order to remove the unbound protein, beads were washed 3 x with PBS. Coated beads were incubated for 2h with increasing amounts of recombinant GST-Jab1/CSN5 (0.5, 1 and 2 µg respectively) on a rotating wheel for 2 h at 4°C in binding buffer containing 25 mM Tris-HCl pH 8.0, 200 mM KCl, 2 mM $MgCl_2$, 1 mM ATP, 1 mM dithiothreitol, 5% glycerol and 1% Triton X–100. As a control, uncoated Ni-NTA beads were incubated with 2 µg GST-Jab1/CSN5. After extensive washing with binding buffer, the beads were boiled in SDS sample buffer for 5 min. Proteins were resolved on SDS-PAGE and either stained with colloidal Coomassie or detected by immunoblotting.

4.2.10.2. GST-Jab1/CSN5 pull-down

1 µg of GST-Jab1/CSN5 was immobilized with 30 µl (50% slurry) of glutathione sepharose beads by incubation 500 µl PBS at RT on a rotating wheel for 1h. After 3x washing with PBS, beads were incubated with His-tagged VCP protein (0.5, 1 and 2 µg respectively) for 2h at 4°C in binding buffer (same as 4.2.11.1) on a rotating wheel for 2h at 4°C. As a control, His-VCP was incubated with uncoated glutathione beads. After extensive washing with binding buffer, GST-Jab1/CSN5 bound proteins were analyzed by immunoblotting.

For ubiquitin binding, GST-Jab1/CSN5 bound to glutathione sepharose beads was incubated with polyubiquitin chains (Ub2–7) in binding buffer (50 mM HEPES, pH 7.5, 150 mM NaCl, 5 mM EDTA, 1% Triton X) for 3h at 4°C. The beads were washed 3x with binding buffer and then boiled in SDS sample buffer for 5 min. Bound material was separated on SDS-PAGE, transferred to nitrocellulose membrane and subjected to immunoblotting.

4.3. Molecular biology methods

4.3.1. Preparation of competent *E. coli* and transformation

For the preparation of competent *E. coli* an inoculating loop was used to streak *E. coli* DH5α directly from a frozen glycerol stock onto an LB agar plate containing no antibiotics. The plate was incubated for 16h at 37°C. A single colony was picked and grown in 5 ml SOB medium overnight by shaking (235 rpm/min) at 37°C. 50 ml pre-warmed SOB medium (2% (w/v) bactotryptone or peptone, 0.5 % (w/v) yeast extract, 10 mM NaCl, 2.5 mM KCl) was inoculated with 0.5 ml from the overnight culture. The cells were grown for 2.5-3.0 h at 37°C under monitoring culture growth by measuring OD_{600} in a spectrophotometer every 20 min. When the culture had reached an OD of 0.45-0.50, the cells was incubated on ice for 20 min. Cells were harvested by centrifugation at 1075 x g for 15 min at 4°C and the supernatant was decanted. The cells were gently resuspended in 100 ml TFB buffer (10 mM MES, 45 mM $MnCl_2$, 10 mM $CaCl_2$, 100 mM KCl, pH 6.2) and incubated on ice for 10-15 min. After centrifugation at 1075 x g for 15 min at 4°C, the buffer was decanted. The cells were resuspended gently in 3.9 ml TFB buffer, 140 µl DMSO followed by 5 min incubation on ice. Then 140 µl of 1M DTT was added and incubation continued for 10 min before another 140 µl DMSO were added for 5 min. For transformation, 200 µl of competent cells were transferred to an Eppendorf tube and kept on ice. 3 to 7 µl of ligation reaction mixture containing 50 ng of plasmid were added to the competent cells and incubated on ice for 30

min. The tubes were transferred to a heat block preheated to 42°C for exactly 45 sec and then cooled on ice again. After 2 min of cooling 800 µl of warm (37°C) SOC medium (SOB medium containing 5 mM glucose) was added to each tube. Incubation for 60 min in a shaking incubator allowed the bacteria to recover and to establish antibiotic resistance. 200 µl of transformed compotent cells were plated onto 90 mm LB agar plates containing the appropriate antibiotic (50 µg/ml). The plates were stored at RT until the liquid had been absorbed. The plates were inverted and incubated at 37°C overnight. One colony was picked and inoculated in 5ml mini culture (SOB medium containing antibiotic).

4.3.2. Plasmid DNA isolation (mini and maxi bacterial culture preparation)

One colony was picked and used for inoculation of a 5 ml mini culture (SOB medium containing antibiotic). The bacterial culture was incubated overnight at 37°C in a shaking incubator. The Promega Minipreps DNA Purification Kit was used for the plasmid DNA isolation according to the manufacturer's recommendation. The standard method for the maxiprep isolation of plasmid DNA includes the same general strategy as the mini scale isolation. However, 200 ml medium containing antibiotic inoculated with plasmid-containing colonies are incubated in a 37°C shaker for 12-16h. Isolated plasmid DNA was subjected to agarose gel electrophoresis.

4.3.3. Agarose gel electrophoresis

Agarose gels (0.8% to 1%) were routinely used to separate DNA fragments ranging in size from 100 bp to 10 kb. The appropriate amount of agarose was dissolved in 1x TAE buffer (40 mM Tris-acetate, 1 mM EDTA pH 8.0) by heating in a microwave oven. After cooling the gel solution was poured into a gel mold, a comb was inserted in order to generate wells for the samples. After 30-40 min the comb was removed, and the gel mounted into an electrophoresis chamber filled with 1x TAE buffer. DNA samples and size marker were mixed with an appropriate volume of DNA sample buffer (3% glycerol, 0.025% bromophenol blue, 0.025% xylene cyanol FF) and pipetted into the wells. The gels were run at 100V (2-10V/cm gel) until the bromophenol blue and xylene cyanol dyes had migrated considerable distance through the gel. After electrophoresis, the gel was immersed in 1x SYBR green staining solution (1:10,000 in 1x TAE buffer) and incubated for 30 min at RT with gentle shaking. Occasionally, SYBR green staining solution was added directly to the sample. The gel was then examined on a 305 nm UV transilluminator and photographed using a gel documentation

system.

4.3.4. Cloning of pN3-CTB-MIF

The MIF cDNA was produced by standard PCR (annealing temperature 52°C for 5 cycles and 56°C for 30 cycles) using the upstream primer C**GAATTC**CGCCACCATGCCTATGTTCATCGTG (Eco RI site in bold) and the downstream primer GAT**GTCGAC**AGCGAAGGTGGAACCGTTCCA (Sal I site in bold) and a pGEX-4T-2 MIF full length expression construct (unpublished) as template. The method of de Boer et al. (de Boer et al., 2003) was employed using the modified tagging construct pN3-CTB developed by Rischitor et al. (Rischitor, 2005). pN3-CTB-MIF was constructed by ligating the Eco RI/Sal I restricted PCR fragment into pN3-CTB opened with Eco RI and Sal I (pN3-CTB-MIF was cloned by Tamara Henke and Dr.Jörg Klug).

4.3.5. Cloning of inserts into the shRNA vector pSUPER

For the knockdown of MIF the shRNA vector pSUPER was used (Brummelkamp et al., 2002). It is based on the RNA polymerase III H1 RNA-gene promoter that is directing the expression of a short hairpin RNA. This shRNA is cleaved by the nuclear RNase Drosha, processed by the cytoplasmic RNase Dicer and eventually incorporated into the RNA-induced silencing complex RISC that is effecting gene specific silencing. The shRNA is defined by cloning a short insert obtained by annealing a pair of custom 64mer oligonucleotides (Sigma) that contains a unique 19-nt sequence derived from the MIF mRNA followed by a 9 bp spacer encoding the RNA hairpin and the reverse complement of the same 19-nt sequence (see Figure 6).

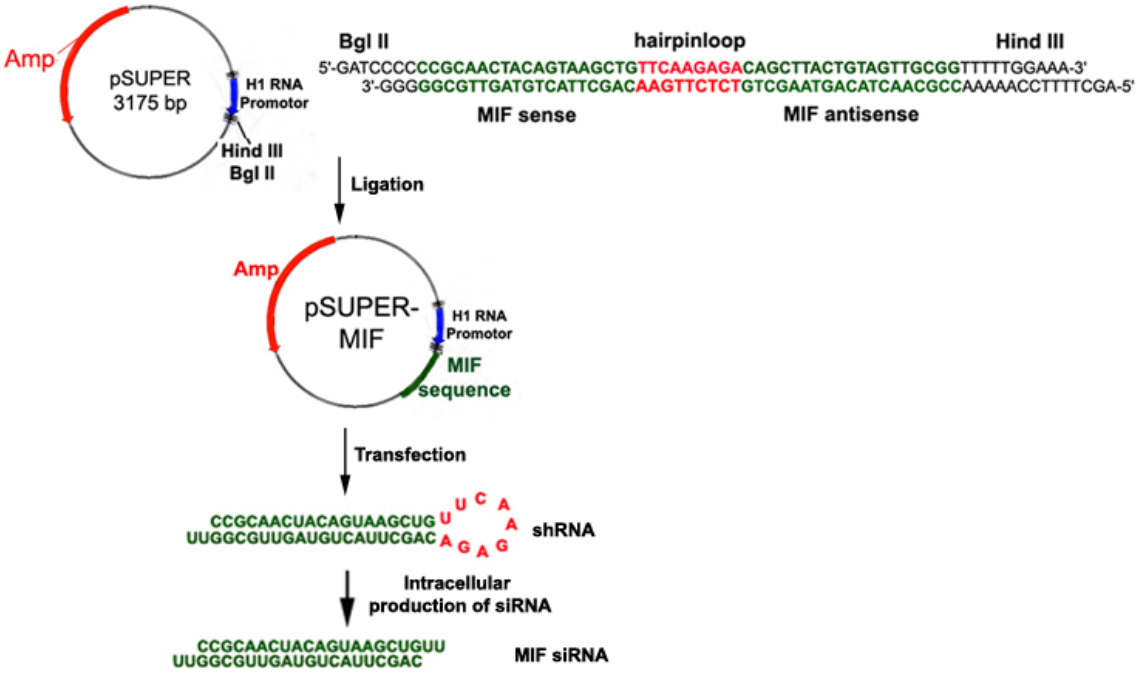

Figure 6: Strategy for cloning the MIF-specific pSUPER vector.

For an experiment utilizing a pSUPER vector general steps were followed as outlined below.

- Annealing of upper and lower strand of the insert
- Linearization of the pSUPER vector with Bgl II and Hind III
- Cloning of annealed oligos into the vector
- Transformation into bacteria, selection of insert containing clones, verification of the insert sequence by DNA sequencing using the T7 promoter primer (Seqlab, Göttingen) and purification of plasmid DNA suitable for transfections
- High efficinecy transfection of pSUPER-MIF into mammalian cells
- Assaying the knock-down effect on protein expression and/or mRNA level

4.3.5.1. Annealing of oligos

The 64mer oligonucleotides were obtained from Sigma and dissolved in Tris-EDTA, pH 8.0 at 100 pmol/µl. 20 µl of each oligonucleotide (approx. 20 µg), 10 µl 10x annealing buffer (100 mM Tris-HCl pH8.0, 10 mM EDTA, 300 mM KCl) and 50 µl water were mixed in a reaction tube. Ample Water was heated in a 500 ml beaker to boiling point, taken off the heat source, and the reaction tube was incubated in the hot water with the aid of a floatable

tube holder. When the water in the beaker had cooled down to room temperature dilutions of the annealed oligonucleotides were made (40 ng/µl and 4 ng/µl) and stored together with the stock solution at -20°C.

4.3.5.2. Ligation into pSUPER

20 µg pSUPER vector were digested with Hind III and Bgl II. The linearized vector was purified over a 1% agarose gel and extracted using a DNA gel purification kit. The ligation reaction was set up by mixing 1 µl pSuper (approx. 100 ng/µl), 2 µl of the annealed oligos (approx. 4 ng/µl), 5 µl of 2x T4 DNA ligase buffer, 1 µl H_2O and 1 µl T4 DNA ligase. Cloning controls included a ligation reaction without insert and a reaction without insert and ligase. Half of the ligation reaction was used to transform competent *E. coli* DH5α (see section 4.3.1). 5 ng of a standard plasmid vector were used as a transformation control.

Bacteria were plated on ampicillin-agar plates and grown overnight. Colonies were picked and grown overnight in ampicilin containing LB medium. Clones were checked by digestion with Bgl II (the Bgl II site is destroyed in positive clones) (Figure 7, lane 4-7). One or two positive clones confirmed by DNA sequencing (Seqlab, Göttingen).

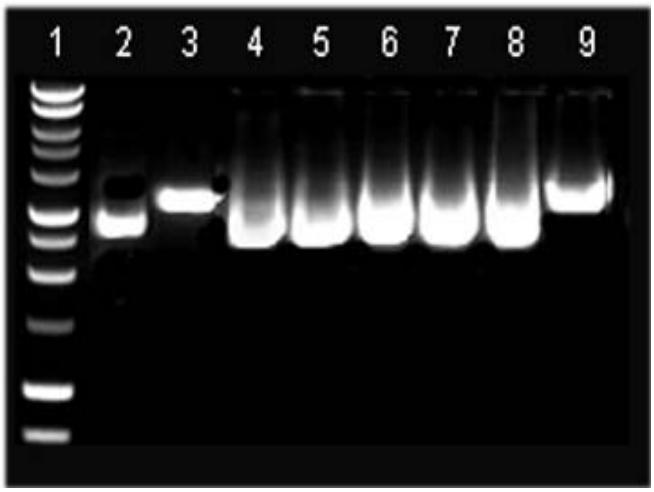

Figure 7: Determination of positive clones digested with Bgl II
Lane 1: 1kb marker; Lane 2: pSUPER vector; Lane 3: pSuper vector digested with Bgl II; Lane 4-5; Lane 6-7: positive clones uncut by Bgl II; and Lane 8-9: negative clone were shown on 1% agarose gel.

4.3.5.3. Transfection of mammalian cells

One day before transfection, cells were cultured in Dulbecco's modified Eagle's medium (DMEM) supplemented with 10% fetal bovine serum so that they reached 50-70% confluence at the time of transfection. Transient transfection was performed with Lipofectamine 2000 (Invitrogen) according to the prodecure recommended by the supplier. The level of suppression of our target gene was measured by immunoblotting (Figure 8).

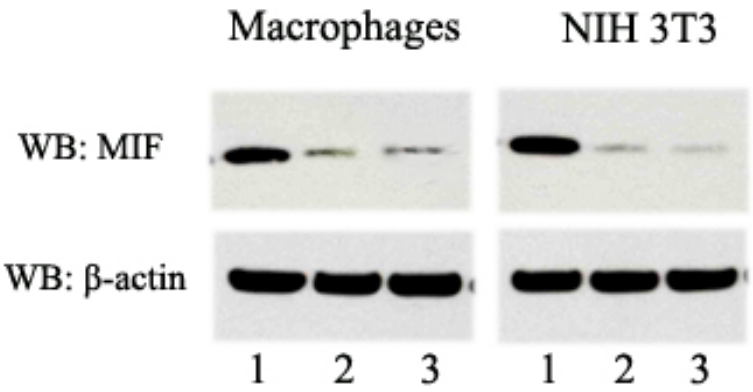

Figure 8: Knockdown of MIF in 264.7 RAW macrophages and NIH 3T3 cells.
264.7 RAW macrophages and NIH 3T3 cells were transfected with either pSUPER vector (lane 1) or MIFsi (lane 2 and 3) for 48 hours. Cytoplasmic fractions were analyzed by Western blotting. The blot was stripped and reprobed with β-actin antibody as a loading control.

4.4. Gel filtration assay

HEK 293T lysates (containing 3 mg of protein) were separated by gel filtration chromatography using a Sephacryl S-200 column 10/30 HR column (Pharmacia) in a buffer containing 25 mM HEPES pH 7.5, 150 mM NaCl, 1 mM EDTA, 1 mM dithiothreitol, 1 mM ATP and 10% glycerol. One-milliliter fractions were collected, 300µl was precipitated with acetone, resolved in SDS containing sample buffer and examined by SDS-PAGE.

4.5. Double immunofluorescence

Immunofluorescence staining was performed on NIH 3T3 mouse fibroblasts to investigate the cellular localization of endogenous MIF and its associated proteins. Cells were cultured on cover slips until 80% confluency. After washing once with 1x PBS, cells were fixed with ice-cold methanol for 10 min at RT. Blocking was performed with 5% BSA and

10% NHS for 1h at RT. Double immunostaining with rabbit anti-VCP (1:400), rabbit anti-Pgk-1, rabbit anti-RPS 19, followed by donkey anti-rabbit IgG conjugated with Cy3 (1:1,000), and mouse anti-MIF (1:200) followed by donkey anti-mouse IgG conjugated with FITC (1:1,000) was performed. Primary antibodies were incubated over night at 4°C and secondary antibodies were incubated for 1h at RT. After incubating with primary and secondary antibodies, three wash steps were performed using 1x PBS. Images were acquired with a confocal laser scanning microscope.

4.6. FRET (Fluorescence Resonance Energy Transfer)

FRET was combined with CLSM (confocal laser scanning microscopy) and double-labeling indirect immunofluorescence to identify associations of proteins. Cells were cultured on the 24-well slides and transfected with different plasmids using the same transfection procedure as described above. Twenty-four hours after transfection, cells were fixed with 4% PFA for 15 min. Jab1/CSN5 and VCP were labeled using conventional indirect double-labeling immunofluorescence technique (anti-Jab1/CSN5 from rabbit labeled with Cy5-conjugated secondary reagent, anti-VCP antibody labeled with Cy3- conjugated secondary reagent). Both primary antibodies were applied simultaneously and incubated overnight at 4^{o}C. After a washing step, Cy3-conjugated donkey anti-mouse-Ig was applied for 1h and after a second washing step the cells were incubated with Cy5-conjugated F(ab')2 donkey anti-rabbit-Ig. For control of the species-specificity of the secondary reagents, only the anti-Jab1/CSN5 antibody and both secondary antibodies were applied. FRET was quantified by the acceptor photobleaching method using a CLSM. FRET was quantified by measurement of the fluorescence intensity in the Cy3 (donor) channel in the bleached area before and after bleaching. Cy5 (acceptor) was bleached 5 times (1.28 s/scan) with highest possible zoom (X32) with 100% laser power of the 633 nm HeNe laser line. To assess changes during the measurements that were not due to FRET, four rectangular region of interest (ROI) of approximately the same size as the bleached area were measured adjacent to the bleached area. The CLSM settings were as follows: Detection of Cy3: 52% laser power at 543 nm, detection at 555–620 nm; Cy5: 20% laser power at 633 nm, detection at 639–738 nm. FRET efficiency was shown as change of fluorescence intensity (absolute increase in fluorescence (ΔIF)=I_{DA}-I_{DB}, where I_{DA} is the donor intensity after bleaching and I_{DB} the donor intensity before bleaching.

Differences among experimental group and control group in the FRET-experiments were analyzed with the Kruskal-Wallis test followed by the Mann-Whitney test using SPSS software, version 12 (SPSS GmbH Software, Munich, Germany), with $p \leq 0.05$ being considered as significant and $p \leq 0.01$ as highly significant.

5. RESULTS

5.1. Identification of MIF interacting proteins

In order to identify new MIF interacting proteins, the following strategy was implied. Initially, a recently developed in vivo biotin tagging method followed by affinity based chromatography methodologies was applied for purification of new MIF interacting proteins. Subsequently, these proteins were identified by MALDI-TOF mass spectrometry. Finally, the putative interaction between MIF and associated proteins were confirmed by Fluorescence Resonance Energy Transfer (FRET), co-immunoprecipitation and *in vitro* pull-down experiments.

5.1.1. *In vivo* biotinylation of MIF

In vivo biotinylation of MIF was conducted by stable cotransfection of pN3-CTB-MIF and BirA enzyme expression vector pBudCE4.1-birA into NIH 3T3 cells. The principle of the specific *in vivo* biotinylation of MIF in NIH 3T3 cells is shown in Figure 9.

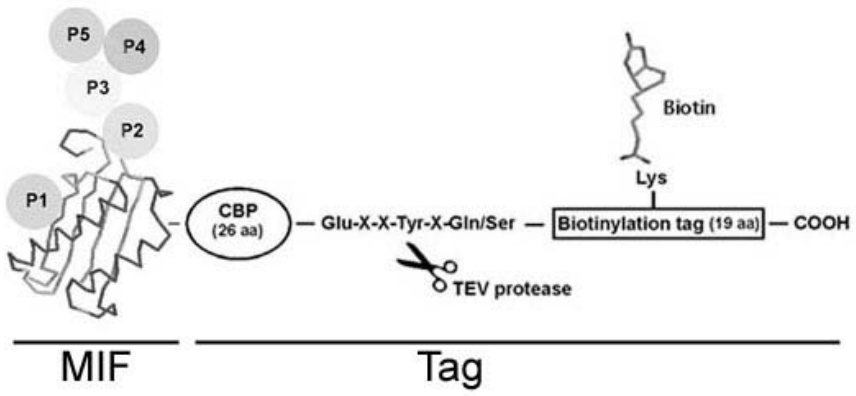

Figure 9: Principle of the *in vivo* biotinylation of MIF stably expressed in NIH 3T3 cells. The MIF backbone is shown together with bound hypothetical interaction partners P1, P2, P3 etc. The tag contains a calmodulin binding peptide (CBP), a TEV protease cleavage site and a biotinylation tag. The bacterial biotin ligase birA required for biotinylation of the tag is stably co-expressed in the same NIH 3T3 clone.

The efficiency of biotinylation of the MIF target protein by stable coexpression of the *Bir*A enzyme *in vivo* was evaluated by SDS-PAGE analysis (Figure 10). Protein extracts from cells expressing tagged MIF and BirA *(*double transfectant) or BirA only (single transfectant)

were applied to 18% SDS gel, transferred to nitrocellulose membranes and probed with anti-MIF antibody (Figure 10, upper panel) to detect endogenous and biotinylated MIF (biotin.MIF). The same membrane was then stripped and reprobed with streptavidin-HRP (Figure 10, lower panel) to detect biotin.MIF. In case of double transfectants, Western blots using the anti-MIF antibody detect a 22 kDa slower-migrating biotin.MIF (Figure 10, upper panel, lane 2, arrow) and 12 kDa endogenous MIF (Figure 10, upper panel, lane 2, and star) in cell extracts. For single transfectants, only the endogenous MIF was detected (Figure 10, lane 3). Next, the successful biotinylation of MIF was confirmed by biotin detection in cell lysates. An increased signal was only detectable in double transfectants (Figure 10, lower panel, lane 2, arrow). No biotinylation was detected in the single transfectant (Figure 10, lower panel, lane 3). These data demonstrate the efficient biotinylation of MIF by BirA in NIH 3T3 cells.

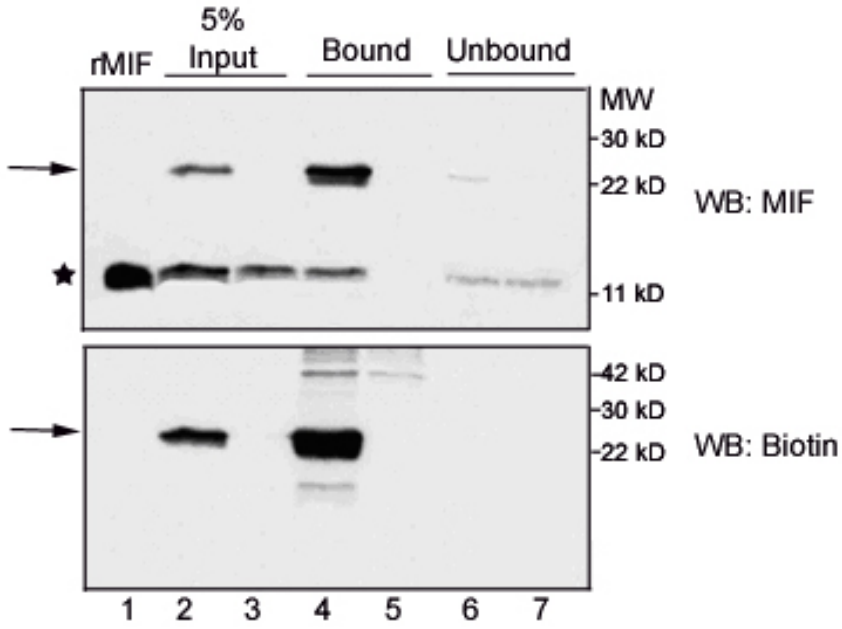

Figure 10: Efficiency of biotinylation of MIF and single-step purification.
Cytoplasmic extracts from NIH 3T3 cells expressing biotin.MIF and biotin ligase birA (lanes 2, 4 and 6) or birA only (lanes 3, 5 and 7) were incubated with streptavidin agarose beads. Supernatants (unbound, lanes 6 and 7), bound proteins (lanes 4 and 5) and input lysate (lanes 2 and 3) were subjected to 18% SDS-PAGE followed by Western blotting (WB) for MIF (upper blot) and biotin (lower blot). Endogenous and recombinant MIF (rMIF) are indicated by asterisk and biotin.MIF is marked by arrows.

Following the confirmation of the successfull *in vivo* biotin tagging, biotin.MIF together with its associated binding proteins were purified from cell extracts by affinity chromatography using streptavidin coated beads. The optimum binding ratio of total protein extracts to streptavidin beads was determined using different amounts of protein extracts and

different incubation times (data not shown). The complete protein extracts (Figure 10, lane 2 and 3), bound material (Figure 10, lane 4 and 5) and unbound supernatants (Figure 10, lane 6 and 7) were analyzed by Western blotting. As shown in figure 10 (lower panel) a number of endogenously biotinylated proteins bound to streptavidin-HRP were also visible. Taken together, these results indicate that biotin.MIF is efficiently recovered from cell extracts by single-step affinity purification.

5.1.2. Purification and visualization of MIF associated proteins

After single step purification by direct binding to streptavidin beads, biotin.MIF was almost completely recovered from extracts as hardly any biotin.MIF could be detected in supernatants. The efficiency of affinity purification was further confirmed by Coomassie blue stained gel of the cell extracts binding to streptavidin beads (Figure 11). Biotin.MIF was only detected in the double transfectants. The presence of biotin.MIF was confirmed by excising the respective band from the gel. The staining pattern of the lane with the co-purified proteins together with biotin.MIF (Figure 11, lane 3) was significantly different to that observed with the background binding (lane 4) indicating enrichment of MIF interacting partners copurified with biotin.MIF. The entire lane from double and single transfectant was excised and divided into corresponding gel pieces subsequently analyzed by mass spectrometry.

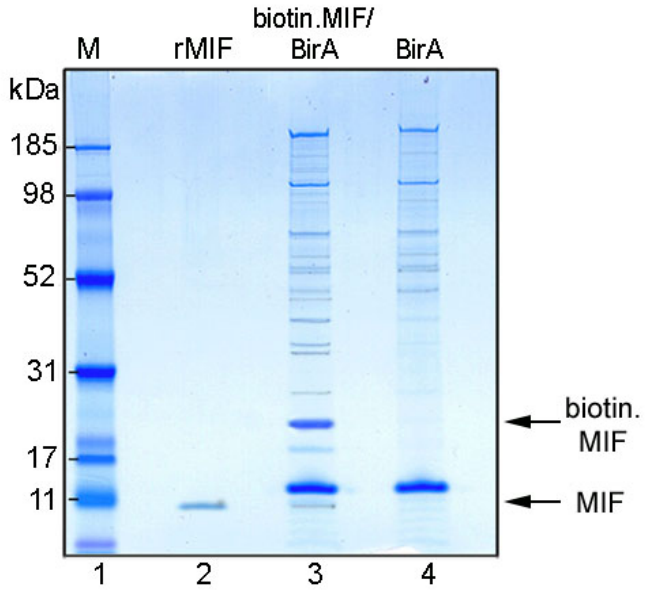

Figure 11: Coomassie blue stained gel of purified biotin.MIF and its interacting partners. Proteins from biotin.MIF and birA (lane 3) and birA only (lane 4) expressing cells bound to streptavidin beads. M = molecular weight marker (lane 1), rMIF (lane 2).

After mass spectrometry analysis, proteins identified in both transfectants (Figure 11, lane 3 and lane 4) were compared to each other. Because biotin.MIF and co-purified proteins (lane 3) may compete for binding with the endogenously expressed biotinylated proteins observed in lane 4, the proteins in single transfectant (Figure 11, lane 4) were further excluded. The proteins identified from 1D-SDS-PAGE, their identities, corresponding NCBI accession numbers and matched peptide fragments are listed in Table III. Identified proteins included the well known MIF binding partners peroxiredoxin–1 and RPS 19 (unpublished data).

As it is possible that addition of the peptide tag or biotinylation may affect the properties of the tagged MIF, it was tested whether biotin.MIF could still undergo protein–protein interactions with established MIF partners such as Jab1/CSN5, peroxiredoxin-1. After pull-down of biotin.MIF Jab1/CSN5, peroxiredoxin-1 (Prx-1) and RP S19 was found to be retrieved from cell extracts expressing biotin.MIF (Figure 12, lane 3), but not from extracts expressing BirA only (Figure 12, lane 4).

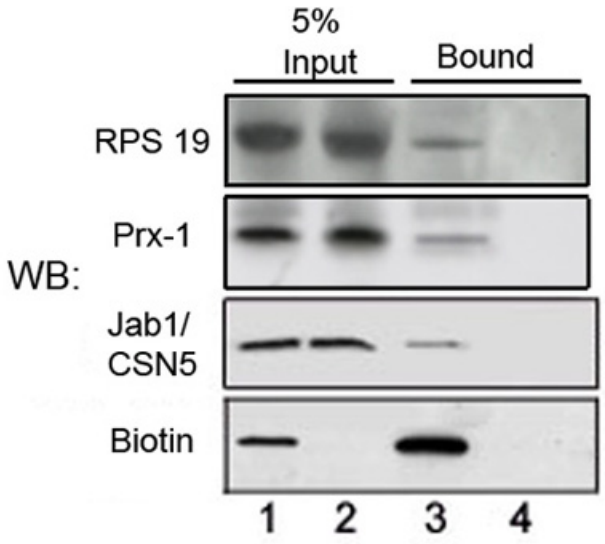

Figure 12: Single step biotin pull-down of MIF together with known interacting proteins. Cell extracts expressing biotinylated MIF and birA (lanes 1 and 3) and birA only (lanes 2 and 4) were incubated with streptavidin beads. Input (lanes 1 and 2) and bound proteins (lanes 3 and 4) were resolved on a 15% SDS gel and analyzed by immunoblotting using antibodies for Jab1/CSN5, peroxiredoxin-1 (Prx-1) and RPS 19 (upper panels) and biotin (lower panel).

5.1.3. TEV-digest on beads and 1D-SDS-PAGE

The specific TEV protease cleavage site present on the biotinylation tag (see figure 9) was used to cleave and elute the tagged protein complex from the streptavidin beads. Beads carrying protein complexes obtained from double and single transfected cells were washed and incubated with the TEV protease. In order to increase protein concentrations, TEV eluates from 3 experiments were combined and proteins subsequently precipitated with acetone. Proteins were separated by 1D-SDS-PAGE and stained with Coomassie blue (Figure 13).

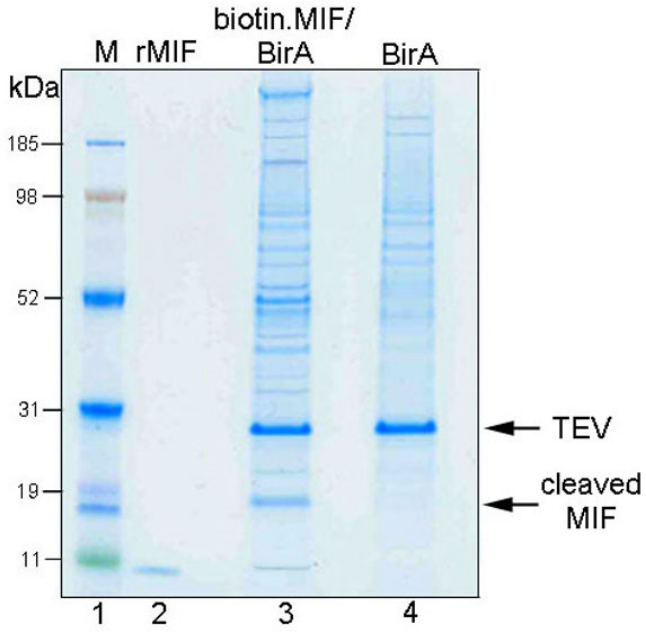

Figure 13: Coomassie blue stained gel of cytoplasmic extracts obtained after binding to streptavidin beads with subsequent elution of bound proteins by cleavage with TEV.
Lane 1: molecular weight marker, lane 2: rMIF, lane 3: eluted proteins from cells expressing biotin.MIF and BirA, lane 4: eluted proteins from cells expressing BirA only.

5.1.4. 2D-SDS-PAGE analysis of protein complexes obtained after TEV protease reaction

In order to obtain a better separation and resolution of purified proteins, TEV eluates from both double and single transfectants were applied to 2D-SDS-PAGE and stained with Silver staining (Figure 14). Proteins spots occurring only in double transfected cells were exzised from silver stained gels and subjected to in-gel trypsin digestion followed by MALDI-MS analysis. Proteins identified by peptide mass fingerprinting analysis are listed in table IV. A total of 30 gel spots were subjected to analysis. Amongst them 4 gene products were also found in 1D-SDS gel analysis of the single-step affinity purification (Figure 11 and table III).

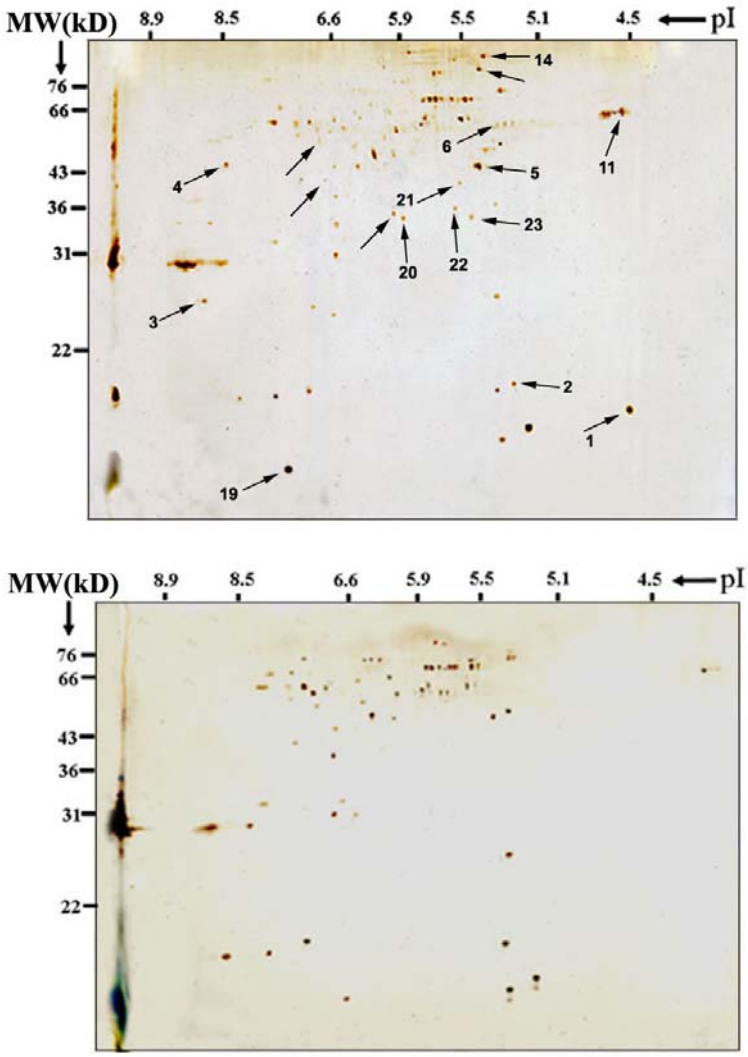

Figure 14: 2D-SDS-PAGE of proteins eluted after TEV protease treatment.
Protein spots from cells expressing biotinylated MIF and BirA (upper panel) were compared with spots from cells expressing BirA only (lower panel). Proteins that were found only in cells expressing biotinylated MIF and BirA were exzised from the gel, digested with trypsin, and identified by MALDI-MS and peptide mass fingerprinting analysis. The numbers in the upper panel refer to the list of identified proteins in table IV.

5.1.5. Co-immunoprecipitation of MIF interacting proteins from NIH 3T3 cells

To verify the *in vivo* biotin tagging approach, the results obtained by MALDI-TOF were reproved with an independent method, i.e. co-immunoprecipitation (co-IP). Peroxiredoxin-1, Fetuin, Pgk-1, RPS 19 and VCP were co-precipitated with MIF (Figure 15A). Extracts from mouse NIH 3T3 fibroblast cells were subjected to co-IP with a polyclonal rabbit anti-rat MIF antibody or with a rabbit control preimmune serum which were previously immobilized on protein G-Sepharose beads. The immune complexes were probed for Peroxiredoxin-1, VCP, Fetuin, RPS 19, Jab1/CSN5 and Pgk-1, stripped and reprobed for MIF

by Western blot analysis. As shown in Figure 15A, anti-MIF antibody efficiently precipitated MIF together with Peroxiredoxin-1, VCP, Fetuin, Pgk-1 and RPS 19 from NIH 3T3 cell lysates. Additionally, mouse and bovine Fetuin were precipitated with MIF (Figure 15B). Importantly, reverse co-IP with anti-RPS 19 antibody followed by anti-MIF Western blot analysis confirmed the interaction (Figure 15C). To further solidify the interaction between endogenous MIF and RPS 19 cell lysates were subjected to immunoprecipition with anti-mouse RPS 19 antibody and mouse Ig control antibody. Immunoprecipitates were analyzed by Western blotting using anti-MIF antibody.

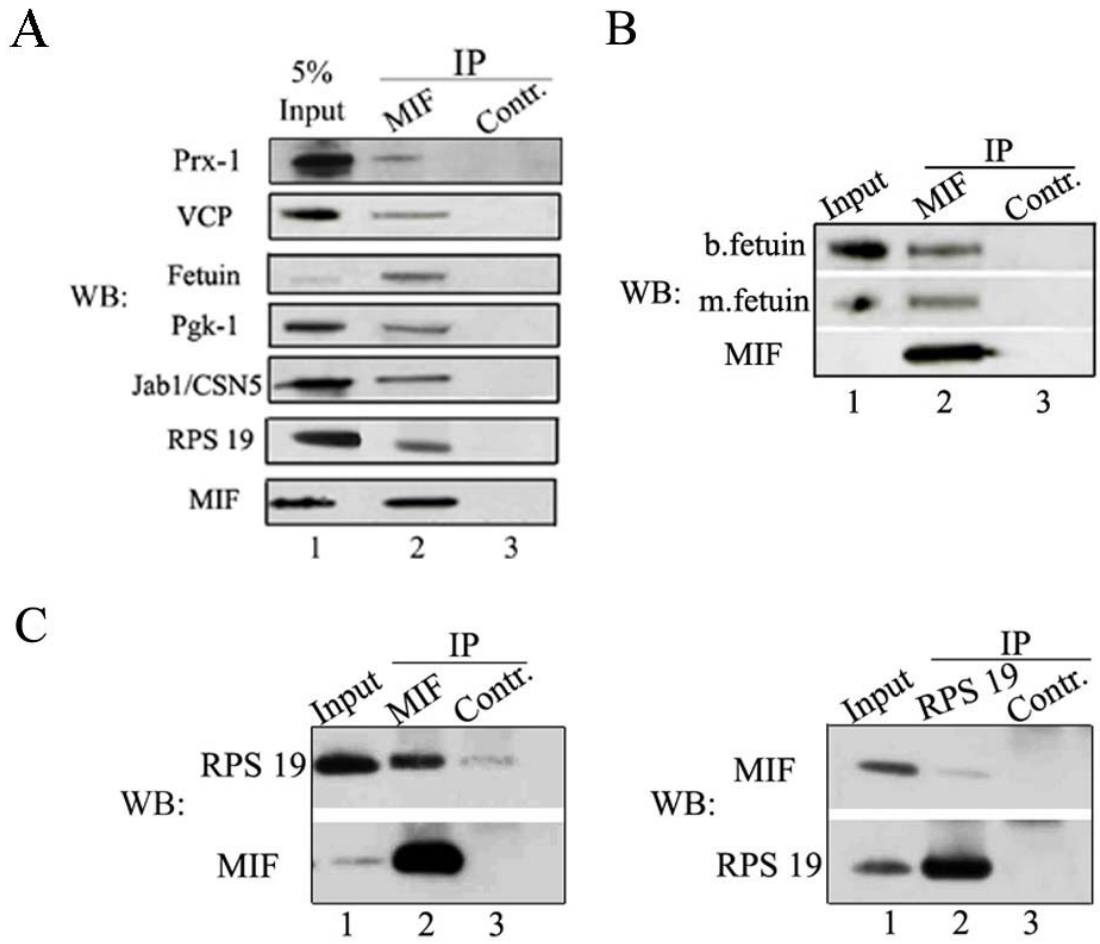

Figure 15: Interaction between endogenous MIF and its binding partners in NIH 3T3 cells. (A) Cell lysates were subjected to immunoprecipitation (IP) with either a rabbit anti-MIF antiserum (lane 2) or rabbit pre-immunserum (lane 3). Co-immunoprecipitated proteins were analyzed by Western blotting as indicated. **(B)** Mouse and bovine serum were assessed with anti-MIF (lane 2) and control (lane 3) IP. Immunoprecipitated proteins were detected with anti-fetuin antibody. **(C)** Interaction between MIF and RPS 19 was further confirmed by reciprocal IP with a monoclonal RP S19 antibody (right panel, lane 2) and isotype control antibody (right panel lane 3). The amount of input is 5% of cell lysate (lane 1).

5.1.6. Co-localization of MIF and its interacting partners

The interaction between MIF and its associated proteins was further confirmed by revealing a cytoplasmic co-localization of proteins with confocal microscopy (Figure 16).

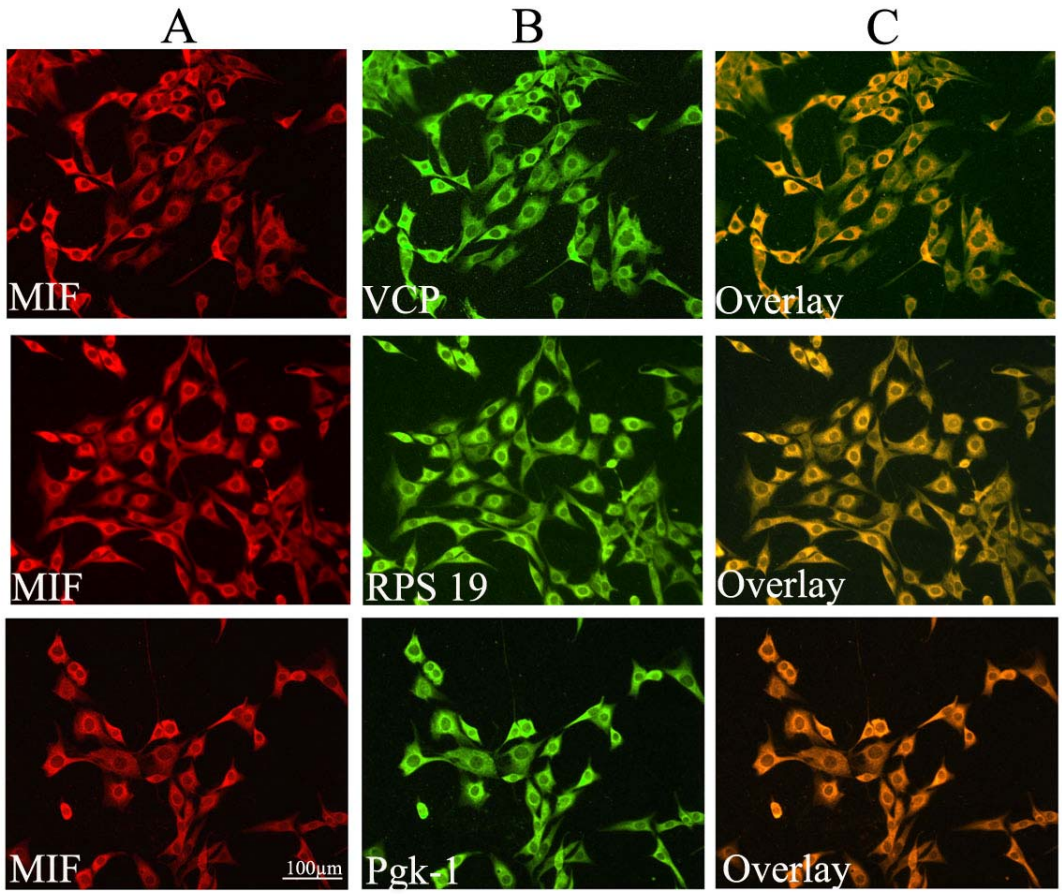

Figure 16: Co-localization of MIF and its interacting proteins in NIH 3T3 cells.
Cells were double immunostained using antibodies raised against MIF and VCP, RPS 19 or Pgk-1, respectively, followed by decoration with fluorescently labeled secondary antibodies. MIF is shown in red **(A),** interacting proteins in green **(B)** Regions with co-localized proteins appear orange in the overlay **(C).**

1D- and 2D-SDS-PAGE results indicate that the screening approach used in this study permits the identification of novel MIF interaction partners. A recent study has shown that MIF regulates the activity of SCF ubiquitin ligases, which are known to play a pivotal role in UPS (ubiquitin proteasome system) (Nemajerova et al., 2007a). Of note, VCP an important component of the UPS, was identified as a new MIF-binding partner in the 2D-SDS-PAGE analysis in this study with the highest peptide score. This prompted us to investigate the association of MIF and VCP further.

5.1.7. Characterization of protein domains involved in interaction between MIF and VCP

To investigate the binding domains involved in the interaction between MIF and VCP, the N-terminal domain (residues 1–202), D1 domain (residues 203–450), D2 domain (residues 451–807) and ND1 domain (residues 1–450) of VCP were co-expressed with MIF in NIH 3T3 cells, respectively. Cell lysates from transfected cells were subjected to MIF-IP and precipitated proteins were detected with an anti-FLAG antibody. However, none of the domains of VCP were precipitated together with MIF (Figure 17B).

Additionally, surface plasmon resonance analysis performed on a Biacore system with the purified recombinant proteins was applied to examine if the interaction between MIF and VCP is direct. However, the dissociation constant of formation of the MIF-VCP complex was not in the range that are commonly observed for protein-protein interactions (cooperation with Carlsson-Skwirut, C, Karolinska Institute, Sweden).

Furthermore, FRET (Fluorescence resonance energy transfer) was used to explore if the molecular proximity between MIF and VCP is closer than 10nm. Although both VCP and MIF were found in the cytoplasm, no significant FRET signal was detected. These results lead to the hypothesis that the interaction between MIF and VCP could be indirectly mediated by a linking cofactor. Amongst known MIF interacting proteins, a potential candidate is Jab1/CSN5. This factor is also involved in the UPS like VCP. To verify if Jab1/CSN5 may serve as a cofactor of VCP, full lenght VCP and its mutants carrying a FLAG tag (Figure 17A) were coexpressed together with wt-Jab1/CSN5 in NIH 3T3 cells. After Jab1/CSN5 pulldown (Figure 17C) only the ND1 domain (lane 11) and full lenght VCP (lane 12), but not the N-terminal domain, the D1 domain or the D2 domain were pulled down together with Jab1/CSN5.

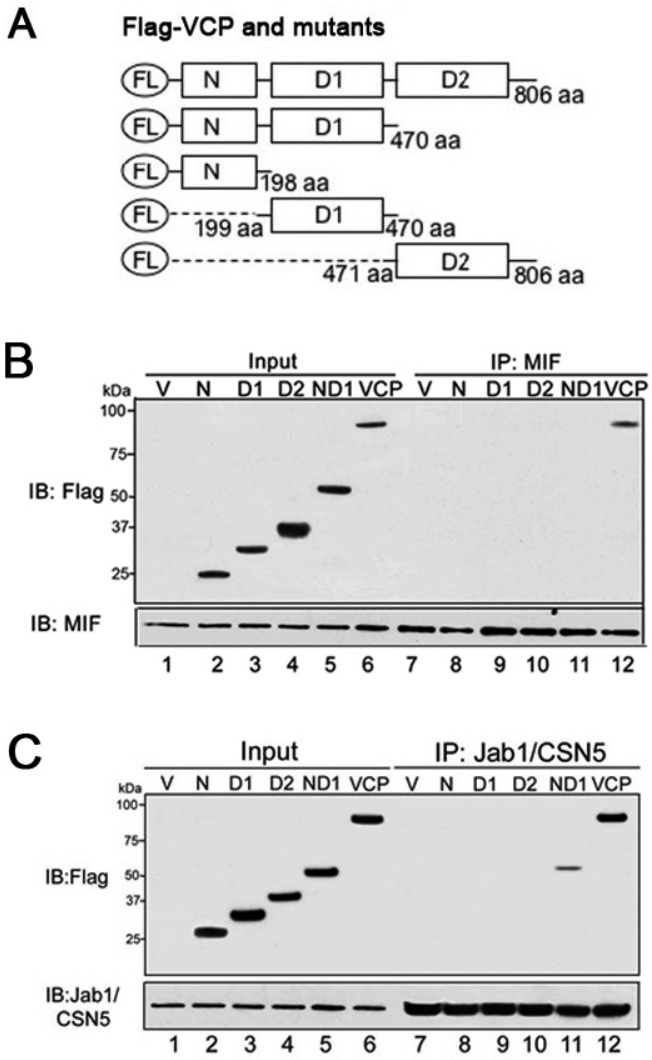

Figure 17: Interaction domains of VCP with MIF and Jab1/CSN5.
(A) Diagram displaying VCP and deletion constructs carrying N-terminal FLAG (FL) tag **(B+C)** Full length VCP or the N-terminal domain (residues 1–202), D1 domain (residues 203–450), D2 domain (residues 451–807) or ND1 domain (residues 1–450) of VCP were ectopically expressed as FLAG-tagged fusion proteins in NIH 3T3 cells. As a control, cells were transfected with the VCP expression vector (V). Simultaneously, MIF **(B)** and Jab1/CSN5 **(C)** were co-expressed ectopically. MIF and Jab1/CSN5 were pulled-down from supernatants of lysed cells using an anti-MIF and anti-Jab1/CSN5 antibodies (lane 7-12). Precipitated proteins were detected by IB with an anti-FLAG antibody (IP: MIF and IP: Jab1/CSN5; lane 7–12). Expression of FLAG, MIF and Jab1/CSN5 constructs in cell lysates was detected by immunoblotting (IB) (input; lanes 1–6).

5.2. MIF interacts with VCP via Jab1/CSN5

5.2.1. Jab1/CSN5 interacts with VCP *in vivo* and *in vitro*

The verification of specific and direct interaction between VCP and Jab1/CSN5 was determined by performing co-IP and *in vitro* pull-down experiments. Initially, the interaction of the endogenous partners with normal expression levels was investigated *in vivo*. Endogenous Jab1/CSN5–VCP complexes were precipitated from NIH 3T3 and HEK293T cells by using anti-Jab1/CSN5 (Figure18A, lane 2) and anti-VCP (Figure 18B, lane 2) antibodies. The cell lysates used for IP was analyzed for VCP and Jab1/CSN5 expression (Figure 18A and B, lane1). Using isotype control antibodies (Figure 18 A+B, lane 3) no co-precipitation was visible.

Furthermore, in order to confirm the interaction between VCP and Jab1/CSN5 ectopically, FLAG-VCP was expressed in NIH 3T3 cells (Figure 18C, lane 2). Cell lysates were prepared and incubated with monoclonal anti-FLAG M2 agarose gel. Precipitated proteins were analysed by Western blotting. As shown in Figure 18C, endogenous Jab1/CSN5 was pulled-down with FLAG-VCP (lane 4), whereas no precipitation of Jab1/CSN5 was observed when cells were transfected with VCP expression vector only (lane 3).

Moreover, *in vitro* pull-down assays were performed to examine a potential direct interaction between Jab1/CSN5 and VCP. For this purpose, increasing concentrations of His-VCP (Figure 18D, lane 1: 0.25 µg, lane 2: 0.50 µg, lane 3: 1 µg, lane 4: 2 µg) were incubated with 1µg of recombinant GST-Jab1/CSN5 immobilized on glutathion agarose beads. As a control, glutathion agarose was incubated with 2 µg of His-VCP (lane 5). After washing the beads, GST-Jab1/CSN5 bound proteins were detected by immunoblotting (Figure 18D). In this experiment, increasing amounts of His-VCP were copurified together with GST-Jab1/CSN5. However, His-VCP did not show unspecific affinity to glutathion. Taken together this suggests a direct interaction of both proteins *in vitro.*

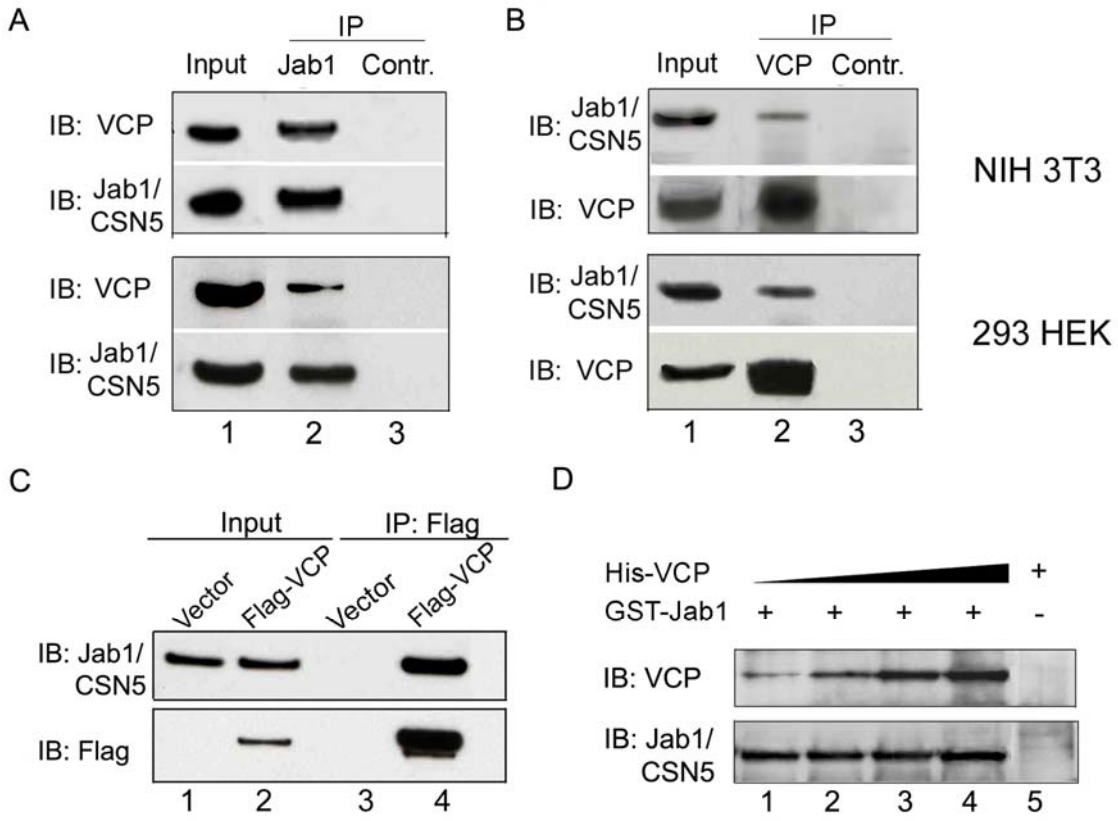

Figure 18: Interaction between Jab1/CSN5 and VCP *in vivo* and *in vitro*.
***(*A)** Lysates from NIH 3T3 and HEK293T cells were analyzed for VCP and Jab1/CSN5 expression by immunoblotting (IB) (input, lane 1). Respective cell lysates were used for immunoprecipitation (IP) with anti-Jab1/CSN5 antibody (lane 2) and isotype control antibody (control, lane 3) **(B)** Reciprocal IP was performed using anti-VCP antibody (lane 2) and isotype control IgG (lane 3). Immunoprecipitates were analyzed with anti-VCP and anti-Jab1/CSN5 antibodies by immunoblotting. **(C)** Jab1/CSN5 expression was analyzed in NIH 3T3 cells transfected with empty VCP expression vector (lane 1) or FLAG-VCP (lane 2). In the supernatant of lysed cells, FLAG-VCP (lane 4) was pulled-down using anti-FLAG antibody. Co-precipitated Jab1/CSN5 was detected by immunoblotting using specific antibody (lane 4). Transfection of empty VCP expression vector served as control for specificity of IP (lane 3). **(D)** His-VCP interacts with purified GST-Jab1/CSN5. Immobilized GST-Jab1/CSN5 was incubated with increasing amounts of purified His-VCP (lane 1-4). Binding of His-VCP to GST-Jab1/CSN5 was detected using anti-VCP antibody (lane 1-4, top). Equal amounts of GST-Jab1/CSN5 (1 µg) were used in the experiments (lane 1-4, bottom). As control, beads without bound GST-Jab1/CSN5 were incubated with 2 µg of His-VCP (lane 5). Input of His-VCP: 0.25 µg (lane 1); 0.5 µg (lane 2); 1 µg (lane 3); 2 µg (lane 4 and 5).

5.2.2. Domains involved in interaction between Jab1/CSN5 and VCP

Previous results in this study showed that Jab1/CSN5 binds to the ND1 domain of VCP (see 5.1.7, figure 17B). To further investigate the domains of Jab1/CSN5 essential for the interaction with VCP, FLAG-VCP, Myc-Jab1/CSN5 and Myc-Jab1/CSN5 deletion mutants (1–191, 1–110, 110–191) were coexpressed in HEK293T cells. A schematic illustration of Jab1/CSN5 and its deletion mutants is described in Figure 19A. Lysates of these transfected cells were prepared and further applied to FLAG-IP (Figure 19B). FLAG-VCP was pulled-down using an anti-FLAG antibody and co-precipitated Myc-Jab1/CSN5 and its deletion mutants were detected by immunoblotting using an anti-Myc antibody. Transfection of Myc-Jab1/CSN5 expression vector served as control for specificity of IP. Immunoprecipitation data indicated that wt-Jab1/CSN5 and its deletion mutants 1–110 and 1–191 bind to FLAG-VCP (Figure 19B, lanes 7, 8, 9), whereas the 110–191 deletion mutant is ineffective (Figure 19B, lane 10). This showed that full lenght Jab1/CSN5 and its 1–191 deletion mutant which harbors an intact Jab1/MPN/Mov34 metalloenzyme motif (MPN) interacts with VCP.

The JAMM motif of the MPN domain is required for the degradation of ubiquitin-proteasome substrates. A mutation of histidines to alanine in the predicted active site stabilized substrates of the ubiquitin pathway (Verma et al., 2002). Since the 110-191 domain of Jab1/CSN5 did not show any interaction, further studies were attempted to investigate whether VCP-Jab1/CSN5 interaction depends on the JAMM motif of Jab1/CSN5. For this purpose, a Myc tagged-JAMM mutant of Jab1/CSN5, in which a histidine residue is changed to alanine, was co-expressed with FLAG-VCP in HEK293T cells. Lysates of transfected cells were applied to Myc and FLAG-IP, respectively. As shown in Figure 19C, the Myc-JAMM mutant Jab1/CSN5 was pulled-down together with FLAG-VCP (Figure 19C, lane 4) and reciprocally, FLAG-VCP was pulled-down together with Myc-Jab1/CSN5 (Figure 19C, lane 8). Cell lysates used for IP experiments are shown in lane 1, 2 and 5, 6. Both FLAG and Myc pull-down assays showed that Jab1/CSN5–VCP interaction is independent of the JAMM motif (Figure 19C).

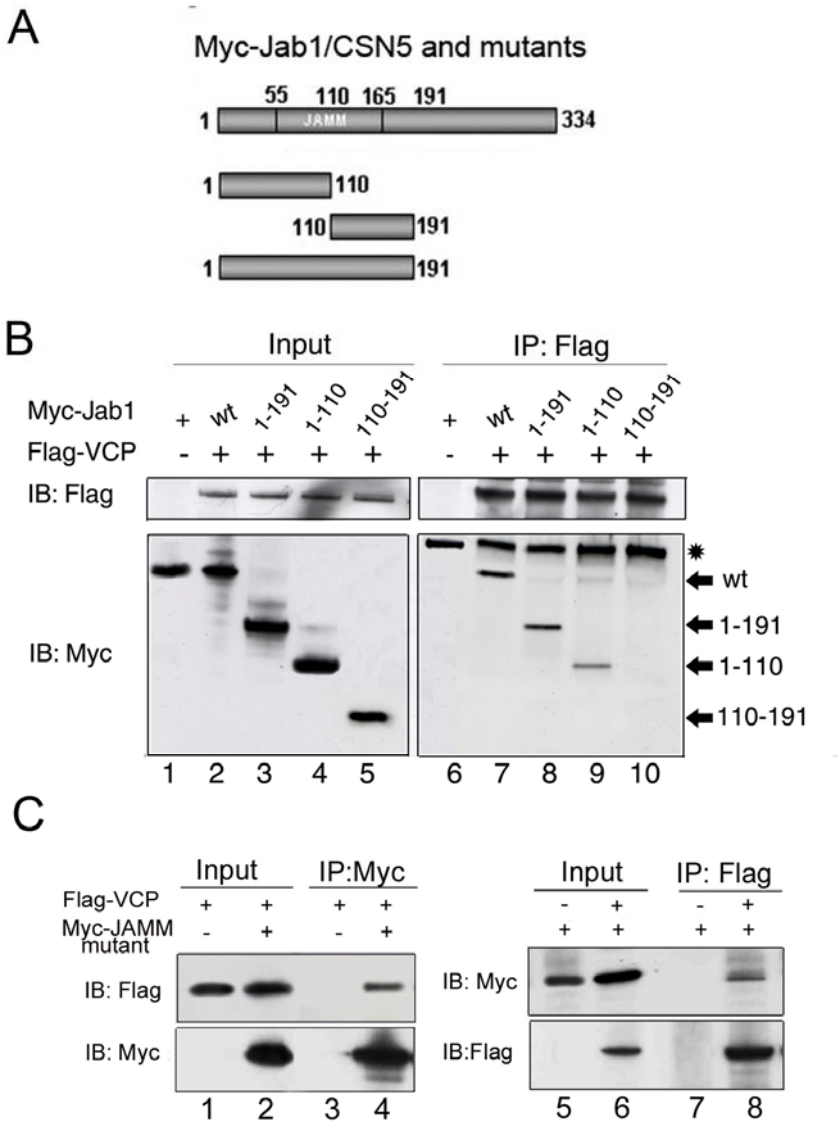

Figure 19: Domains of Jab1/CSN5 involved in interaction with VCP
(A) Schematic illustration of Jab1/CSN5 and its deletion mutants. **(B)** Interaction of FLAG-VCP with the N-terminal domain of Jab1/CSN5. The plasmids expressing FLAG-VCP and Myc-Jab1 (WT, 1-334), the deletion mutants Myc–1–110, Myc–1–191 or Myc–110–191 were co-transfected into HEK293T cells. Respective expression (input, lane 1–5) and FLAG-IP (lanes 6–10) were detected using anti-FLAG or anti-Myc antibodies. The *asterix* indicates presence of the heavy chain of IgG. **(C)** Interaction of JAMM mutant-Jab1/CSN5 with VCP. Plasmids expressing FLAG-VCP and Myc-Jab1/CSN5 mutant were co-transfected in HEK 293T cells. Inputs (lane 1, 2, 5 and 6) and IP (lane 3, 4, 7 and 8) were detected by immunoblotting using anti-Myc and anti-FLAG antibodies.

5.2.3. FRET-CLSM analysis of Jab1/CSN5-VCP association

To investigate whether VCP and Jab1/CSN5 proteins are localized in such proximity in cells that protein-protein interaction is likely, FRET combined with CLSM was applied (Truong and Ikura, 2001; Konig et al., 2006). Proteins were co-expressed in NIH 3T3 cells and detected by indirect double-immunofluorescence. Overexpressed VCP and Jab1/CSN5 were detected primarily in the cytoplasm. In acceptor bleaching experiments, the fluorescence of the donor (VCP, Cy3 labeled) and of the acceptor (Jab1/CSN5, Cy5 labeled) were determined and their intensities were measured before and after the Cy5 fluorophore bleaching in a defined region of interest (ROI). Photobleaching of the acceptor (Jab1/CSN5) fluorophore (Cy5) led to an almost complete removal of the pseudocolored fluorescence intensity (Figure 20D). In donors of the Cy3 (donor) channel, an concominant increase was detected in the same ROI (Figure 20B). A total of eighteen to twenty cells in each experiment (n=76 for the experimental group and n=85 for the control group obtained from 4 different experiments) were analysed. Positive FRET signal was robustly detected in every experiment. A distinct increase of fluorescence (ΔIF) was observed in the bleached area with a median value of 7.87 (Figure 20E). A false-positive FRET signal that can potentially be caused by unspesific cross-reactivity of the secondary antibodies was excluded by performing control experiments. Here, both secondary antibodies were applied in an incubation with anti-Jab1/CSN5 antibody (acceptor) only (median ΔIF = 2.75) (Figure 20E).

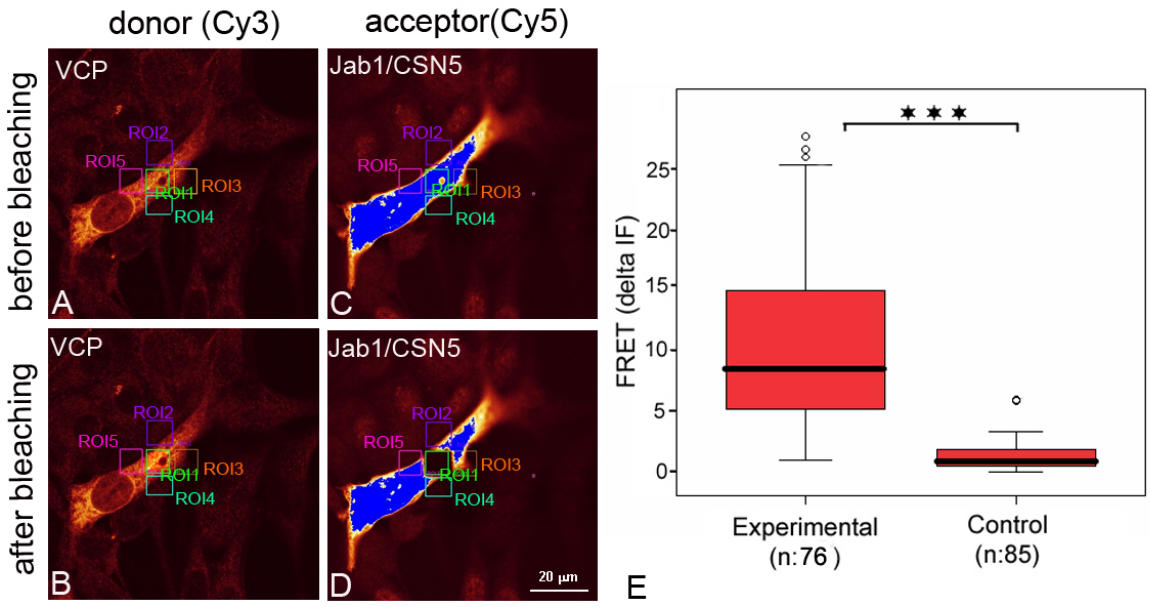

Figure 20: Close proximity of VCP and Jab1/CSN5 proteins in NIH 3T3 cells shown by double-labeling indirect immunofluorescence (IF) combined with FRET analysis.

Immunofluorescence detection of VCP (donor labeled with Cy3-conjugated secondary antibody; **A and B**) and Jab1/CSN5 (acceptor labeled with Cy5-conjugated secondary antibody; **C+D**). Cy5 was bleached in region of interest (ROI) 1 (compare ROI 1 in **C** and **D**). ROI 2-5: control areas outside the bleached area. **(E)** Changes in ΔIF in experimental compared to control group. ***=p ≤ 0.001, Mann-Whitney test; n = number of measurements (4 experiments). Boxplots: percentiles 0, 25, median, 75, 100. O: extreme values of data set. Bar: 20µm

5.2.4. Interactions between VCP and COP9 signalosome (CSN) subunits

The CSN complex, also known as the Jab1/CSN5-containing signalosome, consists of eight subunits termed CSN1-CSN8 (Deng et al., 2000). The interaction of Jab1/CSN5 with VCP found in this study prompted us to investigate whether the other subunits of the CSN complex also interact with VCP. To verify this hypothesis CSN1 pull-down experiments were performed. CSN1-based pull-downs have been shown previously to efficiently precipitate the entire CSN complex (Tsuge et al., 2001).Pull-down of the CSN complex by an anti-CSN1 antibody revealed that the CSN complex indeed interacts with VCP (Figure 21A). Pull-down specificity was confirmed by immunoblotting with a Jab1/CSN5 antibody (Figure 21A).

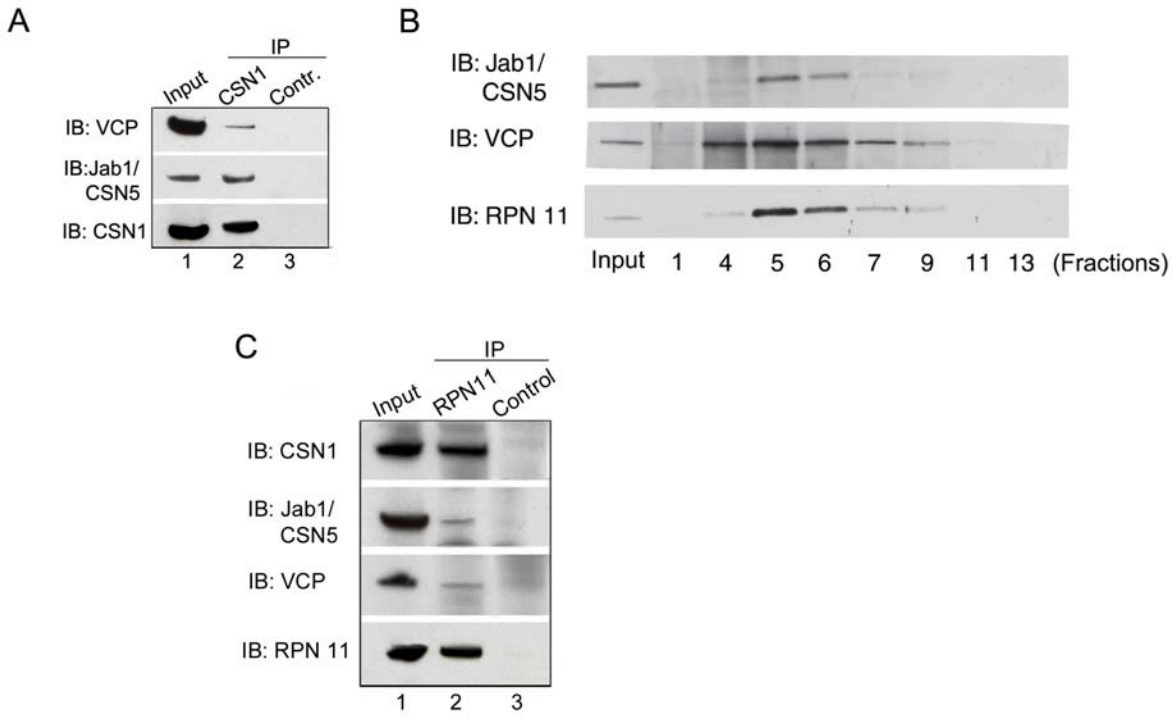

Figure 21: Interaction of VCP with the entire CSN complex and the proteasome lid
(A) Cell lysates from HEK293T cells were analyzed for expression of VCP, Jab1/CSN5 and CSN1 by immunoblot analysis (IB, lane 1). Subsequently, lysates were subjected to co-IP using anti-CSN1 antibody (lane 2) and isotype control antibody (lane 3). Using immunoblot analysis, separated proteins were probed with anti-VCP antibody and anti-Jab1/CSN5

antibody, followed by stripping and reprobed with anti-CSN1 antibody to confirm pull-down of the whole CSN complex **(B)** Copurification of VCP and Jab1/CSN5 with the proteasome subunit RPN 11 in a Sephacryl S-200 column. HEK293T cell lysates were separated using gel filtration. Fractionated proteins were resolved in a 12.5% SDS-PAGE and immunoblot analysis was performed using the antibodies indicated on the left. Fraction numbers are provided at the bottom of the picture **(C)** RPN-11 immunoprecipitation (IP) was performed using fractions 5 and 6 and the presence of CSN1, VCP, Jab1/CSN5 and PRN11 were verified in precipitates using specific antibodies (lane 2). Isotype control antibody was applied as control (lane 3). Lane 1: 2% of input.

5.2.5. Interaction of VCP with Jab1/CSN5 in the proteasome lid complex (RPN 11/S13)

VCP has been shown to copurify and coimmunoprecipitate with the 26S proteasome, to have ATPase activity, and to be a multiubiquitin chain-targeting factor required for degradation by the ubiquitin-proteasome pathway (Dai and Li, 2001). However, it has not been shown which subunit of the proteasome interacts directly with VCP. Since Jab1/CSN5 and the proteasome lid complex subunit (RPN 11) share the same domain (MPN^+ or JAMM), it is possible that VCP could also interact with the lid complex of the proteasome. To study this hypothesis, total protein extracts from HEK293T cells were prepared and resolved by gel filtration chromatography using a Sephacryl S-200 column. Fractions were analyzed by immunoblotting to identify if RPN 11 containining fractions also show VCP and Jab1/CSN5. RPN11 was found in fractions 5-7 (Figure 21B). VCP and Jab1/CSN5 were observed in fractions 5 and 6 suggesting an association with the proteasome. To confirm the hypothesis that Jab1/CSN5 and VCP interact with RPN 11, cell lysates of fractions 5 and 6 were used for immunoprecipitation of RPN 11. Precipitated proteins were analyzed by immunoblotting for using antibodies directed aginst VCP and CSN subunits. Interestingly, RPN 11 appears to interact stronger with CSN than VCP (Figure 21C).

5.2.6. Jab1/CSN5-polyubiquitin interaction *in vivo* and *in vitro*

The Jab1/CSN5-VCP interaction found in this study raised the question whether Jab1/CSN5 could interact with ubiquitin chains via the MPN domain, a known ubiquitin binding domain. Binding of gold labelled polyubiquitin chains (Ub4) to the CSN was demonstrated by electron microscopical study (Hetfeld et al., 2005). It remained, however, unanswered to which subunit of CSN binds to polyubiquitin chains. For this reason, Jab1/CSN5-ubiquitin binding was examined *in vitro* and *in vivo*. To examine the Jab1/CSN5-

ubiquitin association *in vitro*, purified GST-Jab1/CSN5 was immobilized an Glutathion Sepharose beads and incubated with Lys48-linked polyubiquitin chains (Ub2–7). *In vitro* binding was detected by immunoblotting using anti-ubiquitin antibodies (Figure 22a, lane 3 and 4).

Since the MPN domain of proteins is known to interact with ubiquitin chains (McCullough et al., 2004; Bellare et al., 2006; Hurley et al., 2006), it was aimed to define whether Jab1/CSN5 interacts with these ubiquitin chains directly via its MPN domain *in vivo*. Therefore, Myc-Jab1/CSN5 and its deletion mutants (1–191, 1–110, 110–191) were overexpressed in HEK293T cells. Lysates were immunoprecipitated using an anti-Myc antibody and immunoblot analysis was performed with anti-ubiquitin antibodies (Figure 22b). As shown in figure 22b, Jab1/CSN5 binds to ubiquitinylated proteins via the N-terminal region harboring the MPN domain (1-191). The 110–191 domain also binds to ubiquitinylated proteins, but in a weaker fashion than the wild type. These results demostrate that Jab1/CSN5 indeed binds to ubiquitinylated proteins via its MPN domain.

VCP is also known to interact with polyubiquitinylated proteins by either binding to them directly with its N-domain or indirectly mediated by cofactors (Dai and Li, 2001). In this study, VCP-polyubiquitin association was used as a positive control. In order to define VCP-polyubiquitin association *in vitro*, purified His-VCP was immobilized on Ni-NTA agarose beads and incubated with Ub(2-7). Binding was detected using immunoblotting (Figure 22A, lane 6). However, no differences between VCP-polyubiquitin and Jab1/CSN5-polyubiquitin association were detected, suggesting that Jab1/CSN5 binds to ubiquitinylated proteins (lane 3 and 4) with the same affinity as shown in association with VCP-polyubiquitin (lane 6).

After proving that both VCP and Jab1/CSN5 bind to ubiquitin chains, the possibility that Jab1/CSN5 and VCP may compete for binding to polyubiquitin chains (Ub2-7) was examined. For that, immobilized His-VCP was loaded with polyubiquitin chains and increasing amounts of GST- Jab1/CSN5 (lane 8: 0.50 µg and lane 9: 1 µg) were passed over the washed column. GST- Jab1/CSN5 was able to compete with His-VCP for polyubiquitins and thus partially removed polyubiquitin chains from the column. These results showed that GST-Jab1/CSN5 interacts with both His-VCP and ubiquitin chains. Additionally, GST-Jab1/CSN5 competes with VCP for binding to ubiquitin chains.

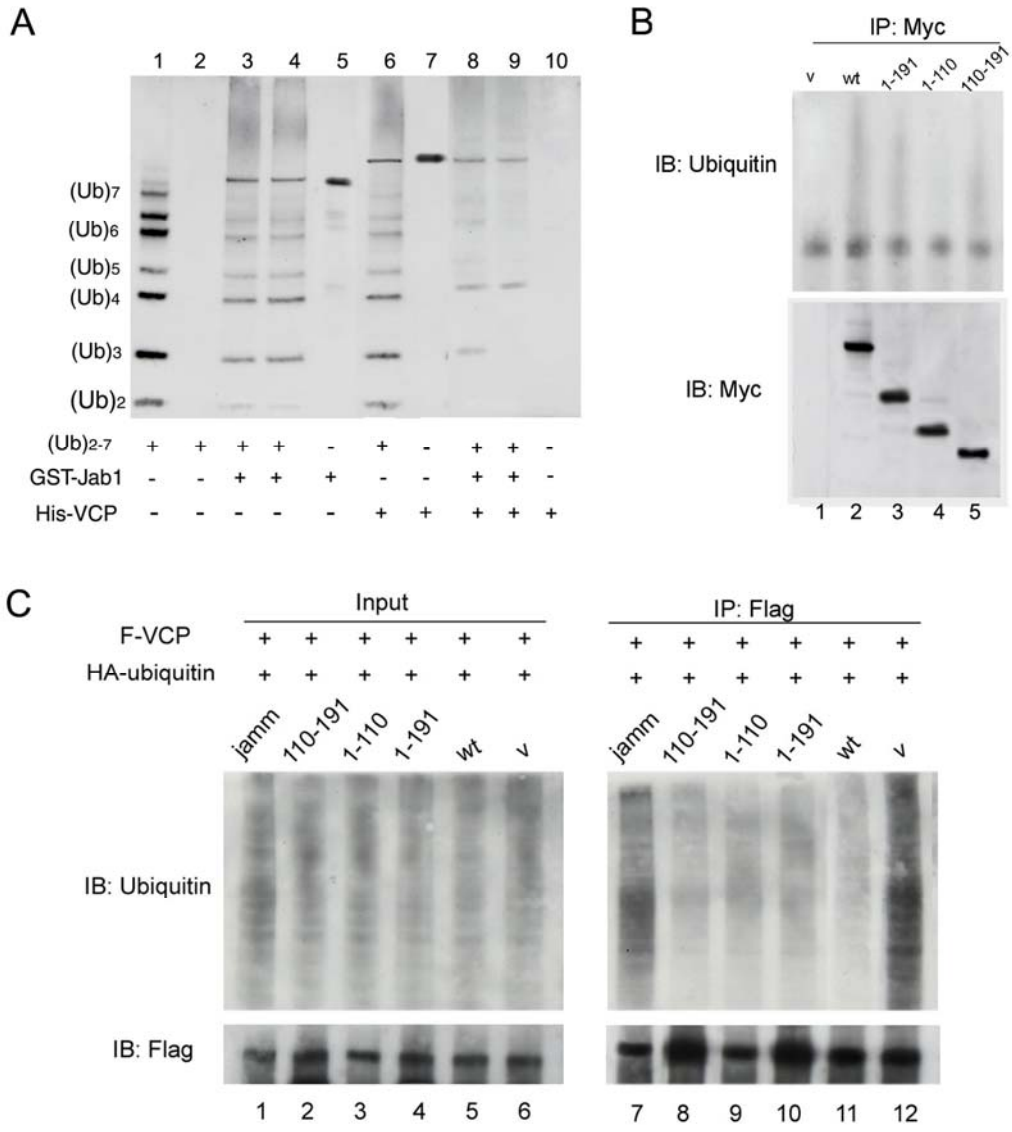

Figure 22: Jab1/CSN5 –polyubiquitin association *in vitro* and *in vivo.*
(A) Binding of Jab1/CSN5 to polyubiquitinated proteins *in vitro*. Polyubiquitin chains (Ub2–7) were incubated both with GST-Jab1/CSN5 immobilized on glutathione-Sepharose 4B and His-VCP immobilized on Ni-NTA agarose *in vitro.* Bound proteins were resolved using SDS-PAGE and polyubiquitin chains associated with GST-Jab1/CSN5 (lane 3 and 4) and His-VCP (lane 6) were detected by immunoblotting using anti-ubiquitin antibodies. Lane 1: 100 ng Ub (2-7), lane 2: GST, lane 5: 200 ng GST-Jab1/CSN5, lane 7: 200 ng His-VCP, lane 10: Ni-NTA agarose. GST-Jab1/CSN5 (lane 8: 0. 5 µg and lane 9: 1 µg) was added to immobilize His-VCP-polyubiquitin. Bound proteins were resolved by SDS-PAGE and polyubiquitin chains were detected by immunoblotting using anti-ubiquitin antibodies **(B)** Binding of Jab1/CSN5 to polyubiquitinated proteins *in vivo.* HEK293T cells transfected with Myc-Jab1/CSN5 expression vector, wt-Myc-Jab1/CSN5 and the deletion mutants of Myc-Jab1/CSN5. Cells were lysed and immunoprecipitated with a monoclonal anti-Myc antibody. Precipitates were analyzed by immunoblotting using anti-Myc and anti-ubiquitin antibodies. **(C)** Jab1/CSN5 effect on VCP-polyubiquitin protein binding. HEK293T cells were transfected with HA-ubiquitin, FLAG-VCP and either Myc-Jab1/CSN5 expression vector or wt-Jab1/CSN5 as well as mutants of Jab1/CSN5. FLAG-VCP was precipitated and the associated ubiquitin proteins were determined by immunoblotting using an anti-ubiquitin antibody.

5.3. Jab1/CSN5 regulates VCP-polyubiquitin association

The main function of VCP is to escort ubiquitinylated proteins to the proteasome and segregate these ubiquitinylated proteins from their binding partners. After extraction of ubiquitinylated substrates from their partners with the aid of a number of substrate-recruiting cofactors, the segregated proteins can either be polyubiquitinylated or deubiquitinylated by a number of substrate-processing cofactors (Jentsch and Rumpf, 2007). Because Jab1/CSN5 in association with the CSN complex is known to possess deubiquitinylase activity (Hetfeld et al., 2005), it is suggested that Jab1/CSN5 may regulate the ubiquitinylation status of proteins bound to VCP. To find out whether the Jab1/CSN5-VCP interaction affects the VCP-polyubiquitin association, HEK293T cells were transfected with FLAG-VCP, HA-ubiquitin and either Myc-Jab1/CSN5 or its deletion mutants. Cell lysates were used for immunoprecipitation of FLAG-VCP *in vivo*. Immunoprecipitated proteins were blotted and probed with an anti-ubiquitin antibody. The number of the ubiquitinylated proteins precipitated together with VCP was decreased in Jab1/CSN5 transfected cells compared to cells transfected with Jab1/CSN5 expression vector and the JAMM mutant of Jab1/CSN5 (Figure 22C). In addition, the proteasome inhibitor MG132 was used to block VCP-mediated degradation of ubiquitinylated substrates in the experimental setup (Figure 23A). A clear difference between Jab1/CSN5 transfected cells and its mutants was observed by means of VCP-polyubiquitin association. Polyubiquitin conjugated proteins bound to VCP were found to accumulate in the JAMM mutant of Jab1/CSN5 transfected cells, whereas no significant change was observed in wild type Jab1/CSN5 transfected cells (Figure 23A).

These results showed that Jab1/CSN5 reduces VCP-polyubiquitin association, suggesting that Jab1/CSN5 could be a new key substrate-processing cofactor that deubiquitinylates the substrates bound to VCP.

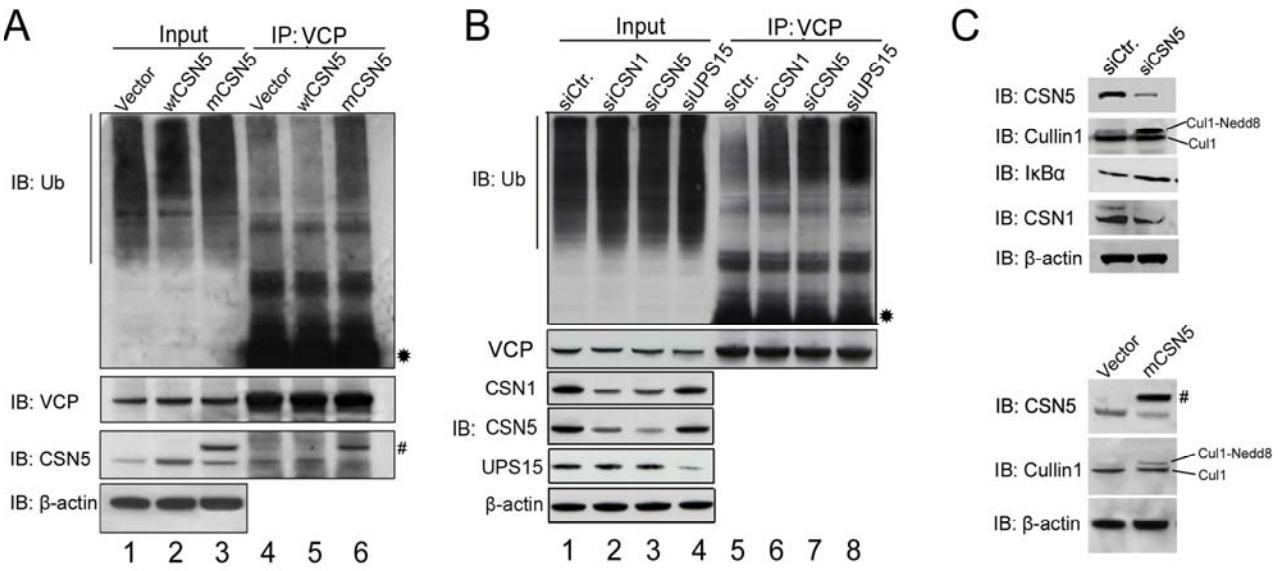

Figure 23: Functional CSN complex with associated USP15 deubiquitinase regulates deubiquitinylation of polyubiquitinated substrates bound to VCP
(A) HEK 293T cells were transfected with empty vector, Jab1/CSN5 (wtCSN5) or the JAMM mutant of CSN5 (mCSN5) and treated with the proteasome inhibitor MG132. VCP was immunoprecipitated (IP) from transfected cell lysates, and precipitates were analyzed by immunoblotting (IB) for ubiquitin, VCP and CSN5. β-actin was used as loading control. **(B)** Cells were transiently transfected with control, CSN1, CSN5 and USP15 siRNAs. After treatment with the proteasome inhibitor MG132 for 1 h cell lysates were analyzed by IB using specific antibodies as indicated on the left. After immunoprecipitation of VCP, ubiquitin was detected in precipitates by IB. Asterisks denote IgG heavy chains, # indicates Myc-tagged CSN5 JAMM mutant. **(C)** Functional controls: lysates of CSN5-knockdown cells were analysed by IB for the presence of CSN5, cullin1, IκBα, CSN1 and ß-actin (upper panel). Lysates of mCSN5-transfected cells were analysed by IB for the presence of CSN5, cullin 1 and ß-actin (lower panel).

Since Jab1/CSN5 exerts its activities within the CSN complex, the functional effect of CSN on the VCP-polyubiquitin association was examined by RNA interference (Figure 23B). Jab1/CSN5 and CSN1 were efficiently knocked down in HEK 293T, which leads to destabilisation of the CSN complex and polyubiquitinylated proteins bound to VCP were detected with an anti-ubiquitin antibody. The amount of ubiquitinylated proteins associated with VCP is increased in Jab1/CSN5 and CSN1 knockdown cells compared to control cells (Figure 23B, lane 6, 7). This confirmed preview results (Figure 22C and 23A) and suggested that the JAMM motif of Jab1/CSN5 (mCSN5) and the CSN complex are required for the deubiquitinylation of ubiquitinylated substrates bound to VCP. Because the CSN is associated with the deubiquitinase USP15 (Hetfeld et al., 2005), USP15 was also knocked down. Like in CSN1 and Jab1/CSN5 knock down experiments polyubiquitinylated proteins bound to VCP

were found to accumulate in USP15 knockdown cells (Figure 23B, lane 8). Therefore, this finding proposes that the activity of USP15 is involved in determining the fate of substrates bound to VCP. The functionality of the knockdown was examined for Jab1/CSN5 (Figure 23C upper panel). Knockdown of Jab1/CSN5 significantly increased the fraction of neddylated cullin 1 as the CSN function is impaired due to inapproriate synthesis of CSN1 or 5, which results in loss of deneddylation. The same effect was observed when the JAMM mutant of Jab1/CSN5 (mCSN5) was overexpressed (Fig. 23C lower panel) demonstrating that the mutant protein is indeed compromising CSN deneddylase activity. Moreover, IκBα accumulated in the Jab1/CSN5 knockdown (Fig. 23C upper panel) due to deregulated deubiquitination by USP15.

5.4. Knockdown of Jab1/CSN5 delays the degradation of ubiquitinylated proteins

It was shown that VCP-Jab1/CSN5 association regulates the fate of the ubiquitinylated proteins in this study (see 5.3). This raised the question if the association could also affect the TNFα inducuded degradation of IκBα, an important and well established substrate for the UPS. Therefore, HEK293T cells were transfected either with Jab1/CSN5^{siRNA} or control^{siRNA} and subsequently stimulated with TNFα (10 ng/ml) for 0-45 min. Lysates were separated using SDS-PAGE and probed with antibodies directed against IκBα, Jab1/CSN5 and β–actin. In cells transfected with control^{siRNA} IκBα was degraded within 5 min after TNFα induction (Figure 17). However, in HEK293T cells transfected with Jab1/CSN5^{siRNA}, TNFα-induced IκBα degradation was delayed. The efficiency of the Jab1/CSN5 knockdown was confirmed by immunoblotting.

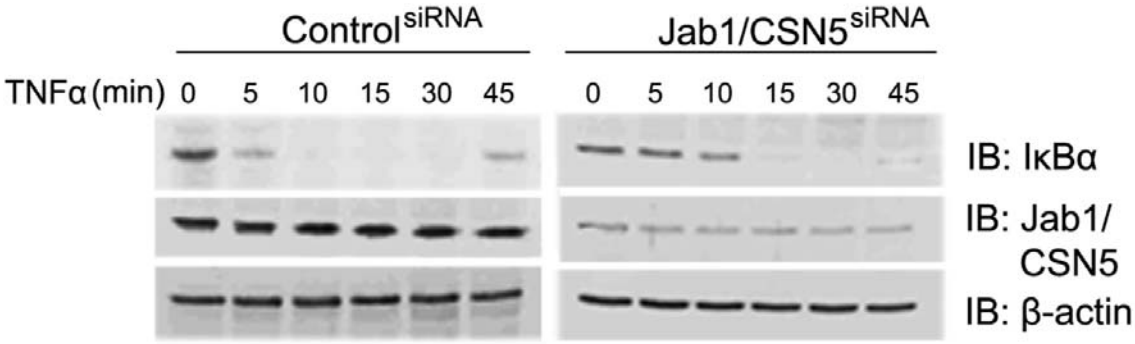

Figure 24: TNFα induced degradation of IκBα is delayed by Jab1/CSN5^{siRNA}
HEK293T cells were transfected with either Jab1/CSN5^{siRNA} or control^{siRNA} for 72 h and subsequently stimulated with TNFα (10 ng/ml) for the indicated periods of time. Lysates were probed using immunoblotting (IB) with antibodies directed against IκBα, Jab1/CSN5 and β–actin (loading control).

Taken together, the results of the knockdown experiments support the hypothesis that Jab1/CSN5 is a key substrate processing factor that deubiquitinylates VCP bound substrates such as IκBα (Figure 23, 24).

5.5. Knockdown of MIF, VCP and Jab1/CSN5 with different RNAi strategies

RNA interference (RNAi) is a novel gene regulatory mechanism by which double-stranded RNA (dsRNA) induces gene silencing by targeting complementary mRNA for degradation. It reduces the expression of a particular gene in nearly all metazoan systems, often by 70-90% or greater and effects the cellular function of the respective gene. The mechanism of RNA interference (RNAi) is summarized in Figure 25.

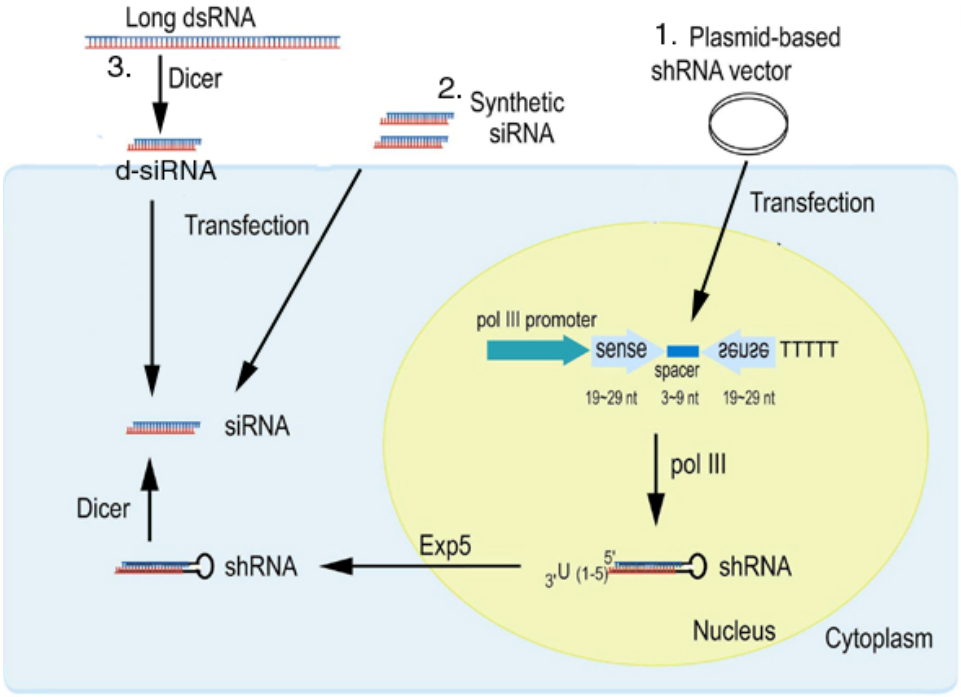

Figure 25: Three Ways to Trigger the RNAi Pathway.
In mammalian systems, RNAi can be triggered by synthetic short interfering RNA (siRNA) molecules (pathway 2) or by DNA based expression vectors designed to express short hairpin RNA (shRNA) molecules (pathway 1). In non-mammalian systems, the RNAi pathway commences when double-stranded RNA (dsRNA; usually longer than 30 bp) is introduced into cells (pathway 3). In each case, gene silencing results from destruction of mRNA that is complementary to the input siRNA (2) or the siRNA molecules created by Dicer cleavage of longer dsRNA (3) or shRNA (1) molecules. Dicer = cytoplasmic nuclease. From (Kim, 2005).

In non-mammalian systems, introducing or expressing long double stranded RNA (dsRNA) triggers the RNAi pathway (Figure 25, pathway 3). The cytoplasmic nuclease Dicer first cleaves the long dsRNA into 21–23 bp small interfering RNAs (siRNAs), then unwind and assemble into RNA-induced silencing complexes (RISCs). The antisense siRNA strand guides RISC to complementary RNA molecules, and RISC cleaves the mRNA, leading to specific gene silencing. Since most mammalian cells mount a potent antiviral response upon introduction of dsRNA longer than 30 bp, researchers induce RNAi in these systems by either transfecting cells with siRNAs (typically 21 bp RNA molecules with 3' dinucleotide overhangs) or by using DNA-based vectors to express short hairpin RNAs (shRNAs) that are processed by Dicer into siRNA molecules (Figure 25, pathways 2 and 1, respectively).

In this study, two main approaches for inducing RNAi into mammalian cells were applied: siRNAs (pathway 2) and shRNA expression vectors (pathway 1) (Figure 25). Knock-down of MIF, Jab1/CSN5 and VCP was aimed to elucidate the function of these genes in specific pathways and also to define the role of Jab1/CSN5-VCP interaction in different cellular functions.

5.5.1. Knock-down of MIF, VCP and Jab1/CSN5 with the shRNA pSUPER vector

The pSUPER RNAi System was used to cause efficient and specific down-regulation of gene expression to inactivate the three genes MIF, VCP and Jab1/CSN5 in NIH 3T3, 264.7 RAW macrophages and HEKT293 cells, respectively (see details in 4.3.5).

5.5.2. Knock-down of VCP and Jab1/CSN5 with siRNAs

To show a functional role of Jab1/CSN5 and VCP in the turnover of UPS proteins, Jab1/CSN5 and VCP gene expression were silenced transiently by using specific siRNAs. 72 h after transfection, HEK293T lysates were examined by immunoblotting. Efficient knockdowns were obtained with Jab1/CSN5 and VCP-siRNAs resulting in almost complete suppression of Jab1/CSN5 and VCP expression. The scrambled control siRNA had no effect (Figure 26). Knock-down of Jab1/CSN5 suppressed CSN1 expression as well, which supports the previous finding that the CSN5 subunit affects assembly of the total CSN (Naumann et al., 1999). Thus, removal of a single CSN subunit is efficient to destabilize the CSN complex and also reduce the level of other CSN related subunits. To confirm the impaired function of the CSN resulting from the knock-down of Jab1/CSN5, the level of Iκβα, a well known UPS

substrate was investigated. Notably, the amount of Iκβα protein was increased in cells showing a knock-down of Jab1/CSN5 (Figure 26A). Furthermore, in line with data published previously (Lue et al., 2007), a decrease in MIF expression and an increase of pAKT in Jab1/CSN5 knock-down cells were observed. This indicates that Jab1/CSN5 regulates MIF expression via AKT pathway.

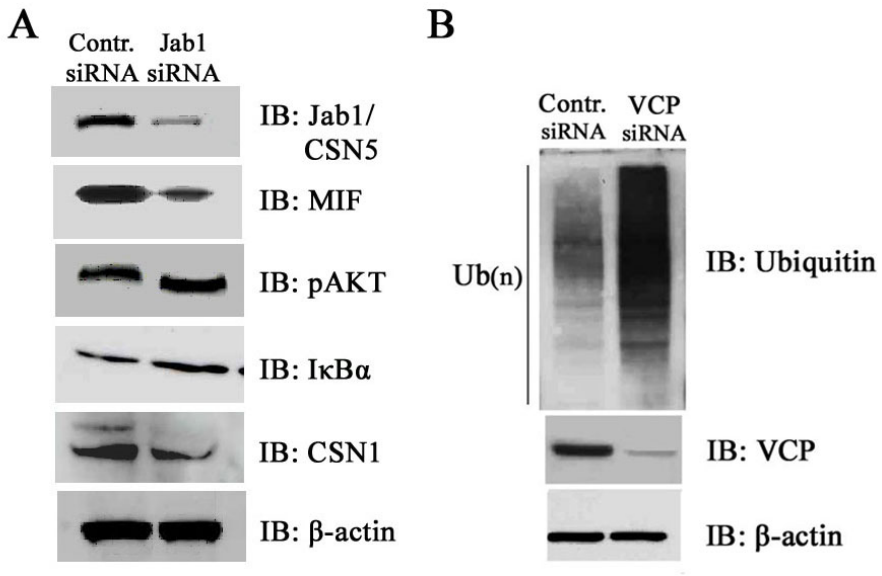

Figure 26: Effect of silencing of Jab1/CSN5 and VCP on selected proteins.
(A) HEK293T cells were transiently transfected with either Jab1/CSN5 siRNA or with a scrambled siRNA (control). After 72 h cell lysates from control and Jab1/CSN5 knockdown cells were analyzed by immunoblotting. Immunodetection of Jab1/CSN5, CSN1, Iκβα, MIF and pAKT (see indicated panels), was performed using specific antibodies. **(B)** HEK293T cells were transiently transfected either with VCP siRNA or a scrambled control siRNA. Efficient knockdown of VCP (indicated panel) was analyzed in cell lysates by immunoblotting. Immunodetection of ubiquitin and VCP were performed using specific antibodies. β-actin served as control for equal sample loading.

To further investigate the impact of VCP knockdown on the assembly of ubiqutinylated proteins, HEK293T cells were transfected with either VCP siRNA or a scrambled control siRNA. Knockdown of VCP caused an accumulation of ubiquitinylated proteins confirming the previous result that VCP is a key chaperone targeting ubiquitinylated proteins to the proteasome (Dai et al., 1998).

5.6. Expression and purification of His-VCP and GST-Jab1/CSN5

5.6.1. Expression of His-VCP and GST-Jab1/CSN5

pET28a $^{(+)}$-VCP and pGEX-4T$_1$-Jab1/CSN5 constructs were used to transform *E. coli* BL21 (DE3) bacterial cells to express His-tagged VCP and GST-tagged Jab1/CSN5. One clone from the successfully transformed bacteria was selected for protein expression. For determining the optimal conditions for protein expression, bacterial VCP and Jab1/CSN5 protein expression were induced with 0.5 mM IPTG at 37°C. The fusion proteins appeared as the major bacterial proteins 3h after induction (Fig. 27A and B; arrows).

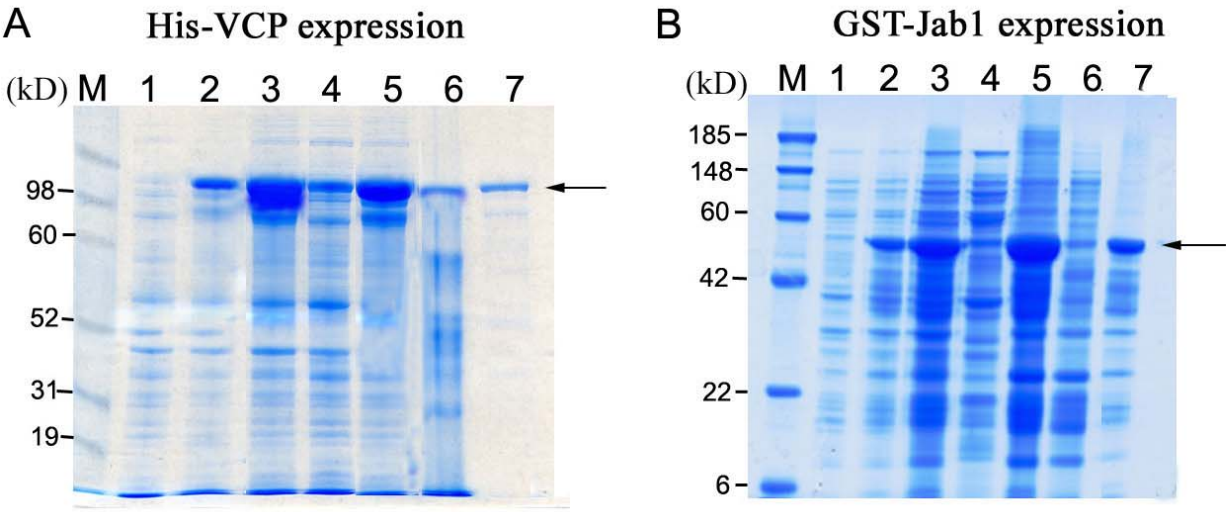

Figure 27: Expression of His-tagged VCP and GST-tagged Jab1/CSN5 in *E. coli*.
500 ml culture of *E. coli* BL21 (DE3) carrying the VCP expression plasmid **(A**, lane 1) and the Jab1/CSN5 expression plasmid **(B**, lane 1) were induced with 0.5 mM IPTG at 37°C. 3 h after induction (lane 2), cells were treated with 1 mg/ml lysozyme and DNAse I (lane 3). Supernatants of the lysated cells (lane 4) were discarded. Resuspended pellets containing inclusion bodies (lane 5) were incubated with denaturation buffer and centrifuged (lane 6) again. The cleared lysate (lane 7) was dialyzed against PBS. Aliquots of each fraction were separated by 12.5% SDS-PAGE. The gel was stained with colloidal Coomassie blue after electrophoresis. (M) = molecular weight marker (kD).

5.6.2. Purification of His-VCP and GST-Jab1/CSN5

His-VCP protein was affinity purified using Ni-NTA agarose beads, whereas the GST–Jab1/CSN5 protein was purified using a glutathion agarose column. Eluted fractions were collected and the purity of each fraction was subsequently investigated by SDS-PAGE (Figure 28A and B).

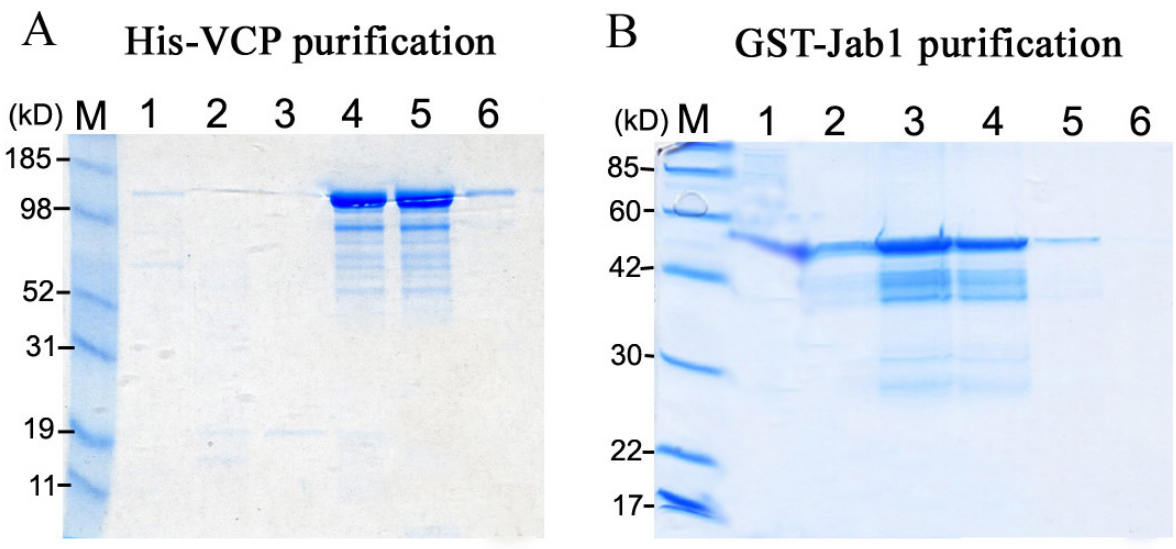

Figure 28: Purification of His tagged VCP and GST tagged Jab1/CSN5
An aliquot from each eluted fraction (lane 1 to 6) was separated by 12.5% SDS-PAGE subsequently stained with Coomassie blue.

5.7. MIF modulates binding between Jab1/CSN5 and VCP

A previous study demonstrated that MIF binds to the MPN domain of Jab1/CSN5 (Burger-Kentischer et al., 2005). In this study, it was shown that the MPN domain of Jab1/CSN5 also interacts with VCP. Since VCP and MIF bind to the same domain of Jab1/CSN5, it is suggested that MIF and VCP could compete for binding to Jab1/CSN5. To examine whether MIF could competitively affect the interaction between Jab1/CSN5 and VCP, HEK293T cells were transfected with pCIneo-Jab1/CSN5, FLAG-VCP and increasing amounts of pCMV-MIF. Cell lysates from transfected cells were subjected to VCP-IP (Figure 29A). Indeed, increasing amounts of MIF decreased Jab1/CSN5 association with VCP (see indicated panel in figure 29A). This study proposes that MIF competes with VCP for Jab1/CSN5 binding. Conversely, transfecting cells with pCIneo-Jab1/CSN5, pCMV-MIF and increasing amounts of FLAG-VCP decreased Jab1/CSN5 interaction with MIF (Figure 29B).

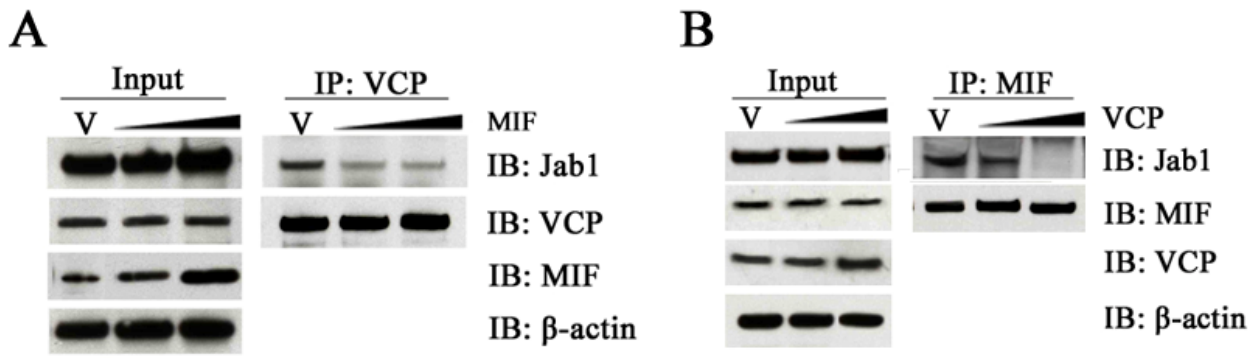

Figure 29: Competition between MIF and VCP in binding to Jab1/CSN5.
(A) HEK293T cells were transfected with Jab1/CSN5, VCP and either vector (v) or increasing amounts of MIF. Cell lysates were used for immunoprecipitation of VCP. Immunoprecipitated proteins were separated by SDS-PAGE and probed with antibodies directed against Jab1/CSN5, VCP, MIF and β-actin. **(B)** HEK293T cells were transfected with Jab1/CSN5, MIF and either vector (v) or increasing amounts of VCP. MIF was immunoprecipitated from cell lysates and precipitated proteins were detected by probing with antibodies directed against Jab1, MIF, VCP and β-actin. Input: 5% of cell lysate used for IP.

Taken together, these results indicate that MIF decreases Jab1/CSN5 binding to VCP. Conversely, VCP also inhibited Jab1/CSN5 binding to MIF, showing competition of both molecules for binding to Jab1/CSN5.

5.8. MIF activates VCP via AKT pathway

It has been shown that MIF prevents apoptosis and enhances cell survival by direct activation of the AKT pathway (Lue et al., 2007). Moreover, VCP was shown as an important target of AKT mediated signaling and to be involved in AKT-mediated anti-apoptotic signaling (Vandermoere et al., 2006). The interaction between MIF and VCP found in this study raised the question whether MIF could enhance the phosphorylation of VCP via AKT signaling. Initially, the phosphorylation of AKT was examined in a time-dependent manner in NIH 3T3 cells. As recognized by PAS (Phospho AKT substrate) antibody MIF mediated AKT activation between 5 and 30 min was shown to cause VCP phosphorylation. (Figure 30). This finding strongly indicates that MIF induces the sustained phosphorylation of VCP.

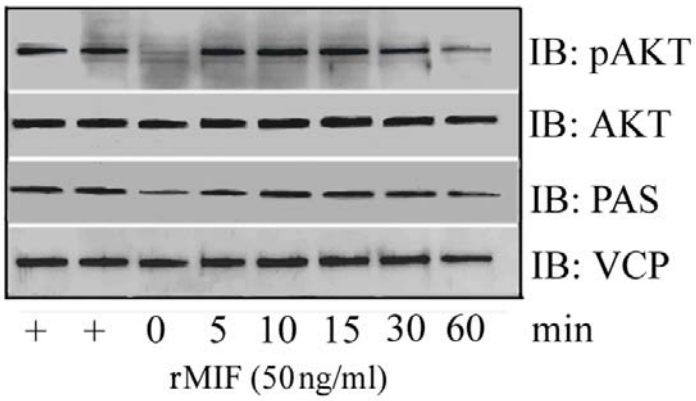

Figure 30: Phosphorylation of AKT and AKT substrates by rMIF.
Time course of AKT and VCP phosphorylation induced by exogenous rMIF (50 ng/ml) in NIH 3T3 fibroblasts. Dose response of phosphorylation of AKT and substrates (PAS) were analyzed by immunoblotting. Immunodetection of pAKT, AKT and VCP was performed using specific antibodies (see indicated right panel). Phosphorylation of VCP was detected using PAS (Phospho AKT substrate) antibody. AKT and VCP served as loading control. +, +: As a positive control PDGF (20 ng/ml) was used.

Table III: MALDI-MS identification of MIF interacting proteins from 1D-SDS-PAGE

	Protein	NCBI entry	Matched peptides	Note
Ribosomal proteins	Ribosomal protein S16	gi|33286940	8	
	Ribosomal protein S3	gi|337514	7	
	Ribosomal protein L13	gi|33286940	5	
	Ribosomal protein S6	gi|337514	5	
	Ribosomal protein S9-like	gi|21594169	5	
	Ribosomal protein S17	gi|950111	4	
	Rpl17 protein	gi|28174920	3	
	Rps15a protein	gi|56541088	3	
	Ribosomal protein L26	gi|56205563	3	
	Ribosomal protein L31	gi|56541054	3	
	Ribosomal protein S19	gi|62663652	3	
	Ribosomal protein L38	gi|12963655	2	
	Ribosomal protein S10	gi|13399310	1	
	60S ribosomal protein L21	gi|2500367	1	
	Ribosomal protein 10	gi|54035586	1	
	40S ribosomal protein SA	gi|125970	1	
Mitochondrial proteins	ATP synthase, H+ transporting mitochondrial	gi|1592878	12	
	ATP synthase beta-subunit	gi|2623222	8	
	ADP,ATP carrier protein	gi|423368	8	
	Solute carrier family 25, member 4	gi|20070838	7	
	Atp5b protein	gi|23272966	5	
	Sideroflexin 3	gi|15126554	3	
	Mitochondrial carrier homolog 2	gi|24416581	3	
	Voltage-dependent anion channel 2	gi|33243895	3	
	H(+)-transporting ATP synthase	gi|102	3	

	Protein	NCBI entry	Matched peptides	Note
Heatschock proteins	Hsc70-ps1	gi|56385	14	
	HSP 90-alpha (HSP 86)	gi|1170383	11	
	Chaperonin subunit 2 (beta)	gi|435839	5	
	Mortalin mot-2	gi|435839	5	
	Chaperonin containing TCP-1 gamma subunit	gi|38969850	3	
	Chaperonin subunit 4 (delta)	gi|32452050	4	
	CCT (chaperonin containing TCP-1) epsilon	gi|468550	4	
	CCT (chaperonin containing TCP-1)beta	gi|5295992	3	
ER proteins	BIP	gi|2598562	13	ERAD component
	T-complex protein 1	gi|13277861	8	ERAD component
	Protein disulfide isomerase	gi|23958822	7	ERAD component
	Clathrin	gi|51259242	5	VCP partner
	Sec61 beta subunit	gi|13324684	1	ERAD component
Ca binding proteins	Annexin A2	gi|13097	9	
	Annexin A1	gi|6754570	4	
	Troponin C-like protein	gi|223036	4	
	S100 calcium binding	gi|14789726	3	
Nuclear proteins	Hist1h4h protein	gi|27692960	5	
	Nucleophosmin 1	gi|55153941	4	
	Histone 1, H1e	gi|13430890	3	
	Hnrpm protein	gi|13543181	2	
	Heterogeneousnuclear ribonucleoprotein C	gi|8393544	1	
Others	Eukaryotic translation elongation factor 2	gi|13938072	13	
	Nonmuscle heavy chain myosin II	gi|17978023	11	
	Lamin A, isoform A	gi|15929761	9	
	Eno1 protein	gi|54114937	8	
	ADP-ribosylation factor 1	gi|21594148	7	

	Protein	NCBI entry	Matched peptides	Note
	Plectin 1	gi|40849908	7	
	Transketolase	gi|11066098	7	
	Eukaryotic translation elongation factor 1-delta	gi|10442752	5	
	Mccc2 protein	gi|20380367	5	
	AHNAK	gi|37675525	6	
	Galectin 3	gi|33859580	5	
	Aldolase 1, A isoform	gi|27695278	4	
	B-cell receptor-associated	gi|6671622	4	
	LDH-A	gi|535924	5	
	Rho GDP dissociation inhibitor (GDI) alpha	gi|56541074	5	
	Eukaryotic translation elongation factor 1 gamma	gi|53237111	4	
	p100 co-activator	gi|6009521	3	
	CPN10-like protein	gi|8777943	3	
	Glutathione S-transferase	gi|30931187	3	
	Prohibitin	gi|56206786	3	
	Ubiquitin	gi|229532	2	
	Proteasome (macropain) subunit, alpha type 4	gi|12805051	2	Proteasome subunit
	Proteasome (macropain) subunit, beta type 5	gi|77415527	1	Proteasome subunit
	Trap1 protein	gi|13905144	2	
	Peroxidase	gi|885932	2	
	Myosin IC	gi|18204814	2	
	Kinesin family member	gi|30794518	2	
	Voltage-dependent anion	gi|13435771	2	
	Ehd2 protein	gi|20072042	2	
	Arpc4 protein	gi|33244031	2	
	Thioredoxin 1	gi|14789654	2	MIF partner
	Eukaryotic translation initiation factor 2	gi|16741332	1	

Table IV: MALDI-MS identification of MIF interacting proteins from 2D-SDS-PAGE

Spot	Protein	NCBI entry	M_r (kDa)	Matched peptides	Note
3	Peroxiredoxin 1	gi|56103807	22	10	MIF and Jab1partner
14	Valosin-containing protein	gi|55217	89	12	ERAD, UPS component
4	Phosphoglycerate kinase 1	gi|987048	45	11	
5	Heterogeneous nuclear ribonucleoprotein F	gi|17390408	46	7	
6	Serine proteinase inhibitor	gi|27806941	49	5	
11	Alpha-2-HS-glycoprotein	gi|27806751	58	5	
2	Eukaryotic translation initiation	gi|124231	19	3	
20	Malate dehydrogenase	gi|164543	36	4	
19	MIF	gi|694108	11	4	
1	Troponin C-like protein	gi|223036	17	2	
21	AHA1, activator of heat shock 90kDa protein	gi|12653109	38	2	
22	Pyrophosphatase	gi|27754065	42	2	
23	Acidic ribosomal phosphoprotein P0	gi|6671569	35	2	

6. DISCUSSION

Macrophage migration inhibitory factor (MIF) was originally identified for its ability to inhibit the random migration of macrophages *in vitro* (Bloom and Bennett, 1966; David, 1966). Later it was shown that MIF is involved in the pathogenesis of inflammatory diseases such as atherosclerosis, sepsis, asthma and rheumatoid arthritis (Calandra et al., 1994). MIF is an unusual cytokine since it is abundantly expressed by several cell types and stored in the cytoplasm (Bacher et al., 1997). Recent investigations identified CD74/CD44 as cellular surface receptor that mediates binding of extracellular MIF (Leng et al., 2003; Shi et al., 2006). Albeit the majority of MIF research has focused on its role as pro-inflammatory mediator, recent studies showed that MIF functions are not limited to immune system. Elevated levels of MIF have been observed in several cancer tissues such as breast, bladder and lung cancer (Bando et al., 2002; Tomiyasu et al., 2002; Meyer-Siegler et al., 2006). Importantly, MIF was found to negatively regulate p53-mediated apoptosis (Hudson et al., 1999). An attractive mechanism explaining the MIF-p53 relationship and MIF's role in tumor development has been put forward (Nemajerova et al., 2007a). The authors propose that MIF plays a key role in regulating the DNA damage checkpoints which control cell cycle progression. It was found that MIF deficiency causes improper degradation of several cell cycle regulators such as p27, E2F1 and Cyclin A2.

MIF exerts its diverse biological effects by interacting with different proteins. Several of the MIF-interacting proteins identified to date are redox proteins or proteins which are directly connected to redox regulation (Thiele and Bernhagen, 2005). The interaction of the proliferation–associated gene product (PAG), a thiol-specific cellular antioxidant protein, with MIF results in inhibition of PAG's antioxidant activity (Jung et al., 2001). In addition to PAG, hepatopoeitin is directly involved in MIF's redox-modulating function (Li et al., 2004). Moreover, Bcl-2/adenovirus E1B interacting protein like (BNIPL), an apoptosis-associated protein was found to interact with MIF and it was suggested that BNIPL can inhibit MIF-mediated cell proliferation (Shen et al., 2003). Recently, MIF was shown to be a functional noncognate ligand for the chemokine receptors CXCR2 and CXCR4 in inflammatory and atherogenic leukocyte recruitment (Bernhagen et al., 2007).

In a search for intracellular MIF-interacting proteins using the yeast two-hybrid system Jab1/CSN5 was identified (Kleemann et al., 2000). Jab1/CSN5 is a component of the COP9 signalosome (CSN) and possesses metalloprotease activity which targets SCF E3

Ubiquitin ligase and deconjugates Nedd8 from cullins (Cope et al., 2002; Zhou et al., 2003; Petroski and Deshaies, 2005). A balanced neddylation status of its cullin component seems to be required for correct SCF E3 ligase activity. It was proposed that MIF is able to control SCF activty via binding to Jab1/CSN5 (Nemajerova et al., 2007a).

Although several MIF-interacting proteins were identified previously, the mechanism of MIF action and the role of interacting proteins in influencing MIF signaling pathways remain unclear and partially controversial. Therefore, my aim was to identify new MIF-interacting proteins and to investigate the impact of MIF-MIF-interacting protein interactions on cellular functions.

6.1. Identification of MIF interacting proteins

In this study, new MIF-interacting proteins were identified using an approach based on specific *in vivo* biotinylation of stably expressed MIF. Taking advantage of the high affinity of biotin to avidin, *in vivo* methods were developed to specifically biotinylate 'bait' proteins (Cronan, 1990; Smith et al., 1998; Beckett et al., 1999; de Boer et al., 2003). Tagged MIF was efficiently biotinylated *in vivo* and associated MIF-interacting proteins were purified by binding to streptavidin. Amongst the affinity-based purification methods, the biotin-avidin system has several advantages. Firstly, as shown here biotinylated MIF can be efficiently purified directly from crude cellular extracts in a single-step procedure, whereas other *in vivo* tagging methods like the tandem affinity purification tag (TAP) strategy require several purification steps (Rigaut et al., 1999). Secondly, unspecific binding is minimized due to the small number of endogenously occurring biotinylated proteins. Thirdly, the very strong affinity of biotin to avidin allows to choose the stringency of washing conditions. This reduces nonspecific background binding, although high stringency washing might also remove MIF-interacting proteins with low affinity. Indeed, a systematic comparison of different tags showed that biotinylation is the best approach in terms of efficiency and purity (Tucker and Grisshammer, 1996). Fourthly, the inclusion of a TEV protease cleavage site downstream of the biotinylation tag was used to specifically cleave bound protein complexes from streptavidin, while leaving endogenously biotinylated proteins bound to the matrix. Moreover, the biotinylated peptide tag did not interfere with the ability of MIF to bind to well established MIF-interacting proteins such as Jab1/CSN5 and peroxiredoxin-1 demonstrating the applicability of the method.

In vivo biotin tagging combined with affinity purification and mass spectrometry had not been applied yet to systematically identify MIF-interacting proteins. My thesis led to the identification of more than 50 new candidates. Some of the identified proteins are presumably transiently or indirectly associated with MIF and have therefore not been identified with other approaches like yeast two-hybrid assays that allow only the detection of direct binding partners, whereas *in vivo* biotin tagging enables the purification of whole complexes consisting of direct and indirect binding partners.

In addition to known MIF-interacting proteins, a number of components of the ubiquitin proteasome system such as VCP, clathrin, ubiquitin, proteasome subunit α4, β5 and of the endoplasmic reticulum associated protein degradation (ERAD) complex such as BIP, ERp57, Sec61 and T-complex protein 1 were identified in this study. Many proteins of eukaryotic cells undergo folding and modification in the lumen of the endoplasmic reticulum (ER). If processing is not succesfull, misfolded proteins and unassembled protein complexes are retro-translocated into the cytosol and degraded by the proteasome. This multi-step process is called ER associated degradation (ERAD) (Zhong et al., 2004). Recent studies revealed that a plethora of factors such as VCP, Ufd1, Npl4, E3 ubiquitin ligases, Derlin-1, -2, and -3, BIP, VIMP, Ubx2, etc. are involved in ERAD (Ye et al., 2001; Lilley and Ploegh, 2005; Neuber et al., 2005; Schuberth and Buchberger, 2005; Mouysset et al., 2006; Oda et al., 2006). Among these proteins the AAA ATPase valosin-containing protein (VCP) seems to be the key factor.

The high number of MIF binding partners in the UPS prompted us to further investigate the association of MIF and VCP. An important question is whether MIF regulates the ERAD pathway by modulating VCP-dependent extraction of proteins from the ER. In the absence of MIF, ERAD substrates may rapidly be extracted from the ER and shuttled to the proteasome for degradation. In the presence of MIF, it could compete with ubiquitinylated proteins or other VCP cofactors for binding to VCP, displacing cofactors from VCP in a competitive manner. This may slow down the extraction of ubiquitinylated proteins, so that they accumulate in the ER. An accumulation of ERAD substrates in the ER increases cellular stress and contributes to disease pathogenesis. Therefore, the interaction between MIF and VCP could be part of a homeostatic mechanism that modulates traffic through the ERAD pathway. Although there are no data showing that MIF monitors and coordinates the ERAD pathway, the identification of ERAD key regulators as MIF interactors makes MIF a potential candidate for such a regulatory protein.

A recent study (Nemajerova et al., 2007b) showed that MIF regulates the activity of cullin 1 containing SCF ubiquitin ligases. The activity of SCF is stimulated by the conjugation of a ubiquitin-like protein called Nedd8 to cullins (Bornstein et al., 2006). Deneddylation of cullins is achieved by the CSN with the Jab1/CSN5 subunit hydrolysing Nedd8 (Cope et al., 2002). MIF binding to Jab1/CSN5 regulates the cycle and activity of the SCF complex. Consistent with these findings, this thesis also provides evidence suggesting a putative role for MIF in the regulation of the UPS.

Another MIF-interacting protein that was identified is phosphoglycerate kinase-1 (Pgk-1), an ATP-generating glycolytic enzyme that forms part of the glycolytic pathway. During glycolysis, Pgk-1 catalyzes the transfer of a high-energy phosphoryl group from the acyl phosphate of 1,3-diphosphoglycerate to ADP to produce ATP. Pgk-1 also catalyzes the reverse reaction during gluconeogenesis where 3-phosphoglycerate and ATP are converted to 1,3-diphosphoglycerate and ADP (Hitzeman et al., 1980; Blake and Rice, 1981). Because Pgk-1 is a highly-expressed gene and its mRNA is relatively stable, it has been the subject of a large number of studies on mRNA stability and decay, protein structure, folding, and kinetics as well as on hypoxia, tumorigenesis and wound healing. Hypoxia inducible transcription factor (HIF-1) plays an important role in controlling the glycolytic pathway when cells are exposed to low oxygen. Recently, HIF-1α was shown to up-regulate Pgk-1 as well as the glucose transporter type 1(GLUT1) and hexokinase 1(HK1) (Luo et al., 2006). In addition, intracellular pH decreases as a result of lactate accumulation caused by accelerated glycolysis. Because intracellular acidosis triggers apoptosis, blocking increased glycolytic activity by down regulating HIF-1α reduces apoptosis of the hypoxic cells. Interestingly, it was shown that the MIF gene contains a Hypoxia Response Element (HRE) within its promoter and is induced under hypoxic conditions (Koong et al., 2000; Bacher et al., 2003; Yao et al., 2005; Maity and Koumenis, 2006). During tissue injury, which leads to hypoxia, an essential part of the inflammatory response is the influx of monocytes/macrophages (Karhausen et al., 2005). In fact, knockout of HIF-1α was shown to cause a profound impairment in myeloid cell motility, invasiveness and bacterial killing (Cramer et al., 2003). Therefore, HIF-1α seems to control the function of myeloid cells in an inflammatory environment. HIF-1α could upregulate MIF to attract inflammatory cells in regions of hypoxia/inflammation. Moreover, MIF has been identified as a hypoxia-induced gene in cancer cells (Koong et al., 2000; Baugh et al., 2006). Based on these findings, both Pgk-1 and MIF seem to play critical roles in hypoxia providing a functional link between MIF and Pgk-1.

Other studies also support a functional role for the interaction between MIF and Pgk-1. Initially, MIF was shown to regulate glucose-induced insulin release in an autocrine fashion (Waeber et al., 1997). In perfusion studies performed with isolated rat islets of Langerhans, immunoneutralization of MIF reduced the glucose induced insulin secretion response by 39% (Waeber et al., 1997). Soon after, MIF was shown to increase the synthesis of fructose 2,6-bisphosphate and cellular glucose uptake (Benigni et al., 2000). MIF is also found to be released by the ischaemic heart, where it stimulates the AMP-activated protein kinase, an important regulator of both glycolysis and glucose uptake during cellular stress (Miller et al., 2008).

The interaction between MIF and the newly identified proteins was verified by co-immunoprecipitation and co-localization studies. Since the interaction between MIF and VCP was found in total cellular extracts of NIH 3T3 cells, immunohistochemical analysis revealed the presence of both proteins in the cytoplasm. A close association of the two proteins in the cytoplasm of NIH 3T3 cells was examined by fluorescence resonance energy transfer (FRET) combined with double-labeling indirect immunofluorescence. Although both proteins were found to co-localize in the cytoplasm, no significant FRET signal was detected indicating that MIF and VCP are not in close proximity excluding a direct interaction. However, FRET in combination with fluorescence labeled antibodies has limitations. For example, resonance energy transfer depends on the proper orientation of donor and acceptor. If this is unfavourable, FRET does not occur even if the proteins interact. In other words, a negative FRET result does not prove non-interaction. But also by using surface plasmon resonance analysis no interaction between MIF and VCP could be detected. Moreover, pull-down experiments were performed *in vivo* with ectopically expressed MIF and deletion mutants of VCP. However, none of the VCP domains interacted with MIF supporting the results of FRET and surface plasmon resonance analyses, which suggest an indirect interaction between MIF and VCP, potentially via a cofactor. Amongst these, a likely candidate is Jab1/CSN5 since VCP and Jab1/CSN5 are both involved in the UPS and MIF interacts with Jab1/CSN5.

6.2. Jab1/CSN5 directly interacts with VCP *in vivo* and *in vitro*

In order to confirm whether Jab1/CSN5 is a linking cofactor between MIF and VCP, a putative direct interaction between Jab1/CSN5 and VCP was investigated. VCP possesses two consecutive AAA ATPase domains (called D1 and D2) and an N-terminal domain (N-domain). The way how VCP associates with cofactors and ubiquitinylated substrates is an

area of active research and two possible mechanisms have been suggested. VCP can bind to proteins directly via its N-domain (Dai and Li, 2001) or indirectly through cofactors (Rape et al., 2001; Meyer et al., 2002; Hartmann-Petersen et al., 2004; Schuberth et al., 2004; Richly et al., 2005) as shown for ubiquitinylated substrates and other proteins. Indeed, the second mechanism may be more common as numerous VCP substrate-recruiting and -processing cofactors have been identified recently, which possess ubiquitin-binding domains and usually interact with VCP through its N-domain. For mapping the interface on VCP, deletion constructs were used for ectopic expression of the N-terminal domain (N), the two individual ATPase domains (D1, D2) and the combined N and D1 domains (ND1). After immunoprecipitation of Jab1/CSN5 neither the N-domain alone, nor the single D1 or D2 domains were co-precipitated. Only the ND1 protein was able to bind to Jab1/CSN5 albeit with less affinity than the wild type protein indicating that it is sufficient for specific binding but that residues in D2 are further contributing to binding affinity. Most substrate-recruiting and –processing cofactors of VCP use the S3/S4 loop of a UBX domain (Jentsch and Rumpf, 2007) for binding into a hydrophobic pocket that separates the N-domain of VCP into two subdomains (Dreveny et al., 2004). Jab1/CSN5 appears to be the first cofactor that is using an MPN core domain instead when interfacing with VCP.

To further validate a direct interaction between Jab1/CSN5 and VCP, pull-down experiments with purified recombinant proteins *in vitro* showed that the interaction between Jab1/CSN5 and VCP occurs directly without the need for a cofactor.

In another line of the study, FRET-CSLM analysis was used to confirm the interaction between Jab1/CSN5 and VCP. Significant FRET occured in the cytoplasm, indicating that VCP and Jab1/CSN5 must be closer than 10 nm in this compartment. There was no indication of co-localization in the nucleus. As reported previously, this thesis confirmed that Jab1/CSN5 is evenly distributed over the nucleus and cytoplasm whereas VCP is mainly located in the cytoplasm (Oh et al., 2006; Vandermoere et al., 2006).

6.3. Jab1/CSN5 binds to ubiquitinylated proteins via its MPN domain

Ubiquitin is a 76-amino-acid polypeptide conjugated to proteins via an isopeptide bond between the C-terminus of ubiquitin and specific lysine residues in the ubiquitinylated protein. Ubiquitin can be attached to proteins as a monomer or as a polyubiquitin chain. Many studies show that ubiquitin and ubiquitinylation of substrates are involved in many biological functions such as protein degradation, endocytosis, protein sorting, subnuclear trafficking, and

gene expression (Pickart, 2001b). Lys48-linked polyubiquitin chains are the principal proteasomal targeting signal, while Lys63-linked chains appear to be nonproteolytic signals (Finley, 2001; Pickart, 2001b). Recent progress in the discovery of new biological roles for ubiquitinylation has gone hand in hand with the discovery of proteins possessing ubiquitin-binding domains (Hicke et al., 2005; Harper and Schulman, 2006).

Amongst these ubiquitin binding domains, JAMM motifs within MPN domains can have different functions. Whereas the JAMM motif of Jab1/CSN5 acts as a NEDD8 isopeptidase, the motifs of RPN 11 and AMSH function as ubiquitin isopeptidases (McCullough et al., 2004). Contrary to these enzymatic examples, the JAMM motif of Mov 34 is unable to complex a zinc ion and is proposed to have primarily a structural role like in the pre-mRNA splicing factor Prp8p whose inactive JAMM motif was shown to be a new ubiquitin binding domain (Bellare et al., 2006). Therefore, it was tested if Jab1/CSN5, apart from being a NEDD8 isopeptidase, can have other functions and binds K48-oligoubiquitin chains. Because Jab1/CSN5 is largely insoluble when produced in various expression systems, a strategy was developed here to refold guanidine HCl denatured GST-CSN5 by using the aggregation suppressor arginine and folding enhancer sucrose (Tresaugues et al., 2004). Refolded GST-Jab1/CSN5 was immobilized on glutathione Sepharose beads and incubated with K48-linked polyubiquitin chains Ub(2–7). Jab1/CSN5 interacted with Ub2-7 and showed a preference for Ub3 and 4. The positive control His-VCP that is known to bind polyubiquitin (Dai and Li, 2001) showed a very similar binding pattern.

To investigate if binding of polyubiquitin is mediated by the JAMM motif, Myc-tagged Jab1/CSN5 and its mutants were ectopically expressed in HEK 293T cells. The wild type protein and the 1-191 mutant containing the entire MPN domain (54-191) were able to bind to ubiquitinylated proteins. Importantly, also the 110-191 mutant harbouring the JAMM motif (129-175) but missing large parts of the MPN core (54-142) (Burger-Kentischer et al., 2005) as well as the conserved glutamate 76 (Cope et al., 2002) could still interact with ubiquitinylated proteins albeit with slightly lower affinity. In contrast, the mutant 1-110 that does not contain the JAMM motif lost binding. Therefore, in addition to conferring NEDD8 isopeptidase activity the JAMM motif of Jab1/CSN5 binds polyubiquitin but does not depolymerize it. Thus, this thesis supports previous experiments suggesting that the JAMM motif possesses ubiquitin deconjugation but not depolymerizing activity (Groisman et al., 2003; Hetfeld et al., 2005)

On the other hand, VCP has also been shown to interact with ubiquitinylated

substrates, to transfer them to the proteasome and to affect the degradation of ERAD and UPS substrates (Ghislain et al., 1996; Dai et al., 1998; Dai and Li, 2001; Jarosch et al., 2002). In contrast to the data presented here that VCP binds to ubiquitinylated proteins (Dai and Li, 2001; Meyer et al., 2002) other studies showed little to no interaction (Doss-Pepe et al., 2003).

6.4. Jab1/CSN5 and VCP bind to the proteasome

Like Jab1/CSN5, RPN 11, the Jab1/CSN5 paralog in the proteasome lid, contains a JAMM/MPN$^+$ motif, which constitutes the major de-ubiquitinylation activity of the 26S proteasome (Verma et al., 2002). Therefore, the question arose whether VCP can also bind to RPN 11. Total protein extracts from HEK 293T cells were separated by Sephacryl S-200 gel filtration chromatography and fractions were immunoblotted for VCP, RPN 11 and Jab1/CSN5. RPN 11 containing fractions were found to also contain VCP and Jab1/CSN5 indicating that both proteins could indeed interact with the proteasome subunit RPN 11. Earlier studies had shown an association of VCP with the 26S proteasome (Dai et al., 1998), however, it remained unclear which subunit of the proteasome is associating with VCP. Although the functional relevance of a VCP-RPN 11 interaction was not investigated here the result suggests that ubiquitinylated proteins bound to VCP are transported to the proteasome where VCP interacts with RPN11 (Elsasser and Finley, 2005).

6.5. Competition between MIF and VCP

Binding experiments in mammalian cells revealed that the N terminal region together with the first ATPase domain D1 (i.e. ND1) of VCP is involved in the association with the MPN domain of Jab1/CSN5. It should be noted that other adaptors of VCP like p47, Ufd1p, SVIP and ataxin3 (Nagahama et al., 2003; Bruderer et al., 2004; Zhong et al., 2004) also bind to the ND1 domain of VCP. Likewise, the MPN domain of Jab1/CSN5 also binds to other proteins (Burger-Kentischer et al., 2005). Individual adaptors can occupy the same site on VCP or Jab1/CSN5, thereby preventing the binding of other proteins in a competitive manner. Indeed, increasing amounts of MIF decreased the amount of Jab1/CSN5 associated with VCP. Conversely, VCP also inhibited Jab1/CSN5 binding to MIF suggesting competition of both proteins for binding to Jab1/CSN5. Therefore, these results provide evidence for the hypothesis that MIF and VCP compete for binding to Jab1/CSN5.

Moreover, it is tempting to speculate that other adaptors of VCP (such as SVIP, p47,

etc.) can also compete with Jab1/CSN5 for binding to the ND1 domain of VCP.

6.6. Jab1/CSN5 regulates the association of VCP with polyubiquitin

VCP binds to ubiquitinylated proteins and targets them to the proteasome. The fate of the ubiquitinylated substrates bound to VCP is defined by VCP partners referred to as substrate recruiting and processing factors (Rumpf and Jentsch, 2006; Jentsch and Rumpf, 2007). Substrate-processing cofactors determine if ubiquitinylated substrates are polyubiquitinylated promoting proteasomal degradation, stably maintain their ubiquitinylation status or are de-ubiquitinylated and released from the complex.

To elucidate whether the interaction between Jab1/CSN5 and VCP results in deubiquitinylation of VCP bound proteins, HEK293T cells were transfected with wt-Jab1/CSN5 and the JAMM mutant of Jab1/CSN5. Cell lysates were used for immunoprecipitation of FLAG-VCP *in vivo*. Polyubiquitin conjugated proteins bound to VCP were found to accumulate in JAMM mutant transfected cells, whereas no significant change was observed in wild type Jab1/CSN5 transfected cells.

Similarly, when CSN1 and Jab1/CSN5 were efficiently knocked down by RNAi, which leads to destabilization of the CSN polyubiquitinylated proteins accumulated on VCP. In conclusion, the JAMM motif of Jab1/CSN5 and a functional CSN complex are required for the deubiquitinylation of ubiquitinylated substrates bound to VCP. Because the CSN is associated with the deubiquitinase USP15 (Hetfeld et al., 2005) this thesis also demonstrated that knock down of USP15 caused the accumulation of polyubiquitinated proteins bound to VCP. Therefore, the activity of USP15 is involved in determining the fate of substrates bound to VCP.

The functionality of the knockdowns was exemplarily shown for Jab1/CSN5. Knockdown significantly increased the fraction of neddylated cullin 1 as a functional CSN is lacking due to inapproriate amounts of CSN1 or 5 resulting in defective deneddylation. The same effect was observed when the JAMM mutant of Jab1/CSN5 was overexpressed demonstrating that the mutant protein is indeed compromising CSN deneddylase activity. However, in line with a previous publication (Cope and Deshaies, 2006) neddylation of

Cullin1 in Jab1/CSN5 knockdown cells was not complete in HEK293T cells. This indicates the presence of other deneddylases which may partially compensate the impaired deneddylase activity of the CSN. Contrary to HEK293T cells, HeLa cells showed hyperneddylation of Cullin1 in Jab1/CSN5 knockdown cells together with reduced expression of Cullin1. It is at present unclear why knockdown of Jab1/CSN5 in HEK293T and in HeLa cells behave differently. Moreover, IκBα accumulated in the Jab1/CSN5 knockdown due to deregulated deubiquitinylation by USP15 (Schweitzer et al., 2007).

In accordance with other studies, this thesis shows that knockdown of single CSN subunits strongly interfered with CSN function (Peth et al., 2007a; Peth et al., 2007b; Schweitzer et al., 2007). For example, knockdown of Jab1/CSN5 causes a 50% downregulation of CSN1. Therefore, it appears that a Jab1/CSN5 knockdown causes the coordinated downregulation of the entire CSN and thus compromises the deubiquitinylase and deneddylase activity of the CSN so that polyubiquitinylated proteins keep associated with VCP.

6.7. VCP interacts with the CSN complex

Because Jab1/CSN5 exerts its activities as part of the CSN complex, it was examined if VCP is interacting with the whole CSN. It is known that CSN1 co-precipitates with other subunits of the CSN complex such as CSN 2, 3, 5 and 8 (Tsuge et al., 2001). Total cell extracts from HEK 293T cells were used to precipate the CSN1 subunit of the CSN. VCP co-precipitated with CSN1 as well as with Jab1/CSN5 indicating that VCP indeed is interacting with the entire CSN complex. This finding leads to the speculation that the CSN together with VCP could form a complex that may be called the CSN particle similar to lid and base of the proteasome that form regulatory particle (Figure 31A and B).

This implies that the proteasomal proteins RPN1, 2, 10 and 13 or paralogous proteins could be part of the CSN particle as well. Currently, VCP is considered as a molecular `gearbox´ that in conjunction with substrate-processing cofactors is able to regulate the ubiquitinylation status of substrates (Jentsch and Rumpf, 2007). Because this thesis has shown that the deneddylase activity of Jab1/CSN5 and the deubiquitinase (DUB) USP15 are involved in the regulation of the ubiquitinylation status of proteins recruited to VCP, it can be hypothesized that both activities are decisive for `switching gears´. Other DUBs could be involved as well as the CSN is associated with at least two different enzymes (Groisman et al., 2003; Hetfeld et al., 2005). A further level of control originates from the association of

1,3,4-trisphosphate 5/6-kinase and protein kinases CK2 and D with the CSN which could be involved in regulating the association of substrate-processing cofactors with VCP through phosphorylation. Therefore, it emerges the picture of a molecular machine that is extracting ubiquitinylated and abnormally folded proteins from larger protein complexes or membranes and decides on their fate by using VCPs N-terminal domain and the CSN as a hub for substrate-processing cofactors and regulatory enzymes.

As the discovery of the interaction of VCP with Jab1/CSN originated from a MIF interactome screen, results of this thesis suggest that MIF is likely to be involved in the regulation of the ubiquitinylation status of substrates through interaction with Jab1/CSN5 (Figure 31).

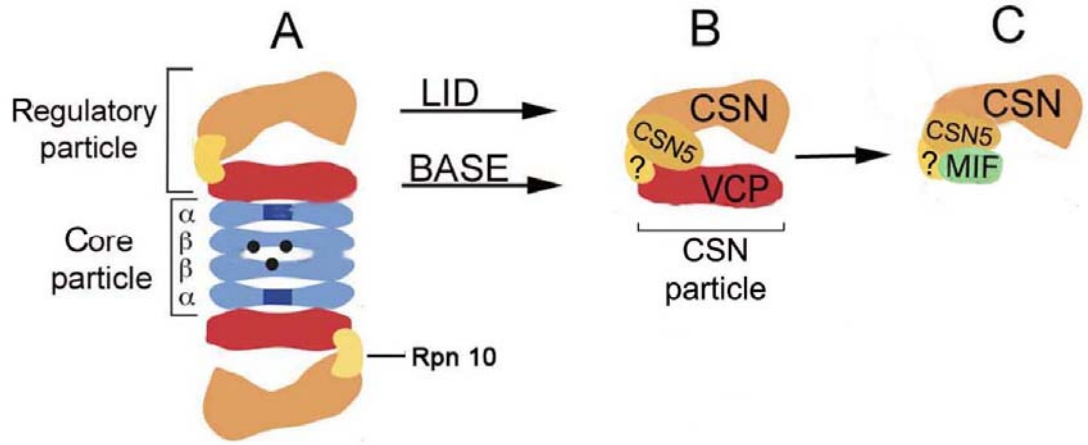

Figure 31: The CSN and VCP form a complex – the CSN particle - that is structurally similar to the 19S proteasome regulatory particle. (A) Schematic representation of the 26S proteasome (adapted from Elsasser and Finley, 2005). The 26S proteasome is composed of one core particle (blue) and two regulatory particles as indicated. The regulatory particle can be further subdivided into the lid (orange) and the base (red). The base contains six ATPases (Rpt1-6), and four non-ATPase subunits (Rpn1, Rpn2, Rpn10, Rpn13). The lid contains six PCI domain-containing proteins (Rpn3, Rpn5–7, Rpn9, and Rpn12) and two MPN domain-containing proteins (Rpn8 and Rpn11). **(B)** Proposed model of the CSN particle in analogy to the proteasome regulatory particle. The CSN particle may represent an alternative form of the regulatory particle. The proteasomol proteins RPN1, 2, 10 and 13 could be part of the CSN particle as indicated here with a question mark (?) **(C)** MIF binds to Jab1/CSN5 and prevents it from interacting with VCP, a mechanism that is likely to be involved in the regulation of the ubiquitinylation status of substrates.

6.8. Effect of VCP-Jab1/CSN5 interaction on IκBα degradation

IκBα was selected as a UPS test substrate for investigations as the role of VCP in targeting substrates to the proteasome was shown (Dai et al., 1998). Deubiqutinylation of IκBα via Jab1/CSN5 has already been examined by others (Schweitzer et al., 2007). Upon

TNFα stimulation, IκBα the inhibitor of NF-κB is hyperphosphorylated, then polyubiquitinylated and targeted to the proteasome for degradation. In order to show the relevance of the VCP-Jab1/CSN5 interaction on IκBα degradation, HEK293T cells were transfected either with Jab1/CSN5^{siRNA} or control^{siRNA} and subsequently stimulated with TNFα in a time dependent manner. In accordance with previous studies (Wang et al., 2006; Schweitzer et al., 2007), TNFα induced IκBα degradation was delayed following knockdown of Jab1/CSN5. Because Jab1/CSN5 deubiquitinylates VCP bound substrates such as IκBα, knockdown of Jab1/CSN5 expression by using siRNA transfection extends the time period of VCP–ubiquitinylated IκBα association. Taken together, these data conclusively show that the CSN not only controls the deubiquitinylation of IκBα, but also the association between VCP and ubiquitinylated IκBα.

Other laboratories also have shown that knockdown of Jab1/CSN5 using siRNA leads to delayed degradation of IκBα and reduced NF-κB activity in synovial fibroblasts of rheumatoid arthritis origin as well as in HeLa cells (Wang et al., 2006; Schweitzer et al., 2007). Jab1/CSN5 was shown to be required for the survival of synovial fibroblasts and knockdown of Jab1/CSN5 caused a high level of apoptosis which was concordant with the accumulation of IκBα. Since MIF was shown to be involved in the pathogenesis of many inflammatory diseases such as rheumatoid arthritis and artherosclerosis, MIF may also activate NF-κB. Indeed, it was shown that MIF activates NF-κB in human mononuclear cells (Amin et al., 2006). Moreover, MIF was shown to regulate AP-1 activity, but not the NF-κB activity in NIH 3T3 cells (Kleemann et al., 2000). This NF-κB activation by MIF may be cell-specific since different cell types were used in those studies. As MIF and Jab1/CSN5 are both involved in the NF-κB pathway, they represent potential therapeutic targets for the treatment of inflammatory diseases.

6.9. MIF activates VCP via the AKT pathway

MIF has been shown to antagonize p53-dependent gene expression (Hudson et al., 1999; Nemajerova et al., 2007a) and to enhance proliferation in various cell types. The inhibition of p53 by MIF requires serial activation of ERK1/2, cPLA2, cyclooxygenase 2 (COX2) and prostaglandin E2 (PGE2) (Mitchell et al., 1999). Although MIF-induced ERK signaling contributes to the anti-apoptotic properties of MIF, a more direct mechanism on MIF mediated cell survival was shown on the AKT signaling pathway via a PI3K-dependent route (Lue et al., 2007).

Activation of AKT by MIF showed MIF's potent anti-apoptotic effects and is in accordance with MIF's cytokine/growth factor-like activity profile in inflammation and cancer (Roger et al., 2003; Mitchell, 2004). Enhancement of cell survival by MIF through PI3K/AKT is in line with observations suggesting a role for PI3K in MIF-dependent endothelial cell migration and angiogenesis (Amin et al., 2006). Interestingly, VCP was shown as an important target of AKT mediated signalling and to be involved in AKT-mediated anti-apoptotic pathways (Vandermoere et al., 2006). In order to examine whether MIF mediated AKT activation causes VCP phosphorylation, AKT activation was examined in a time-dependent manner in NIH 3T3 cells. This thesis shows that MIF-induced AKT activation leads to phosphorylation of AKT substrates amongst them VCP. Data were strengthed as MIF-induced VCP phosphorylation was studied separately in fibroblasts, HEK293T and HeLa cells.

VCP phosphorylation has been also examined by other authors. Tyrosine phosphorylation of VCP was suggested to play a role in membrane fusion and the presentation of polyubiquitinylated proteins to the proteosome (Rabouille et al., 1995; Madeo et al., 1998; Dai and Li, 2001). In another study, VCP tyrosine dephosphorylation caused destabilization of VCP/ER membrane association thereby promoting ER transitional assembly (Lavoie et al., 2000). Moreover, VCP tyrosine phosphorylation has been shown to regulate cell proliferation and apoptosis (Imamura et al., 2003). In accordance with these studies, MIF-mediated VCP phosphorylation also appears to be involved in cell survival and anti-apoptotic pathways.

7. SUMMARY

Macrophage migration inhibitory factor (MIF) is a conserved 12.5 kD protein that serves many critical functions in the regulation of gene expression, proliferation, apoptosis and development. Over the last few years evidence has accumulated that MIF may function in the inhibition of the deneddylase activity of the COP9 signalosome (CSN) by interacting with its subunit Jab1/CSN5. The target of the CSN deneddylase activity is the cullin component of SCF E3 ubiquitin ligases that are significantly more active when neddylated. These ligases are responsible for the selective ubiquitinylation of substrates which are hydrolysed in the 26S proteasome. The latter consists of a 19S reguatory and a 20S core particle. Thus, ubiquitinylating enzymes and the proteasome form the two main pillars of the ubiquitin proteasome system (UPS). To better understand the biological role of MIF in the UPS, a systematic interactome screen was performed in NIH3T3 cells that are constitutively expressing biotinylated MIF.

Biotinylated MIF and its associated proteins were purified by streptavidin binding. Subsequent identification of MIF interacting proteins by mass spectrometry detected a number of already known MIF interacting proteins including MIF itself, peroxiredoxin 1 and RPS19, thus emphasizing the validity of the approach. Besides other new candidates, endoplasmic reticulum (ER) associated chaperones amongst them BiP, ERp57 Sec61ß and the AAA ATPase valosin-containing protein (VCP), which are all involved in ER-associated degradation were identified. As many new MIF interacting partners are involved in the UPS, further investigations were concentrated on the association of MIF with Jab1/CSN5 and VCP. Whilst the binding of MIF to VCP seems to be indirectly mediated by Jab1/CSN5, the interaction of VCP with Jab1/CSN5 is direct and robust as was verified independently by co-immunoprecipitation (co-IP), *in vitro* pull-down assays and fluorescence resonance energy transfer experiments.

The interaction interface between VCP and Jab1/CSN5 was investigated by transient transfection of wild type and mutant proteins followed by co-IP. It emerged that Jab1/CSN5 associates with VCP via the core of its MPN domain that is contacting the N-terminal domain and the D1 domain of VCP. Its binding is independent of the JAMM motif harboring the NEDD8 isopeptidase activity. The JAMM motif was also shown to bind, but not to depolymerize poly-ubiquitinylated chains. Using gel filtration chromatography, VCP co-

migrated with the CSN and co-IP experiments confirmed that the interaction of VCP is not restricted to Jab1/CSN5, but involves the whole CSN complex in the association. The CSN consists of eight proteins that all have paralogs in the 19S regulatory particle of the proteasome. VCP is a homohexameric ATPase with structural homology to the heterohexameric ring of ATPases in the 19S regulatory particle.

RNA interference mediated knockdowns demonstrated that the JAMM motif of CSN5, a functional CSN complex and the CSN-associated deubiquitinase USP15 are all required for deubiquitinylation of substrates bound to VCP.

Taken together, these results suggest that the CSN together with VCP forms a complex. Apart from interacting with at least one deubiquitinylase, the CSN is also known to be associated with three kinases that could regulate the connection of substrate-processing cofactors with VCP via phosphorylation. Therefore, we hypothesize that the CSN together with VCP could have the function to extract ubiquitinylated and abnormal folded proteins from larger protein complexes or membranes and to determine their fate by means of associated substrate-processing cofactors and regulatory enzymes.

8. ZUSAMMENFASSUNG

Der Makrophagen Migrations-Inhibitionsfaktor (MIF) ist ein konserviertes 12,5 kD großes Protein, das zahlreiche kritische Funktionen bei der Genexpression, der Proliferation, der Apoptose und der Entwicklung erfüllt. In den letzten Jahren wurde deutlich, dass eine wichtige Funktion von MIF in der Inhibition der Deneddylase-Aktivität des COP9-Signalosoms (CSN) durch Interaktion mit seiner Untereinheit Jab1/CSN5 bestehen könnte. Substrat für die CSN Deneddylase-Aktivität ist die Cullin-Komponente von SCF E3-Ubiquitin-Ligasen, die im neddylierten Zustand signifikant aktiver sind. Sie sind verantwortlich für die selektive Ubiquitinylierung von Substraten, die dann im 26S Proteasom, das aus einem 19S regulatorischen Partikel und einem 20S Kernpartikel besteht, hydrolysiert werden. Ubiquitinylierungsenzyme und das Proteasom bilden somit die beiden Hauptkomponenten des Ubiquitin-Proteasom-Systems (UPS). Um zu einem verbesserten Verständnis der biologischen Rolle von MIF innerhalb des UPS beizutragen, wurde das MIF-Interaktom mit Hilfe von NIH3T3-Zellen, die konstitutiv biotinmarkiertes MIF exprimieren, untersucht.

Biotinyliertes MIF und damit assoziierte Proteine wurden zunächst über Streptavidin-Bindung aufgereinigt. Die Validierung der Methode erfolgte mittels Massenspektrometrie und der Identifizierung von einigen bereits bekannten MIF Interaktionspartnern wie MIF selbst, Peroxiredoxin 1 und RPS19. Zusätzlich wurden zahlreiche neue MIF-Interaktionspartner gefunden. Auffällig war, dass sich darunter viele mit dem Endoplasmatischen Retikulum (ER) assoziierte Chaperone wie BiP, ERp57, Sec61ß und die AAA ATPase VCP befanden, die alle bei der ER-assoziierten Degradation eine Rolle spielen. Aufgrund der vielen in das UPS eingebundenen neu identifizierten Interaktionspartner konzentrierten sich die anschließenden Untersuchungen auf die Interaktionen zwischen MIF, Jab1/CSN5 und VCP. Die Ergebnisse dieser Arbeit zeigen, dass die Bindung zwischen MIF und VCP indirekt über Jab1/CSN5 vermittelt wird, wogegen eine direkte und robuste Interaktion zwischen VCP und Jab1/CSN5 durch Co-Immunpräzipitationen (Co-IPs), *in vitro* Pull-down-Assays sowie Fluoreszenzresonanz-Energietransfer-Untersuchungen bestätigt werden konnte.

Die an der Interaktion zwischen Jab1/CSN5 und VCP beteiligten Domänen wurden mit Co-IP nach transienter Transfektion der Wildtyp-Proteine sowie einer Reihe von Mutanten untersucht. Hierbei wurde gefunden, dass Jab1/CSN5 mit Hilfe seiner MPN-Kerndomäne an die N-terminale Domäne sowie die D1-Domäne von VCP bindet. Die

Bindung ist unabhängig vom JAMM-Motiv, das Teil der MPN Domäne ist und die NEDD8-Isopeptidase-Aktivität vermittelt. Das JAMM-Motiv dagegen bindet auch oligo-ubiquitinylierte Ketten, ohne diese jedoch depolymerisieren zu können. In Gelfiltrationsuntersuchungen co-migriert VCP mit dem CSN Komplex. Mit Co-IPs konnte gezeigt werden, dass nicht nur Jab1/CSN5, sondern der gesamte CSN-Komplex mit VCP interagiert. Der CSN-Komplex besteht aus acht Proteinen, die allesamt Paraloge im 19S regulatorischen Partikel des Proteasoms haben. VCP ist eine homohexamere ATPase, die strukturelle Ähnlichkeit mit dem heterohexameren Ring von ATPasen im 19S regulatorischen Partikel aufweist.

Durch RNA-Interferenz vermittelte Knockdowns konnte weiterhin gezeigt werden, dass das JAMM-Motiv von Jab1/CSN5, ein funktioneller CSN-Komplex sowie die CSN-assoziierte Deubiquitinase USP15 sämtlich essentiell für die Deubiquitinylierung von an VCP gebundenen Substraten sind.

Zusammengenommen legen diese Ergebnisse nahe, dass das CSN mit VCP einen Komplex bildet. Neben der Assoziation mit mindestens einer Deubiquitinase (DUB) ist das CSN mit drei Kinasen assoziiert, die die Bindung von substratprozessierenden Cofaktoren an VCP durch Phosphorylierung regulieren könnten. Das CSN mit VCP könnte damit die Funktion aufweisen, ubiquitinylierte und fehlgefaltete Proteine aus größeren Proteinkomplexen oder Membranen zu extrahieren und über ihre weitere Verwendung mit Hilfe von substratprozessierenden Cofaktoren und regulatorischen Enzymen zu entscheiden.

9. REFERENCES

Amin, M.A., Haas, C.S., Zhu, K., Mansfield, P.J., Kim, M.J., Lackowski, N.P., and Koch, A.E. (2006). Migration inhibitory factor up-regulates vascular cell adhesion molecule-1 and intercellular adhesion molecule-1 via Src, PI3 kinase, and NFkappaB. Blood *107*, 2252-2261.

Aravind, L., and Ponting, C.P. (1998). Homologues of 26S proteasome subunits are regulators of transcription and translation. Protein Sci *7*, 1250-1254.

Bacher, M., Meinhardt, A., Lan, H.Y., Mu, W., Metz, C.N., Chesney, J.A., Calandra, T., Gemsa, D., Donnelly, T., Atkins, R.C., and Bucala, R. (1997). Migration inhibitory factor expression in experimentally induced endotoxemia. Am J Pathol *150*, 235-246.

Bacher, M., Metz, C.N., Calandra, T., Mayer, K., Chesney, J., Lohoff, M., Gemsa, D., Donnelly, T., and Bucala, R. (1996). An essential regulatory role for macrophage migration inhibitory factor in T-cell activation. Proc Natl Acad Sci U S A *93*, 7849-7854.

Bacher, M., Schrader, J., Thompson, N., Kuschela, K., Gemsa, D., Waeber, G., and Schlegel, J. (2003). Up-regulation of macrophage migration inhibitory factor gene and protein expression in glial tumor cells during hypoxic and hypoglycemic stress indicates a critical role for angiogenesis in glioblastoma multiforme. Am J Pathol *162*, 11-17.

Bando, H., Matsumoto, G., Bando, M., Muta, M., Ogawa, T., Funata, N., Nishihira, J., Koike, M., and Toi, M. (2002). Expression of macrophage migration inhibitory factor in human breast cancer: association with nodal spread. Jpn J Cancer Res *93*, 389-396.

Barnes, P.J., and Karin, M. (1997). Nuclear factor-kappaB: a pivotal transcription factor in chronic inflammatory diseases. N Engl J Med *336*, 1066-1071.

Baugh, J.A., and Bucala, R. (2002). Macrophage migration inhibitory factor. Crit Care Med *30*, S27-S35.

Baugh, J.A., Gantier, M., Li, L., Byrne, A., Buckley, A., and Donnelly, S.C. (2006). Dual regulation of macrophage migration inhibitory factor (MIF) expression in hypoxia by CREB and HIF-1. Biochem Biophys Res Commun *347*, 895-903.

Bech-Otschir, D., Kraft, R., Huang, X., Henklein, P., Kapelari, B., Pollmann, C., and Dubiel, W. (2001). COP9 signalosome-specific phosphorylation targets p53 to degradation by the ubiquitin system. Embo J *20*, 1630-1639.

Beckett, D., Kovaleva, E., and Schatz, P.J. (1999). A minimal peptide substrate in biotin holoenzyme synthetase-catalyzed biotinylation. Protein Sci *8*, 921-929.

Bellare, P., Kutach, A.K., Rines, A.K., Guthrie, C., and Sontheimer, E.J. (2006). Ubiquitin binding by a variant Jab1/MPN domain in the essential pre-mRNA splicing factor Prp8p. Rna *12*, 292-302.

Bendrat, K., Al-Abed, Y., Callaway, D.J., Peng, T., Calandra, T., Metz, C.N., and Bucala, R. (1997). Biochemical and mutational investigations of the enzymatic activity of macrophage

migration inhibitory factor. Biochemistry *36*, 15356-15362.

Benigni, F., Atsumi, T., Calandra, T., Metz, C., Echtenacher, B., Peng, T., and Bucala, R. (2000). The proinflammatory mediator macrophage migration inhibitory factor induces glucose catabolism in muscle. J Clin Invest *106*, 1291-1300.

Bernhagen, J., Bacher, M., Calandra, T., Metz, C.N., Doty, S.B., Donnelly, T., and Bucala, R. (1996). An essential role for macrophage migration inhibitory factor in the tuberculin delayed-type hypersensitivity reaction. J Exp Med *183*, 277-282.

Bernhagen, J., Calandra, T., Cerami, A., and Bucala, R. (1994). Macrophage migration inhibitory factor is a neuroendocrine mediator of endotoxaemia. Trends Microbiol *2*, 198-201.

Bernhagen, J., Calandra, T., Mitchell, R.A., Martin, S.B., Tracey, K.J., Voelter, W., Manogue, K.R., Cerami, A., and Bucala, R. (1993). MIF is a pituitary-derived cytokine that potentiates lethal endotoxaemia. Nature *365*, 756-759.

Bernhagen, J., Krohn, R., Lue, H., Gregory, J.L., Zernecke, A., Koenen, R.R., Dewor, M., Georgiev, I., Schober, A., Leng, L.*, et al.* (2007). MIF is a noncognate ligand of CXC chemokine receptors in inflammatory and atherogenic cell recruitment. Nat Med *13*, 587-596.

Berse, M., Bounpheng, M., Huang, X., Christy, B., Pollmann, C., and Dubiel, W. (2004). Ubiquitin-dependent degradation of Id1 and Id3 is mediated by the COP9 signalosome. J Mol Biol *343*, 361-370.

Blake, C.C., and Rice, D.W. (1981). Phosphoglycerate kinase. Philos Trans R Soc Lond B Biol Sci *293*, 93-104.

Bloom, B.R., and Bennett, B. (1966). Mechanism of a reaction in vitro associated with delayed-type hypersensitivity. Science *153*, 80-82.

Blum, H., Beier, H., and Gross, H. (1987). Improved silver staining of plant proteins, RNA and
DNA in polyacrylamide gels. Electrophoresis *8*, 93-99.

Bornstein, G., Ganoth, D., and Hershko, A. (2006). Regulation of neddylation and deneddylation of cullin1 in SCFSkp2 ubiquitin ligase by F-box protein and substrate. Proc Natl Acad Sci U S A *103*, 11515-11520.

Bozza, M., Satoskar, A.R., Lin, G., Lu, B., Humbles, A.A., Gerard, C., and David, J.R. (1999). Targeted disruption of migration inhibitory factor gene reveals its critical role in sepsis. J Exp Med *189*, 341-346.

Braun, S., Matuschewski, K., Rape, M., Thoms, S., and Jentsch, S. (2002). Role of the ubiquitin-selective CDC48(UFD1/NPL4)chaperone (segregase) in ERAD of OLE1 and other substrates. Embo J *21*, 615-621.

Brown, F.G., Nikolic-Paterson, D.J., Metz, C., Bucala, R., Atkins, R.C., and Lan, H.Y. (1999). Up-regulation of macrophage migration inhibitory factor in acute renal allograft rejection in the rat. Clin Exp Immunol *118*, 329-336.

Bruderer, R.M., Brasseur, C., and Meyer, H.H. (2004). The AAA ATPase p97/VCP interacts with its alternative co-factors, Ufd1-Npl4 and p47, through a common bipartite binding mechanism. J Biol Chem *279*, 49609-49616.

Brummelkamp, T.R., Bernards, R., and Agami, R. (2002). A system for stable expression of short interfering RNAs in mammalian cells. Science *296*, 550-553.

Bucala, R. (1996). MIF rediscovered: cytokine, pituitary hormone, and glucocorticoid-induced regulator of the immune response. Faseb J *10*, 1607-1613.

Burger-Kentischer, A., Finkelmeier, D., Thiele, M., Schmucker, J., Geiger, G., Tovar, G.E., and Bernhagen, J. (2005). Binding of JAB1/CSN5 to MIF is mediated by the MPN domain but is independent of the JAMM motif. FEBS Lett *579*, 1693-1701.

Calandra, T., Bernhagen, J., Mitchell, R.A., and Bucala, R. (1994). The macrophage is an important and previously unrecognized source of macrophage migration inhibitory factor. J Exp Med *179*, 1895-1902.

Calandra, T., and Bucala, R. (1995). Macrophage migration inhibitory factor: a counter-regulator of glucocorticoid action and critical mediator of septic shock. J Inflamm *47*, 39-51.

Callige, M., Kieffer, I., and Richard-Foy, H. (2005). CSN5/Jab1 is involved in ligand-dependent degradation of estrogen receptor {alpha} by the proteasome. Mol Cell Biol *25*, 4349-4358.

Cao, K., Nakajima, R., Meyer, H.H., and Zheng, Y. (2003). The AAA-ATPase Cdc48/p97 regulates spindle disassembly at the end of mitosis. Cell *115*, 355-367.

Cardozo, T., and Pagano, M. (2004). The SCF ubiquitin ligase: insights into a molecular machine. Nat Rev Mol Cell Biol *5*, 739-751.

Cope, G.A., and Deshaies, R.J. (2003). COP9 signalosome: a multifunctional regulator of SCF and other cullin-based ubiquitin ligases. Cell *114*, 663-671.

Cope, G.A., and Deshaies, R.J. (2006). Targeted silencing of Jab1/Csn5 in human cells downregulates SCF activity through reduction of F-box protein levels. BMC Biochem *7*, 1.

Cope, G.A., Suh, G.S., Aravind, L., Schwarz, S.E., Zipursky, S.L., Koonin, E.V., and Deshaies, R.J. (2002). Role of predicted metalloprotease motif of Jab1/Csn5 in cleavage of Nedd8 from Cul1. Science *298*, 608-611.

Cramer, T., Yamanishi, Y., Clausen, B.E., Forster, I., Pawlinski, R., Mackman, N., Haase, V.H., Jaenisch, R., Corr, M., Nizet, V., *et al.* (2003). HIF-1alpha is essential for myeloid cell-mediated inflammation. Cell *112*, 645-657.

Cronan, J.E., Jr. (1990). Biotination of proteins in vivo. A post-translational modification to label, purify, and study proteins. J Biol Chem *265*, 10327-10333.

Dai, R.M., Chen, E., Longo, D.L., Gorbea, C.M., and Li, C.C. (1998). Involvement of

valosin-containing protein, an ATPase Co-purified with IkappaBalpha and 26 S proteasome, in ubiquitin-proteasome-mediated degradation of IkappaBalpha. J Biol Chem *273*, 3562-3573.

Dai, R.M., and Li, C.C. (2001). Valosin-containing protein is a multi-ubiquitin chain-targeting factor required in ubiquitin-proteasome degradation. Nat Cell Biol *3*, 740-744.

David, J.R. (1966). Delayed hypersensitivity in vitro: its mediation by cell-free substances formed by lymphoid cell-antigen interaction. Proc Natl Acad Sci U S A *56*, 72-77.

de Boer, E., Rodriguez, P., Bonte, E., Krijgsveld, J., Katsantoni, E., Heck, A., Grosveld, F., and Strouboulis, J. (2003). Efficient biotinylation and single-step purification of tagged transcription factors in mammalian cells and transgenic mice. Proc Natl Acad Sci U S A *100*, 7480-7485.

de Jong, Y.P., Abadia-Molina, A.C., Satoskar, A.R., Clarke, K., Rietdijk, S.T., Faubion, W.A., Mizoguchi, E., Metz, C.N., Alsahli, M., ten Hove, T.*, et al.* (2001). Development of chronic colitis is dependent on the cytokine MIF. Nat Immunol *2*, 1061-1066.

Deng, X.W., Dubiel, W., Wei, N., Hofmann, K., Mundt, K., Colicelli, J., Kato, J., Naumann, M., Segal, D., Seeger, M.*, et al.* (2000). Unified nomenclature for the COP9 signalosome and its subunits: an essential regulator of development. Trends Genet *16*, 202-203.

Denkinger, C.M., Denkinger, M., Kort, J.J., Metz, C., and Forsthuber, T.G. (2003). In vivo blockade of macrophage migration inhibitory factor ameliorates acute experimental autoimmune encephalomyelitis by impairing the homing of encephalitogenic T cells to the central nervous system. J Immunol *170*, 1274-1282.

Doss-Pepe, E.W., Stenroos, E.S., Johnson, W.G., and Madura, K. (2003). Ataxin-3 interactions with rad23 and valosin-containing protein and its associations with ubiquitin chains and the proteasome are consistent with a role in ubiquitin-mediated proteolysis. Mol Cell Biol *23*, 6469-6483.

Dreveny, I., Kondo, H., Uchiyama, K., Shaw, A., Zhang, X., and Freemont, P.S. (2004). Structural basis of the interaction between the AAA ATPase p97/VCP and its adaptor protein p47. EMBO J *23*, 1030-1039.

Elsasser, S., and Finley, D. (2005). Delivery of ubiquitinated substrates to protein-unfolding machines. Nat Cell Biol *7*, 742-749.

Fingerle-Rowson, G., Koch, P., Bikoff, R., Lin, X., Metz, C.N., Dhabhar, F.S., Meinhardt, A., and Bucala, R. (2003). Regulation of macrophage migration inhibitory factor expression by glucocorticoids in vivo. Am J Pathol *162*, 47-56.

Finley, D. (2001). Signal transduction. An alternative to destruction. Nature *412*, 283, 285-286.

Frohlich, K.U., Fries, H.W., Rudiger, M., Erdmann, R., Botstein, D., and Mecke, D. (1991). Yeast cell cycle protein CDC48p shows full-length homology to the mammalian protein VCP and is a member of a protein family involved in secretion, peroxisome formation, and gene

expression. J Cell Biol *114*, 443-453.

Ghislain, M., Dohmen, R.J., Levy, F., and Varshavsky, A. (1996). Cdc48p interacts with Ufd3p, a WD repeat protein required for ubiquitin-mediated proteolysis in Saccharomyces cerevisiae. Embo J *15*, 4884-4899.

Glickman, M.H., Rubin, D.M., Fried, V.A., and Finley, D. (1998). The regulatory particle of the Saccharomyces cerevisiae proteasome. Mol Cell Biol *18*, 3149-3162.

Groisman, R., Polanowska, J., Kuraoka, I., Sawada, J., Saijo, M., Drapkin, R., Kisselev, A.F., Tanaka, K., and Nakatani, Y. (2003). The ubiquitin ligase activity in the DDB2 and CSA complexes is differentially regulated by the COP9 signalosome in response to DNA damage. Cell *113*, 357-367.

Harper, J.W., and Schulman, B.A. (2006). Structural complexity in ubiquitin recognition. Cell *124*, 1133-1136.

Hartmann-Petersen, R., Wallace, M., Hofmann, K., Koch, G., Johnsen, A.H., Hendil, K.B., and Gordon, C. (2004). The Ubx2 and Ubx3 cofactors direct Cdc48 activity to proteolytic and nonproteolytic ubiquitin-dependent processes. Curr Biol *14*, 824-828.

Henke, W., Ferrell, K., Bech-Otschir, D., Seeger, M., Schade, R., Jungblut, P., Naumann, M., and Dubiel, W. (1999). Comparison of human COP9 signalsome and 26S proteasome lid'. Mol Biol Rep *26*, 29-34.

Hetfeld, B.K., Helfrich, A., Kapelari, B., Scheel, H., Hofmann, K., Guterman, A., Glickman, M., Schade, R., Kloetzel, P.M., and Dubiel, W. (2005). The zinc finger of the CSN-associated deubiquitinating enzyme USP15 is essential to rescue the E3 ligase Rbx1. Curr Biol *15*, 1217-1221.

Hicke, L., Schubert, H.L., and Hill, C.P. (2005). Ubiquitin-binding domains. Nat Rev Mol Cell Biol *6*, 610-621.

Hitchcock, A.L., Krebber, H., Frietze, S., Lin, A., Latterich, M., and Silver, P.A. (2001). The conserved npl4 protein complex mediates proteasome-dependent membrane-bound transcription factor activation. Mol Biol Cell *12*, 3226-3241.

Hitzeman, R.A., Clarke, L., and Carbon, J. (1980). Isolation and characterization of the yeast 3-phosphoglycerokinase gene (PGK) by an immunological screening technique. J Biol Chem *255*, 12073-12080.

Huang, X.R., Chun Hui, C.W., Chen, Y.X., Wong, B.C., Fung, P.C., Metz, C., Cho, C.H., Hui, W.M., Bucala, R., Lam, S.K., and Lan, H.Y. (2001). Macrophage migration inhibitory factor is an important mediator in the pathogenesis of gastric inflammation in rats. Gastroenterology *121*, 619-630.

Hudson, J.D., Shoaibi, M.A., Maestro, R., Carnero, A., Hannon, G.J., and Beach, D.H. (1999). A proinflammatory cytokine inhibits p53 tumor suppressor activity. J Exp Med *190*, 1375-1382.

Hurley, J.H., Lee, S., and Prag, G. (2006). Ubiquitin-binding domains. Biochem J *399*, 361-372.

Imamura, S., Ojima, N., and Yamashita, M. (2003). Cold-inducible expression of the cell division cycle gene CDC48 and its promotion of cell proliferation during cold acclimation in zebrafish cells. FEBS Lett *549*, 14-20.

Jarosch, E., Taxis, C., Volkwein, C., Bordallo, J., Finley, D., Wolf, D.H., and Sommer, T. (2002). Protein dislocation from the ER requires polyubiquitination and the AAA-ATPase Cdc48. Nat Cell Biol *4*, 134-139.

Jentsch, S., and Rumpf, S. (2007). Cdc48 (p97): a "molecular gearbox" in the ubiquitin pathway? Trends Biochem Sci *32*, 6-11.

Jung, H., Kim, T., Chae, H.Z., Kim, K.T., and Ha, H. (2001). Regulation of macrophage migration inhibitory factor and thiol-specific antioxidant protein PAG by direct interaction. J Biol Chem *276*, 15504-15510.

Karhausen, J., Haase, V.H., and Colgan, S.P. (2005). Inflammatory hypoxia: role of hypoxia-inducible factor. Cell Cycle *4*, 256-258.

Karin, M., and Ben-Neriah, Y. (2000). Phosphorylation meets ubiquitination: the control of NF-[kappa]B activity. Annu Rev Immunol *18*, 621-663.

Kim, B.C., Lee, H.J., Park, S.H., Lee, S.R., Karpova, T.S., McNally, J.G., Felici, A., Lee, D.K., and Kim, S.J. (2004). Jab1/CSN5, a component of the COP9 signalosome, regulates transforming growth factor beta signaling by binding to Smad7 and promoting its degradation. Mol Cell Biol *24*, 2251-2262.

Kim, M. (2003). Expressionsklonierung und Aufreinigung des Makrophagen-Migrations-Inhibitions-Faktor. In Fachbereich Humanmedizin (marburg, Inst. für Anatomie und Zellbiologie, Philipps-Universität Marburg).

Kim, V.N. (2005). Small RNAs: classification, biogenesis, and function. Mol Cells *19*, 1-15.

Kitaichi, N., Matsuda, A., Kotake, S., Namba, K., Tagawa, Y., Sasamoto, Y., Ogasawara, K., Iwabuchi, K., Onoe, K., Matsuda, H., and Nishihira, J. (2000). Inhibition of experimental autoimmune uveoretinitis with anti-macrophage migration inhibitory factor antibodies. Curr Eye Res *20*, 109-114.

Kleemann, R., Hausser, A., Geiger, G., Mischke, R., Burger-Kentischer, A., Flieger, O., Johannes, F.J., Roger, T., Calandra, T., Kapurniotu, A., *et al.* (2000). Intracellular action of the cytokine MIF to modulate AP-1 activity and the cell cycle through Jab1. Nature *408*, 211-216.

Kleemann, R., Kapurniotu, A., Frank, R.W., Gessner, A., Mischke, R., Flieger, O., Juttner, S., Brunner, H., and Bernhagen, J. (1998a). Disulfide analysis reveals a role for macrophage migration inhibitory factor (MIF) as thiol-protein oxidoreductase. J Mol Biol *280*, 85-102.

Kleemann, R., Kapurniotu, A., Mischke, R., Held, J., and Bernhagen, J. (1999). Characterization of catalytic centre mutants of macrophage migration inhibitory factor (MIF) and comparison to Cys81Ser MIF. Eur J Biochem *261*, 753-766.

Kleemann, R., Mischke, R., Kapurniotu, A., Brunner, H., and Bernhagen, J. (1998b). Specific reduction of insulin disulfides by macrophage migration inhibitory factor (MIF) with glutathione and dihydrolipoamide: potential role in cellular redox processes. FEBS Lett *430*, 191-196.

Kondo, H., Rabouille, C., Newman, R., Levine, T.P., Pappin, D., Freemont, P., and Warren, G. (1997). p47 is a cofactor for p97-mediated membrane fusion. Nature *388*, 75-78.

Konig, P., Krasteva, G., Tag, C., Konig, I.R., Arens, C., and Kummer, W. (2006). FRET-CLSM and double-labeling indirect immunofluorescence to detect close association of proteins in tissue sections. Lab Invest *86*, 853-864.

Koong, A.C., Denko, N.C., Hudson, K.M., Schindler, C., Swiersz, L., Koch, C., Evans, S., Ibrahim, H., Le, Q.T., Terris, D.J., and Giaccia, A.J. (2000). Candidate genes for the hypoxic tumor phenotype. Cancer Res *60*, 883-887.

Lan, H.Y., Nikolic-Paterson, D.J., Mu, W., and Atkins, R.C. (1996). Local macrophage proliferation in progressive renal injury. Contrib Nephrol *118*, 100-108.

Lavoie, C., Chevet, E., Roy, L., Tonks, N.K., Fazel, A., Posner, B.I., Paiement, J., and Bergeron, J.J. (2000). Tyrosine phosphorylation of p97 regulates transitional endoplasmic reticulum assembly in vitro. Proc Natl Acad Sci U S A *97*, 13637-13642.

Leech, M., Metz, C., Santos, L., Peng, T., Holdsworth, S.R., Bucala, R., and Morand, E.F. (1998). Involvement of macrophage migration inhibitory factor in the evolution of rat adjuvant arthritis. Arthritis Rheum *41*, 910-917.

Leng, L., Metz, C.N., Fang, Y., Xu, J., Donnelly, S., Baugh, J., Delohery, T., Chen, Y., Mitchell, R.A., and Bucala, R. (2003). MIF signal transduction initiated by binding to CD74. J Exp Med *197*, 1467-1476.

Li, S., Liu, X., and Ascoli, M. (2000). p38JAB1 binds to the intracellular precursor of the lutropin/choriogonadotropin receptor and promotes its degradation. J Biol Chem *275*, 13386-13393.

Li, Y., Lu, C., Xing, G., Zhu, Y., and He, F. (2004). Macrophage migration inhibitory factor directly interacts with hepatopoietin and regulates the proliferation of hepatoma cell. Exp Cell Res *300*, 379-387.

Lilley, B.N., and Ploegh, H.L. (2005). Multiprotein complexes that link dislocation, ubiquitination, and extraction of misfolded proteins from the endoplasmic reticulum membrane. Proc Natl Acad Sci U S A *102*, 14296-14301.

Lin, S.G., Yu, X.Y., Chen, Y.X., Huang, X.R., Metz, C., Bucala, R., Lau, C.P., and Lan, H.Y. (2000). De novo expression of macrophage migration inhibitory factor in atherogenesis in

rabbits. Circ Res *87*, 1202-1208.

Liu, J., Furukawa, M., Matsumoto, T., and Xiong, Y. (2002). NEDD8 modification of CUL1 dissociates p120(CAND1), an inhibitor of CUL1-SKP1 binding and SCF ligases. Mol Cell *10*, 1511-1518.

Lue, H., Kleemann, R., Calandra, T., Roger, T., and Bernhagen, J. (2002). Macrophage migration inhibitory factor (MIF): mechanisms of action and role in disease. Microbes Infect *4*, 449-460.

Lue, H., Thiele, M., Franz, J., Dahl, E., Speckgens, S., Leng, L., Fingerle-Rowson, G., Bucala, R., Luscher, B., and Bernhagen, J. (2007). Macrophage migration inhibitory factor (MIF) promotes cell survival by activation of the Akt pathway and role for CSN5/JAB1 in the control of autocrine MIF activity. Oncogene *26*, 5046-5059.

Luo, F., Liu, X., Yan, N., Li, S., Cao, G., Cheng, Q., Xia, Q., and Wang, H. (2006). Hypoxia-inducible transcription factor-1alpha promotes hypoxia-induced A549 apoptosis via a mechanism that involves the glycolysis pathway. BMC Cancer *6*, 26.

Madeo, F., Schlauer, J., Zischka, H., Mecke, D., and Frohlich, K.U. (1998). Tyrosine phosphorylation regulates cell cycle-dependent nuclear localization of Cdc48p. Mol Biol Cell *9*, 131-141.

Maity, A., and Koumenis, C. (2006). HIF and MIF--a nifty way to delay senescence? Genes Dev *20*, 3337-3341.

Makita, H., Nishimura, M., Miyamoto, K., Nakano, T., Tanino, Y., Hirokawa, J., Nishihira, J., and Kawakami, Y. (1998). Effect of anti-macrophage migration inhibitory factor antibody on lipopolysaccharide-induced pulmonary neutrophil accumulation. Am J Respir Crit Care Med *158*, 573-579.

Marsin, A.S., Bertrand, L., Rider, M.H., Deprez, J., Beauloye, C., Vincent, M.F., Van den Berghe, G., Carling, D., and Hue, L. (2000). Phosphorylation and activation of heart PFK-2 by AMPK has a role in the stimulation of glycolysis during ischaemia. Curr Biol *10*, 1247-1255.

Maurizi, M.R., and Li, C.C. (2001). AAA proteins: in search of a common molecular basis. International Meeting on Cellular Functions of AAA Proteins. EMBO Rep *2*, 980-985.

Maytal-Kivity, V., Reis, N., Hofmann, K., and Glickman, M.H. (2002). MPN+, a putative catalytic motif found in a subset of MPN domain proteins from eukaryotes and prokaryotes, is critical for Rpn11 function. BMC Biochem *3*, 28.

McCullough, J., Clague, M.J., and Urbe, S. (2004). AMSH is an endosome-associated ubiquitin isopeptidase. The Journal of cell biology *166*, 487-492.

Medzhitov, R. (2001). Toll-like receptors and innate immunity. Nat Rev Immunol *1*, 135-145.

Medzhitov, R., Preston-Hurlburt, P., and Janeway, C.A., Jr. (1997). A human homologue of the Drosophila Toll protein signals activation of adaptive immunity. Nature *388*, 394-397.

Meinhardt, A., Bacher, M., McFarlane, J.R., Metz, C.N., Seitz, J., Hedger, M.P., de Kretser, D.M., and Bucala, R. (1996). Macrophage migration inhibitory factor production by Leydig cells: evidence for a role in the regulation of testicular function. Endocrinology *137*, 5090-5095.

Meyer-Siegler, K.L., Iczkowski, K.A., Leng, L., Bucala, R., and Vera, P.L. (2006). Inhibition of macrophage migration inhibitory factor or its receptor (CD74) attenuates growth and invasion of DU-145 prostate cancer cells. J Immunol *177*, 8730-8739.

Meyer, H.H., Wang, Y., and Warren, G. (2002). Direct binding of ubiquitin conjugates by the mammalian p97 adaptor complexes, p47 and Ufd1-Npl4. Embo J *21*, 5645-5652.

Mikulowska, A., Metz, C.N., Bucala, R., and Holmdahl, R. (1997). Macrophage migration inhibitory factor is involved in the pathogenesis of collagen type II-induced arthritis in mice. J Immunol *158*, 5514-5517.

Miller, E.J., Li, J., Leng, L., McDonald, C., Atsumi, T., Bucala, R., and Young, L.H. (2008). Macrophage migration inhibitory factor stimulates AMP-activated protein kinase in the ischaemic heart. Nature *451*, 578-582.

Mitchell, R.A. (2004). Mechanisms and effectors of MIF-dependent promotion of tumourigenesis. Cell Signal *16*, 13-19.

Mitchell, R.A., Liao, H., Chesney, J., Fingerle-Rowson, G., Baugh, J., David, J., and Bucala, R. (2002). Macrophage migration inhibitory factor (MIF) sustains macrophage proinflammatory function by inhibiting p53: regulatory role in the innate immune response. Proc Natl Acad Sci U S A *99*, 345-350.

Mitchell, R.A., Metz, C.N., Peng, T., and Bucala, R. (1999). Sustained mitogen-activated protein kinase (MAPK) and cytoplasmic phospholipase A2 activation by macrophage migration inhibitory factor (MIF). Regulatory role in cell proliferation and glucocorticoid action. J Biol Chem *274*, 18100-18106.

Mouysset, J., Kahler, C., and Hoppe, T. (2006). A conserved role of Caenorhabditis elegans CDC-48 in ER-associated protein degradation. J Struct Biol *156*, 41-49.

Muhlhahn, P., Bernhagen, J., Czisch, M., Georgescu, J., Renner, C., Ross, A., Bucala, R., and Holak, T.A. (1996). NMR characterization of structure, backbone dynamics, and glutathione binding of the human macrophage migration inhibitory factor (MIF). Protein Sci *5*, 2095-2103.

Nagahama, M., Suzuki, M., Hamada, Y., Hatsuzawa, K., Tani, K., Yamamoto, A., and Tagaya, M. (2003). SVIP is a novel VCP/p97-interacting protein whose expression causes cell vacuolation. Mol Biol Cell *14*, 262-273.

Naumann, M., Bech-Otschir, D., Huang, X., Ferrell, K., and Dubiel, W. (1999). COP9 signalosome-directed c-Jun activation/stabilization is independent of JNK. J Biol Chem *274*, 35297-35300.

Nemajerova, A., Mena, P., Fingerle-Rowson, G., Moll, U.M., and Petrenko, O. (2007a).

Impaired DNA damage checkpoint response in MIF-deficient mice. Embo J *26*, 987-997.

Nemajerova, A., Moll, U.M., Petrenko, O., and Fingerle-Rowson, G. (2007b). Macrophage migration inhibitory factor coordinates DNA damage response with the proteasomal control of the cell cycle. Cell Cycle *6*, 1030-1034.

Neuber, O., Jarosch, E., Volkwein, C., Walter, J., and Sommer, T. (2005). Ubx2 links the Cdc48 complex to ER-associated protein degradation. Nat Cell Biol *7*, 993-998.

Neuwald, A.F., Aravind, L., Spouge, J.L., and Koonin, E.V. (1999). AAA+: A class of chaperone-like ATPases associated with the assembly, operation, and disassembly of protein complexes. Genome Res *9*, 27-43.

Oda, Y., Okada, T., Yoshida, H., Kaufman, R.J., Nagata, K., and Mori, K. (2006). Derlin-2 and Derlin-3 are regulated by the mammalian unfolded protein response and are required for ER-associated degradation. J Cell Biol *172*, 383-393.

Ogura, T., and Wilkinson, A.J. (2001). AAA+ superfamily ATPases: common structure--diverse function. Genes Cells *6*, 575-597.

Oh, W., Lee, E.W., Sung, Y.H., Yang, M.R., Ghim, J., Lee, H.W., and Song, J. (2006). Jab1 induces the cytoplasmic localization and degradation of p53 in coordination with Hdm2. J Biol Chem *281*, 17457-17465.

Pamnani, V., Tamura, T., Lupas, A., Peters, J., Cejka, Z., Ashraf, W., and Baumeister, W. (1997). Cloning, sequencing and expression of VAT, a CDC48/p97 ATPase homologue from the archaeon Thermoplasma acidophilum. FEBS Lett *404*, 263-268.

Peth, A., Berndt, C., Henke, W., and Dubiel, W. (2007a). Downregulation of COP9 signalosome subunits differentially affects CSN complex and target protein stability. BMC Biochem *8*, 27.

Peth, A., Boettcher, J.P., and Dubiel, W. (2007b). Ubiquitin-dependent proteolysis of the microtubule end-binding protein 1, EB1, is controlled by the COP9 signalosome: possible consequences for microtubule filament stability. J Mol Biol *368*, 550-563.

Petrenko, O., Fingerle-Rowson, G., Peng, T., Mitchell, R.A., and Metz, C.N. (2003). Macrophage migration inhibitory factor deficiency is associated with altered cell growth and reduced susceptibility to Ras-mediated transformation. J Biol Chem *278*, 11078-11085.

Petroski, M.D., and Deshaies, R.J. (2005). Function and regulation of cullin-RING ubiquitin ligases. Nat Rev Mol Cell Biol *6*, 9-20.

Pickart, C.M. (2001a). Mechanisms underlying ubiquitination. Annu Rev Biochem *70*, 503-533.

Pickart, C.M. (2001b). Ubiquitin enters the new millennium. Mol Cell *8*, 499-504.

Pickart, C.M., and Cohen, R.E. (2004). Proteasomes and their kin: proteases in the machine age. Nat Rev Mol Cell Biol *5*, 177-187.

Rabouille, C., Levine, T.P., Peters, J.M., and Warren, G. (1995). An NSF-like ATPase, p97, and NSF mediate cisternal regrowth from mitotic Golgi fragments. Cell *82*, 905-914.

Rape, M., Hoppe, T., Gorr, I., Kalocay, M., Richly, H., and Jentsch, S. (2001). Mobilization of processed, membrane-tethered SPT23 transcription factor by CDC48(UFD1/NPL4), a ubiquitin-selective chaperone. Cell *107*, 667-677.

Richly, H., Rape, M., Braun, S., Rumpf, S., Hoege, C., and Jentsch, S. (2005). A series of ubiquitin binding factors connects CDC48/p97 to substrate multiubiquitylation and proteasomal targeting. Cell *120*, 73-84.

Rigaut, G., Shevchenko, A., Rutz, B., Wilm, M., Mann, M., and Seraphin, B. (1999). A generic protein purification method for protein complex characterization and proteome exploration. Nat Biotechnol *17*, 1030-1032.

Rischitor, G. (2005). Transcription factor Sp3 as target for SUMOylation in vivo. (Marburg, Philipps-Universität Marburg), p. 197.

Roger, T., David, J., Glauser, M.P., and Calandra, T. (2001). MIF regulates innate immune responses through modulation of Toll-like receptor 4. Nature *414*, 920-924.

Roger, T., Froidevaux, C., Martin, C., and Calandra, T. (2003). Macrophage migration inhibitory factor (MIF) regulates host responses to endotoxin through modulation of Toll-like receptor 4 (TLR4). J Endotoxin Res *9*, 119-123.

Rosengren, E., Aman, P., Thelin, S., Hansson, C., Ahlfors, S., Bjork, P., Jacobsson, L., and Rorsman, H. (1997). The macrophage migration inhibitory factor MIF is a phenylpyruvate tautomerase. FEBS Lett *417*, 85-88.

Rumpf, S., and Jentsch, S. (2006). Functional division of substrate processing cofactors of the ubiquitin-selective Cdc48 chaperone. Mol Cell *21*, 261-269.

Russell, R.R., 3rd, Bergeron, R., Shulman, G.I., and Young, L.H. (1999). Translocation of myocardial GLUT-4 and increased glucose uptake through activation of AMPK by AICAR. Am J Physiol *277*, H643-649.

Russell, R.R., 3rd, Li, J., Coven, D.L., Pypaert, M., Zechner, C., Palmeri, M., Giordano, F.J., Mu, J., Birnbaum, M.J., and Young, L.H. (2004). AMP-activated protein kinase mediates ischemic glucose uptake and prevents postischemic cardiac dysfunction, apoptosis, and injury. J Clin Invest *114*, 495-503.

Sakai, Y., Masamune, A., Satoh, A., Nishihira, J., Yamagiwa, T., and Shimosegawa, T. (2003). Macrophage migration inhibitory factor is a critical mediator of severe acute pancreatitis. Gastroenterology *124*, 725-736.

Santoro, M.G., Rossi, A., and Amici, C. (2003). NF-kappaB and virus infection: who controls whom. Embo J *22*, 2552-2560.

Schnell, J.D., and Hicke, L. (2003). Non-traditional functions of ubiquitin and ubiquitin-

binding proteins. J Biol Chem *278*, 35857-35860.

Schuberth, C., and Buchberger, A. (2005). Membrane-bound Ubx2 recruits Cdc48 to ubiquitin ligases and their substrates to ensure efficient ER-associated protein degradation. Nat Cell Biol *7*, 999-1006.

Schuberth, C., Richly, H., Rumpf, S., and Buchberger, A. (2004). Shp1 and Ubx2 are adaptors of Cdc48 involved in ubiquitin-dependent protein degradation. EMBO Rep *5*, 818-824.

Schwechheimer, C., and Deng, X.W. (2001). COP9 signalosome revisited: a novel mediator of protein degradation. Trends Cell Biol *11*, 420-426.

Schweitzer, K., Bozko, P.M., Dubiel, W., and Naumann, M. (2007). CSN controls NF-kappaB by deubiquitinylation of IkappaBalpha. EMBO J *26*, 1532-1541.

Seeger, M., Kraft, R., Ferrell, K., Bech-Otschir, D., Dumdey, R., Schade, R., Gordon, C., Naumann, M., and Dubiel, W. (1998). A novel protein complex involved in signal transduction possessing similarities to 26S proteasome subunits. Faseb J *12*, 469-478.

Shaulian, E., and Karin, M. (2002). AP-1 as a regulator of cell life and death. Nat Cell Biol *4*, E131-136.

Shen, L., Hu, J., Lu, H., Wu, M., Qin, W., Wan, D., Li, Y.Y., and Gu, J. (2003). The apoptosis-associated protein BNIPL interacts with two cell proliferation-related proteins, MIF and GFER. FEBS Lett *540*, 86-90.

Shevchenko, A., Wilm, M., Vorm, O., and Mann, M. (1996). Mass spectrometric sequencing of proteins silver-stained polyacrylamide gels. Anal Chem *68*, 850-858.

Shi, X., Leng, L., Wang, T., Wang, W., Du, X., Li, J., McDonald, C., Chen, Z., Murphy, J.W., Lolis, E., *et al.* (2006). CD44 is the signaling component of the macrophage migration inhibitory factor-CD74 receptor complex. Immunity *25*, 595-606.

Smith, P.A., Tripp, B.C., DiBlasio-Smith, E.A., Lu, Z., LaVallie, E.R., and McCoy, J.M. (1998). A plasmid expression system for quantitative in vivo biotinylation of thioredoxin fusion proteins in Escherichia coli. Nucleic Acids Res *26*, 1414-1420.

Song, G., Ouyang, G., and Bao, S. (2005). The activation of Akt/PKB signaling pathway and cell survival. J Cell Mol Med *9*, 59-71.

Sugimoto, H., Suzuki, M., Nakagawa, A., Tanaka, I., and Nishihira, J. (1996). Crystal structure of macrophage migration inhibitory factor from human lymphocyte at 2.1 A resolution. FEBS Lett *389*, 145-148.

Sukhodub, A., Jovanovic, S., Du, Q., Budas, G., Clelland, A.K., Shen, M., Sakamoto, K., Tian, R., and Jovanovic, A. (2007). AMP-activated protein kinase mediates preconditioning in cardiomyocytes by regulating activity and trafficking of sarcolemmal ATP-sensitive K(+) channels. J Cell Physiol *210*, 224-236.

Suzuki, M., Sugimoto, H., Nakagawa, A., Tanaka, I., Nishihira, J., and Sakai, M. (1996). Crystal structure of the macrophage migration inhibitory factor from rat liver. Nat Struct Biol *3*, 259-266.

Swope, M., Sun, H.W., Blake, P.R., and Lolis, E. (1998). Direct link between cytokine activity and a catalytic site for macrophage migration inhibitory factor. Embo J *17*, 3534-3541.

Takeda, K., Kaisho, T., and Akira, S. (2003). Toll-like receptors. Annu Rev Immunol *21*, 335-376.

Thiele, M., and Bernhagen, J. (2005). Link between macrophage migration inhibitory factor and cellular redox regulation. Antioxid Redox Signal *7*, 1234-1248.

Tomiyasu, M., Yoshino, I., Suemitsu, R., Okamoto, T., and Sugimachi, K. (2002). Quantification of macrophage migration inhibitory factor mRNA expression in non-small cell lung cancer tissues and its clinical significance. Clin Cancer Res *8*, 3755-3760.

Tresaugues, L., Collinet, B., Minard, P., Henckes, G., Aufrere, R., Blondeau, K., Liger, D., Zhou, C.Z., Janin, J., Van Tilbeurgh, H., and Quevillon-Cheruel, S. (2004). Refolding strategies from inclusion bodies in a structural genomics project. J Struct Funct Genomics *5*, 195-204.

Truong, K., and Ikura, M. (2001). The use of FRET imaging microscopy to detect protein-protein interactions and protein conformational changes in vivo. Curr Opin Struct Biol *11*, 573-578.

Tsuge, T., Matsui, M., and Wei, N. (2001). The subunit 1 of the COP9 signalosome suppresses gene expression through its N-terminal domain and incorporates into the complex through the PCI domain. J Mol Biol *305*, 1-9.

Tucker, J., and Grisshammer, R. (1996). Purification of a rat neurotensin receptor expressed in Escherichia coli. Biochem J *317 (Pt 3)*, 891-899.

Vale, R.D. (2000). AAA proteins. Lords of the ring. J Cell Biol *150*, F13-19.

Vandermoere, F., El Yazidi-Belkoura, I., Slomianny, C., Demont, Y., Bidaux, G., Adriaenssens, E., Lemoine, J., and Hondermarck, H. (2006). The valosin-containing protein (VCP) is a target of Akt signaling required for cell survival. J Biol Chem *281*, 14307-14313.

Verma, R., Aravind, L., Oania, R., McDonald, W.H., Yates, J.R., 3rd, Koonin, E.V., and Deshaies, R.J. (2002). Role of Rpn11 metalloprotease in deubiquitination and degradation by the 26S proteasome. Science *298*, 611-615.

Wadgaonkar, R., Dudek, S.M., Zaiman, A.L., Linz-McGillem, L., Verin, A.D., Nurmukhambetova, S., Romer, L.H., and Garcia, J.G. (2005). Intracellular interaction of myosin light chain kinase with macrophage migration inhibition factor (MIF) in endothelium. J Cell Biochem *95*, 849-858.

Waeber, G., Calandra, T., Roduit, R., Haefliger, J.A., Bonny, C., Thompson, N., Thorens, B.,

Temler, E., Meinhardt, A., Bacher, M., *et al.* (1997). Insulin secretion is regulated by the glucose-dependent production of islet beta cell macrophage migration inhibitory factor. Proc Natl Acad Sci U S A *94*, 4782-4787.

Wan, M., Cao, X., Wu, Y., Bai, S., Wu, L., Shi, X., and Wang, N. (2002). Jab1 antagonizes TGF-beta signaling by inducing Smad4 degradation. EMBO Rep *3*, 171-176.

Wang, Q., Song, C., and Li, C.C. (2004). Molecular perspectives on p97-VCP: progress in understanding its structure and diverse biological functions. J Struct Biol *146*, 44-57.

Wang, Q., Song, C., Yang, X., and Li, C.C. (2003). D1 ring is stable and nucleotide-independent, whereas D2 ring undergoes major conformational changes during the ATPase cycle of p97-VCP. J Biol Chem *278*, 32784-32793.

Wei, N., Chamovitz, D.A., and Deng, X.W. (1994). Arabidopsis COP9 is a component of a novel signaling complex mediating light control of development. Cell *78*, 117-124.

Wei, N., and Deng, X.W. (1999). Making sense of the COP9 signalosome. A regulatory protein complex conserved from Arabidopsis to human. Trends Genet *15*, 98-103.

Wei, N., and Deng, X.W. (2003). The COP9 signalosome. Annu Rev Cell Dev Biol *19*, 261-286.

Wei, N., Tsuge, T., Serino, G., Dohmae, N., Takio, K., Matsui, M., and Deng, X.W. (1998). The COP9 complex is conserved between plants and mammals and is related to the 26S proteasome regulatory complex. Curr Biol *8*, 919-922.

Weiser, W.Y., Temple, P.A., Witek-Giannotti, J.S., Remold, H.G., Clark, S.C., and David, J.R. (1989). Molecular cloning of a cDNA encoding a human macrophage migration inhibitory factor. Proc Natl Acad Sci U S A *86*, 7522-7526.

Wetzker, R., and Bohmer, F.D. (2003). Transactivation joins multiple tracks to the ERK/MAPK cascade. Nat Rev Mol Cell Biol *4*, 651-657.

Wojcik, C., Yano, M., and DeMartino, G.N. (2004). RNA interference of valosin-containing protein (VCP/p97) reveals multiple cellular roles linked to ubiquitin/proteasome-dependent proteolysis. J Cell Sci *117*, 281-292.

Xing, Y., Musi, N., Fujii, N., Zou, L., Luptak, I., Hirshman, M.F., Goodyear, L.J., and Tian, R. (2003). Glucose metabolism and energy homeostasis in mouse hearts overexpressing dominant negative alpha2 subunit of AMP-activated protein kinase. J Biol Chem *278*, 28372-28377.

Yang, N., Isbel, N.M., Nikolic-Paterson, D.J., Li, Y., Ye, R., Atkins, R.C., and Lan, H.Y. (1998). Local macrophage proliferation in human glomerulonephritis. Kidney Int *54*, 143-151.

Yao, K., Shida, S., Selvakumaran, M., Zimmerman, R., Simon, E., Schick, J., Haas, N.B., Balke, M., Ross, H., Johnson, S.W., and O'Dwyer, P.J. (2005). Macrophage migration inhibitory factor is a determinant of hypoxia-induced apoptosis in colon cancer cell lines. Clin

Cancer Res *11*, 7264-7272.

Ye, Y., Meyer, H.H., and Rapoport, T.A. (2001). The AAA ATPase Cdc48/p97 and its partners transport proteins from the ER into the cytosol. Nature *414*, 652-656.

Yun, J., Tomida, A., Andoh, T., and Tsuruo, T. (2004). Interaction between glucose-regulated destruction domain of DNA topoisomerase IIalpha and MPN domain of Jab1/CSN5. J Biol Chem *279*, 31296-31303.

Zhong, X., Shen, Y., Ballar, P., Apostolou, A., Agami, R., and Fang, S. (2004). AAA ATPase p97/valosin-containing protein interacts with gp78, a ubiquitin ligase for endoplasmic reticulum-associated degradation. J Biol Chem *279*, 45676-45684.

Zhou, C., Wee, S., Rhee, E., Naumann, M., Dubiel, W., and Wolf, D.A. (2003). Fission yeast COP9/signalosome suppresses cullin activity through recruitment of the deubiquitylating enzyme Ubp12p. Mol Cell *11*, 927-938.

Zwickl, P., and Baumeister, W. (1999). AAA-ATPases at the crossroads of protein life and death. Nat Cell Biol *1*, E97-98.

10. ACKNOWLEDGEMENTS

I would first like to thank my advisor Prof. Andreas Meinhardt. He provided an environment for me that exceeded all I could wish for. I am indebted to Andreas for giving me the opportunity to learn so much in his lab and for providing me everything I needed to become a better scientist.

I would like to thank Dr. J Klug, who constantly challenged me with new ideas, provided remarkable insight into my project and corrected my thesis.

Many thanks to Dr. Ana-Maria Bulau, who took me under her wing when I first joined the Meinhardt lab, guided me in my first year in the lab and corrected my thesis.

Special thanks to Suada Fröhlich, Eva Schneider and Dr. Monika Fijak for their support, encouragement, friendship and insight over the years. I am grateful for having the opportunity to work with them.

I would also like to thank other members of the Meinhardt lab, past and present— Patricia Berger, Sudhanshu Bhushan, Sylvia Schirmer, Philipp Lacher, Iris Eckhardt, Benjamin Schwab, Sven Moos, Julis Chapiro and Stefan Binder.

I extend my appreciation to Dr. Henning Urlaub for giving me the opportunity to join his lab and to practice mass spectrometry (MALDI).

I thank Dr. Gabriela Krasteva for helping me with FRET experiments.

I extend my appreciation to Dr. Gabor Huszar and Prof. Ramazan Demir for giving me support and feedback when I needed it.

I am indebted to my family, who always encouraged me to do my best. My parents always supported me throughout my entire education

Last but not least, I would like to thank my husband Fatih, who was always there for me to provide support, encouragement, and help when I needed it the most.

11. CURRICULUM VITAE

Name: Sevil Cayli

Place of birth: Ankara, Turkey

Date of birth: February 12, 1977

Citizenship: Turkey

Address: Department of Anatomy and Cell Biology,
Justus-Liebig University
Aulweg 123, D-35385, Giessen, Germany
Phone: +49(0)6419947032

e-mail: Sevil.Cayli@ anatomie.med.uni-giessen.de

Education and scientifical experience:

2005-2008	Faculty Fellowship in the research group of Prof.Dr. Andreas Meinhardt, Department of Anatomy and Cell Biology, Justus-Liebig University, Giessen, Germany
2002-2005	PhD student and Research Assistant in Akdeniz University, Department of Histology and Embryology, Antalya, Turkey
2002-2003	Research fellow in Obstetrics and Gynecology, Sperm Physiology Laboratuvary, Yale University School of Medicine, New Haven, USA
1999-2002	Master students in Akdeniz University, Department of Histology and Embryology, Antalya, Turkey
1995-1999	Bachelor in Biology, University of Hacettepe, Ankara, Turkey
1984-1995	'Mustafa Kemal' Primary and High School, Ankara, Turkey

12. OWN PUBLICATIONS

12.1. Publications originally from this thesis

1- **Sevil Cayli**, Jörg Klug , Suada Fröhlich , Gabriela Krasteva , Lukas Orel, Andreas Meinhardt. The CSN and p97/VCP form a complex that is structurally similar to the 19S proteasome regulatory particle. **EMBO Rep, under rewiev. Submitted May 2008.**

2- **Sevil Cayli**, Suada Fröhlich, Tamara Henke, Henning Urlaub, Andreas Meinhardt and Jörg Klug. Proteomics analysis of proteins interacting with Macrophage Migration Inhibitory Factor indicates its involvement in the regulation of protein degradation pathways. **manuscript in preparation.**

3- Ana-Maria Bulau, Jörg Klug, **Sevil Cayli,** Suada Fröhlich, Tamara Henke, Patrick Bulau, Regina Eickhoff, Monika Linder, Henning Urlaub, Jürgen Bernhagen, Andreas Meinhardt. Ribosomal Protein S19 Interacts with Macrophage Migration Inhibitory Factor and attenuates its Pro-Inflammatory Function. **J Biol Chem, resubmission invited.**

12.2. Other publications

1- Acar, N., Korgun, E. T., **Cayli, S.**, Sahin, Z., Demir, R., and Ustunel, I. (2008). Is there a relationship between PCNA expression and diabetic placental development during pregnancy? Acta Histochem.

2- Korgun, E. T.**, Cayli, S.,** Asar, M., and Demir, R. (2007). Distribution of laminin, vimentin and desmin in the rat uterus during initial stages of implantation. J Mol Histol *38*, 253-260.

3- Huszar, G., Jakab, A., Sakkas, D., Ozenci, C. C., **Cayli, S.,** Delpiano, E., and Ozkavukcu, S. (2007). Fertility testing and ICSI sperm selection by hyaluronic acid binding: clinical and genetic aspects. Reprod Biomed Online *14*, 650-663.

4- Korgun, E. T., Celik-Ozenci, C., Acar, N., **Cayli, S.**, Desoye, G., and Demir, R. (2006). Location of cell cycle regulators cyclin B1, cyclin A, PCNA, Ki67 and cell cycle inhibitors p21, p27 and p57 in human first trimester placenta and deciduas. Histochem Cell Biol *125*, 615-624.

5- Huszar, G., Ozkavukcu, S., Jakab, A., Celik-Ozenci, C., Sati, G. L., and **Cayli, S.** (2006). Hyaluronic acid binding ability of human sperm reflects cellular maturity and fertilizing potential: selection of sperm for intracytoplasmic sperm injection. Curr Opin Obstet Gynecol *18*, 260-267.

6- Kayisli, U. A., **Cayli, S.,** Seval, Y., Tertemiz, F., Huppertz, B., and Demir, R. (2006). Spatial and temporal distribution of Tie-1 and Tie-2 during very early development of the human placenta. Placenta *27*, 648-659.

7- Demir, R., Kayisli, U. A., **Cayli, S.**, and Huppertz, B. (2006). Sequential steps during vasculogenesis and angiogenesis in the very early human placenta. Placenta *27*, 535-539.

8- Jakab, A., Sakkas, D., Delpiano, E., **Cayli, S.**, Kovanci, E., Ward, D., Revelli, A., and Huszar, G. (2005). Intracytoplasmic sperm injection: a novel selection method for sperm with normal frequency of chromosomal aneuploidies. Fertil Steril *84*, 1665-1673.

9- Huszar, G., Celik-Ozenci, C., **Cayli, S**., Kovacs, T., Vigue, L., and Kovanci, E. (2004). Semen characteristics after overnight shipping: preservation of sperm concentrations, HspA2 ratios, CK activity, cytoplasmic retention, chromatin maturity, DNA integrity, and sperm shape. J Androl *25*, 593-604.

10- Cayli, S., Sakkas, D., Vigue, L., Demir, R., and Huszar, G. (2004). Cellular maturity and apoptosis in human sperm: creatine kinase, caspase-3 and Bcl-XL levels in mature and diminished maturity sperm. Mol Hum Reprod *10*, 365-372.

11- Cayli, S., Jakab, A., Ovari, L., Delpiano, E., Celik-Ozenci, C., Sakkas, D., Ward, D., and Huszar, G. (2003). Biochemical markers of sperm function: male fertility and sperm selection for ICSI. Reprod Biomed Online *7*, 462-468.

12- Huszar, G., Ozenci, C. C., **Cayli, S.**, Zavaczki, Z., Hansch, E., and Vigue, L. (2003). Hyaluronic acid binding by human sperm indicates cellular maturity, viability, and unreacted acrosomal status. Fertil Steril *79 Suppl 3*, 1616-1624.

13- Ustunel, I., **Cayli, S.**, Guney, K., Celik-Ozenci, C., Tanriover, G., Sahin, Z., Balkan, E., and Demir, R. (2003). Immunohistochemical distribution patterns of collagen type II, chondroitin 4-sulfate, laminin and fibronectin in human nasal septal cartilage. Acta Histochem *105*, 109-114.

14- Cayli, S., Ustunel, I., Celik-Ozenci, C., Korgun, E. T., and Demir, R. (2002). Distribution patterns of PCNA and ANP in perinatal stages of the developing rat heart. Acta Histochem *104*, 271-277.

15- Bayram, Z., Asar, M., **Cayli, S.,** and Demir, R. (2002). Immunocytochemical detection of neuronal nitric oxide synthase (nNOS)-IR in embryonic rat stomach between days 13 and 21 of gestation. J Histochem Cytochem *50*, 671-680.

13. EHRENWÖRTLICHE ERKLÄRUNG

Ich erkläre: die vorgelegte Dissertation selbstständig, ohne unerlaubte fremde Hilfe und nur mit den Hilfen angefertigt zu haben, die in der Dissertation angegeben sind.
Alle Textstellen, die wörtlich oder sinngemäß aus veröffentlichten oder nicht veröffentlichen Schriften entnommen sind, und alle Angaben, die auf mündlichen Auskünften beruhen, sind als solche kenntlich gemacht. Bei den von mir durchgeführten und in der Dissertation erwähnten Untersuchungen habe ich die Grundsätze guter wissenschaftlicher Praxis, wie sie in der „Satzung der Justus-Liebig-Universität Giessen zur Sicherung guter wissenschaftlicher Praxis“ niedergelegt sind, eingehalten.

Sevil Cayli
Giessen, Juli 2008